



Misr University for Science and Technology

College of Information Technology

A Graduation Project Report Submission in Partial Fulfillment of the
Requirements for the award of the degree

Bachelor of Information Technology

Cancer Detection Using Deep Learning Approach

Under Supervision of

Prof./ Rania El-Gohary

Dr./ Mohamed Badawi

Mentors

T.A/ Shaimaa Bahaa

T.A/ Shereen Youssef

June 2024



Misr University for Science and Technology

College of Information Technology

A Graduation Project Report Submission in Partial Fulfillment of the
Requirements for the award of the degree

Bachelor of Information Technology

Cancer Detection Using Deep Learning Approach

Submitted by

Student	ID	Dept.
<i>Mostafa Tarek</i>	<i>94071</i>	<i>Artificial Intelligence</i>
<i>Mohamed Ezz</i>	<i>94303</i>	<i>Artificial Intelligence</i>
<i>Abdelrahman Ahmed</i>	<i>94218</i>	<i>Artificial Intelligence</i>
<i>Amr Samir</i>	<i>90369</i>	<i>Artificial Intelligence</i>
<i>Nour Ehab</i>	<i>90330</i>	<i>Artificial Intelligence</i>

Under Supervision of

Prof./ Rania Elgohary

Dr./ Mohamed Badawi

Mentors

T.A/ Shaimaa Bahaa

T.A/ Shereen Youssef

June 2024

ABSTRACT

This thesis presents a comprehensive exploration of advanced computational techniques in the domain of medical diagnostics, focusing on the localization and classification of skin cancer lesions and the segmentation of brain tumors. Through the development and implementation of a multifaceted project comprising a website, desktop application, and Streamlit app, the research endeavors to leverage technology for early detection and precise delineation of these critical health conditions.

Utilizing prominent datasets such as HAM1000 and PH2 for skin cancer analysis and the LGG dataset for brain tumor segmentation, the study establishes a robust foundation for diagnostic innovation. Employing state-of-the-art machine learning algorithms, including Convolutional Neural Networks (CNNs) and U-Net, the project aims to extract and interpret complex patterns inherent in medical imaging data, thereby facilitating accurate diagnosis and treatment planning.

In addition to showcasing the technical prowess of modern computational methodologies, the thesis underscores the importance of interdisciplinary collaboration in addressing healthcare challenges. By seamlessly integrating cutting-edge technology with clinical expertise, the research endeavors to bridge the gap between traditional healthcare practices and emerging computational paradigms.

As the digital landscape continues to evolve, the fusion of technology and medicine holds immense promise for revolutionizing diagnostic processes and improving patient outcomes. Through this endeavor, we glimpse a future where the boundaries between disciplines blur, ushering in an era of precision medicine and personalized healthcare interventions.

ACKNOWLEDGMENT

We express our sincerest gratitude to the Dean of our faculty, Prof. Rania Elgohary, for her unwavering dedication to the growth and success of our academic community. Additionally, we are immensely thankful to our instructor, Dr. Mohamed Badawi, and our Teaching Assistants, T.A. Shaimaa Bahaa and T.A. Shereen Youssef. Your guidance, expertise, and unwavering commitment have been invaluable in shaping our learning journey.

TABLE OF CONTENTS

List of Figures	VI
List of Tables.....	VIII
List of Acronyms.....	IX
Chapter 1: Introduction	1
1.1: Introduction.....	1
1.1.1: Possible Beneficiaries	2
1.2: Research Motivation	2
1.3: Challenges and Solutions.....	3
1.4: Problem Definition	4
1.5: Research Objectives	5
1.6: Benefits and Drawbacks	5
1.6.1: Benefits	5
1.6.2: Drawbacks	6
1.7: Original Key Contribution	7
1.7.1: Features.....	7
1.7.2: Explian the way.....	7
1.8: Research Organization	8
Chapter 2: Related Works	9
2.1: Introduction.....	9
2.2: Scientific Background	9
2.2.1: Machine Learning in Classification	9
2.2.2: Convolutional Neural Networks (CNN).....	9
2.2.3. U-Net for Segmentation.....	10
2.2.4. Transfer Learning in Medical Image Analysis.....	10
2.3. Literal Review.....	11
2.4. Synthesis and Comparison.....	17
2.5. implications and Future Directions.....	17
2.6. Conclusion.....	18

Chapter 3: System Analysis and Design	19
3.1: Introduction.....	19
3.2. The Role of System Analysis and Design.....	19
3.3. The context diagram.....	20
3.4. The class diagram.....	21
3.5. An Entity-Relationship Diagram (ERD).....	23
3.7. Use Case Diagram.....	26
3.8. A Data Flow Diagram (DFD).....	27
3.9. Process Model Diagram.....	28
3.10. Sequence Diagram.....	30
Chapter 4: Implementation.....	32
4.1: Introduction.....	32
4.2. Definitions.....	32
4.3. Proposed System.....	34
4.4. Methodology.....	35
4.4.1. Data Collection.....	35
4.4.2. Data Preprocessing.....	36
4.4.3. Data Augmentation.....	36
4.4.4. Model Architecture.....	37
4.5. Tools Used.....	41
Chapter 5: Testing & Results.....	43
5.1: Introduction.....	43
5.2. Datasets Used.....	43
5.2.1. Skin Cancer Classification Dataset.....	43
5.2.2. Skin Cancer Segmentation Dataset.....	45
5.2.3. Brain Tumor Segmentation Dataset.....	45
5.3. Evaluation Metrics for both classification and segmentation.....	45
5.4. Results.....	47
5.4.1. Results for Skin Cancer Classification.....	47
5.4.2. Results for Skin Cancer Segmentation.....	53
5.4.3. Proposed Skin Cancer Models Predictions.....	55
5.4.4. Results for Brain Tumor Segmentation.....	58
5.4.3. Proposed Brain Tumor Model Predictions.....	60
5.5. Business Value.....	61

5.6. The Platforms GUI.....	61
Chapter 6: Conclusion.....	64
Future Work.....	65
References	66

LIST OF FIGURES

Figure 2.1: Performance Analysis: Metric Comparison across Training Algorithms ..	13
Figure 2.2: Performance Analysis: Metric Comparison across Testing Algorithms....	13
Figure 3.1: system analysis.....	19
Figure 3.2: Context Diagram.....	21
Figure 3.3: Class Diagram.....	23
Figure 3.4: ERD.....	24
Figure 3.5: State Chart.....	25
Figure 3.6: Use Case Diagram.....	26
Figure 3.7: Data Flow Diagram.....	28
Figure 3.8: Process Model Diagram.....	29
Figure 3.9: Sequence Diagram.....	31
Figure 4.1: Proposed System for Skin Cancer.....	35
Figure 4.2: Proposed System for Brain Tumor.....	35
Figure 4.3: Proposed Classification Model Architectural Framework.....	37
Figure 4.4: Segmentation Model Architectural Framework.....	39
Figure 4.5: Segmentation Model Architectural Framework.....	40
Figure 5.1: Class Distribution Analysis of the dataset.....	44
Figure 5.2: All Class Distribution after using the factor.....	45
Figure 5.3: Performance Analysis: Metric Comparison across Training Algorithms ..	48
Figure 5.4: Performance Analysis: Metric Comparison across Testing Algorithms....	49
Figure 5.5: Tracking Progress: Evaluation of Accuracy and Loss.....	49
Figure 5.6: Visualizing Model Performance: Confusion Matrix Graph for Test.....	50
Figure 5.7: Benchmarking Proposed Method Against Existing Papers	53
Figure 5.8: Performance Analysis: Metric Comparison across Training Testing Sets.	54
Figure 5.9: Evaluation of Jaccard Loss and Accuracy for the Model Architecture	54
Figure 5.10: Evaluation of DC and IoU for Proposed Model Architecture	55
Figure 5.11: Evaluation of precision and recall for Proposed Model Architecture	55
Figure 5.12: Sample classification predictions from the suggested model.....	56
Figure 5.13: Sample predictions from the segmentation model.....	56
Figure 5.14: Segmentation-Driven Skin Cancer Diagnosis Model.....	57

Figure 5.15: Performance Analysis: Metric Comparison across Brain Training Set....	58
Figure 5.16: Performance Analysis: Metric Comparison across Brain Testing Set....	59
Figure 5.17: Benchmarking Proposed Method Against Existing Papers.....	60
Figure 5.18 Sample prediction from the Brain segmentation model.....	60
Figure 5.19 Home for the website.....	61
Figure 5.20 Streamlit APP for skin cancer.....	62
Figure 5.21 Desktop APP.....	62
Figure 5.22 Streamlit APP for brain tumor.....	63

LIST OF TABLES

Table 2.1: Performance Analysis: Metric Comparison across Training and Testing.....	12
Table 2.2: Performance Analysis: Metric Comparison across data classes.....	15
Table 2.3: Synthesis and Comparison for two papers.....	17
Table 4.1: Hyperparameters for Skin Classification process.	38
Table 4.2: Hyperparameters for Skin Segmentation process.....	39
Table 4.3: Hyperparameters for Brain Segmentation process.....	41
Table 5.1: Class Distribution Analysis of the dataset.....	43
Table 5.2: Class Distribution after using the factor.....	44
Table 5.3: Performance Analysis: Metric Comparison across Training Algorithm....	47
Table 5.4: Performance Analysis: Metric Comparison across Testing Algorithms....	48
Table 5.5: Comparison between the proposed method and the other papers.....	52
Table 5.6: Performance Analysis: Metric Comparison across Training Testing Sets..	53
Table 5.7: Performance Analysis: Metric Comparison across Brain Training Set.....	58
Table 5.8: Performance Analysis: Metric Comparison across Brain Testing Set.....	58
Table 5.9: Comparison between the proposed method and the other papers.....	59

LIST OF ACRONYMS

ACRONYM	Definition of Acronym
CNN	Convolutional Neural Network
VGG	Visual Geometry Group
Resnet	Residual Network
IOU	Intersection over Union
Lr	Learning Rate
SSD-KD	Single Shot MultiBox Detector with Knowledge Distillation
Xception	Extreme Inception
SVM	Support Vector Machine

CHAPTER ONE

INTRODUCTION

1.1. Introduction

Skin cancer and brain tumors are two significant health concerns that affect millions of people worldwide. While they manifest in different parts of the body and have distinct characteristics, both present serious risks to health and well-being. Understanding their dangers and taking preventive measures is crucial. Furthermore, harnessing the power of artificial intelligence (AI) can play a pivotal role in early detection, treatment, and prevention strategies.

Skin cancer is one of the most common forms of cancer globally, with incidences rising steadily over the years. Excessive exposure to ultraviolet (UV) radiation from the sun or artificial sources like tanning beds is the primary cause of skin cancer. The three main types of skin cancer include basal cell carcinoma (BCC), squamous cell carcinoma (SCC), and melanoma, with melanoma being the most aggressive and potentially lethal form.

Brain tumors, while less common than skin cancer, pose significant risks due to their complex nature and location. These abnormal growths can arise from brain tissue or spread to the brain from other parts of the body. The symptoms of brain tumors vary widely depending on their size, location, and rate of growth. Common symptoms include headaches, seizures, cognitive impairment, and changes in behavior or personality.

Artificial intelligence (AI) has emerged as a powerful tool in the fight against cancer, including skin cancer and brain tumors. AI algorithms can analyze vast amounts of medical data, including images, pathology reports, and patient histories, to identify patterns and detect abnormalities that may indicate the presence of cancer. In the case of skin cancer, AI-powered dermatology tools can assist healthcare providers in the early detection of suspicious lesions by analyzing photographs and identifying features associated with malignancy. These tools can help prioritize high-risk cases for further evaluation and biopsy, potentially leading to earlier diagnosis and treatment. AI algorithms can analyze medical imaging scans, such as MRI and CT scans, to aid in the detection and characterization of brain tumors. By identifying subtle abnormalities and tracking changes over time, AI can help radiologists and oncologists make more accurate diagnoses and treatment recommendations.

1.1.1. Possible Beneficiaries

The innovative website and desktop application designed for skin cancer and brain tumor detection have the potential to benefit various stakeholders within the healthcare ecosystem. These beneficiaries encompass patients, healthcare providers, remote communities, healthcare systems, researchers, and educators. Patients can access the platform's convenience by uploading medical images for automated analysis, facilitating early detection and improving outcomes. Healthcare providers, including specialists in dermatology, oncology, neurology, and radiology, can use the platform as a diagnostic aid, supporting informed decision-making and enabling remote collaboration. Remote communities gain access to specialized care through the platform, overcoming geographical barriers. For healthcare systems, the platform offers streamlined workflows, reducing unnecessary referrals and optimizing resource allocation. Researchers and educators benefit from the anonymized data for advancing medical imaging research and educating future healthcare professionals. Overall, the platform presents a promising opportunity to enhance healthcare accessibility, efficiency, and innovation.

1.2. Research Motivations

The development of a website and desktop application for detecting skin cancer and brain tumors is fueled by various factors at the nexus of healthcare, technology, and societal welfare. These drivers guide the research with a multi-faceted approach:

Primarily, the endeavor aims to rectify healthcare disparities prevalent in regions lacking specialized services like dermatology and neurology, ensuring equitable access to diagnosis through a remote image analysis platform. Secondly, by facilitating early detection and intervention, the project seeks to mitigate delays caused by limited healthcare access, potentially saving lives and alleviating disease burden. Leveraging rapid advancements in AI and medical imaging, the research endeavors to pioneer innovative solutions, enhancing diagnostic accuracy and efficiency to shape the future of healthcare delivery. Additionally, empowering patients and healthcare providers is fundamental, achieved through user-friendly interfaces and automated analysis results, fostering active patient participation and facilitating collaboration between patients and providers.

Lastly, the project aspires to contribute to medical research and education by leveraging data to glean insights into disease dynamics and treatment outcomes. This effort not only advances various fields including dermatology, oncology, and neurology but also serves as a valuable educational resource, empowering future healthcare professionals in image interpretation and AI algorithm utilization, thus driving continued progress in healthcare.

1.3. Challenges and Solutions

The landscape of medical imaging analysis presents a myriad of challenges that hinder effective diagnosis and treatment of skin cancer and brain tumors. However, innovative solutions offer promising avenues to address these challenges and revolutionize healthcare delivery.

Challenge 1: Limited Accessibility to Specialized Healthcare Services

Many individuals, particularly those in remote or underserved areas, face significant barriers to accessing specialized healthcare services. Long wait times for appointments, geographic distance from healthcare facilities, and shortages of trained healthcare professionals exacerbate delays in diagnosis and treatment initiation.

Solution: Telemedicine and Remote Consultation

Telemedicine platforms offer a solution by enabling remote consultations between patients and healthcare providers. Through video conferencing and secure messaging, patients can connect with dermatologists, oncologists, and neurologists, regardless of their location. Telemedicine not only reduces the need for in-person visits but also facilitates timely access to expert medical advice, improving patient outcomes and satisfaction.

Challenge 2: Variability in Interpretation and Diagnosis

The subjective nature of visual assessment and manual interpretation of medical images introduce variability and inconsistency into the diagnostic process. Dermatologists and radiologists may differ in their interpretations, leading to discrepancies in diagnosis and treatment recommendations.

Solution: AI-Powered Image Analysis

Artificial intelligence (AI) algorithms offer a solution by automating the analysis of medical images and standardizing diagnostic practices. Machine learning algorithms can learn from vast datasets of annotated images to identify patterns and features indicative of skin cancer and brain tumors. By leveraging AI-powered image analysis, healthcare providers can achieve greater consistency and accuracy in diagnosis, ultimately improving patient care and outcomes.

Challenge 3: Logistical and Computational Constraints

The exponential growth of medical imaging data presents logistical and computational challenges for healthcare providers. Traditional methods of image analysis are time-consuming and labor-intensive, requiring significant resources and expertise.

Solution: Cloud-Based Image Analysis Platforms

Cloud-based image analysis platforms offer a solution by providing scalable and efficient solutions for processing and interpreting medical images. By leveraging the

computational power of the cloud, healthcare providers can analyze large volumes of imaging data in real-time, accelerating the diagnostic process and optimizing resource utilization. Furthermore, cloud-based platforms enable seamless collaboration and data sharing among healthcare professionals, enhancing efficiency and patient care.

Challenge 4: Privacy and Security Concerns

The collection and storage of sensitive patient data raise privacy and security concerns, particularly in the context of digital healthcare solutions. Healthcare organizations must adhere to strict regulations and standards to protect patient privacy and prevent unauthorized access to medical records.

Solution: Robust Data Encryption and Access Controls

Robust data encryption protocols and stringent access controls offer a solution to privacy and security concerns in medical imaging analysis. By implementing encryption algorithms and multi-factor authentication mechanisms, healthcare organizations can safeguard patient confidentiality and ensure compliance with regulatory requirements. Additionally, regular audits and security assessments can help identify and mitigate potential vulnerabilities, strengthening the overall security posture of digital healthcare platforms.

1.4. Problem Definition

The problem at hand is deeply rooted in the complexities of healthcare delivery and medical imaging analysis. One significant challenge is the global burden of skin cancer and brain tumors, which continue to pose significant health risks and economic burdens on healthcare systems worldwide. Despite advancements in medical technology and treatment modalities, the early detection and accurate diagnosis of these conditions remain paramount for effective management and improved patient outcomes.

Access to specialized healthcare services is a critical barrier faced by many individuals, particularly those living in remote or underserved areas. Limited availability of dermatologists, oncologists, and neurologists, coupled with geographic and socioeconomic disparities, often results in delays in diagnosis and treatment initiation. As a consequence, patients may experience progression of their conditions, leading to worse prognoses and reduced survival rates.

The subjective nature of visual assessment and the reliance on manual interpretation of medical images introduce inherent variability and subjectivity into the diagnostic process. Dermatologists and radiologists may differ in their interpretations of skin lesions or brain scans, leading to discrepancies in diagnosis and treatment recommendations. Standardizing and automating the analysis of medical images can help mitigate these challenges and ensure consistency and accuracy across diagnoses.

Furthermore, the exponential growth of medical imaging data presents logistical and computational challenges for healthcare providers. Traditional methods of image analysis and interpretation are time-consuming and labor-intensive, requiring significant resources and expertise. As the volume and complexity of medical imaging data continue to increase, there is a pressing need for efficient and scalable solutions to streamline the diagnostic process and alleviate the burden on healthcare systems.

Privacy and security concerns surrounding the collection and storage of sensitive patient data add another layer of complexity to the problem. Healthcare organizations must adhere to strict regulations and standards to protect patient privacy and prevent unauthorized access to medical records. Any digital solution aimed at improving medical imaging analysis must prioritize data security and implement robust measures to safeguard patient confidentiality and comply with regulatory requirements.

1.5. Research Objectives

The research into the creation of a website and desktop application for detecting skin cancer and brain tumors is driven by a comprehensive set of objectives aimed at advancing healthcare and technology. Firstly, the focus is on developing an innovative diagnostic platform, with user-friendly interfaces and advanced image analysis algorithms, seamlessly integrating with existing healthcare systems. Secondly, the aim is to improve diagnostic accuracy and efficiency through AI and machine learning, enabling timely intervention. Thirdly, the research targets equal access to specialized care by enabling remote image upload and analysis, transcending geographical barriers. Additionally, the objective includes fostering collaboration between patients and healthcare providers, enabling remote consultation and enhancing patient care. Furthermore, the research aims to contribute to medical research and education by collecting anonymized data, driving innovations in medical imaging analysis and training future professionals. Lastly, ensuring data privacy and security is prioritized to build trust and encourage widespread adoption of the platform.

1.6. Benefits and Drawbacks

The development of the website and desktop application for skin cancer and brain tumor detection offers a range of potential benefits and drawbacks, each of which warrants careful consideration.

1.6.1. Benefits:

1.6.1.1. Enhanced Accessibility: One of the primary benefits of the platform is its ability to enhance accessibility to advanced diagnostic tools. By enabling users to upload medical images remotely, the platform has access to specialized healthcare services, particularly in underserved communities with limited access to dermatologists, oncologists, and neurologists.

1.6.1.2. Early Detection and Intervention: The platform facilitates early detection and intervention by providing users with automated analysis results in a timely manner. By leveraging advanced algorithms for image analysis, the platform enhances diagnostic accuracy and efficiency, potentially leading to earlier detection of skin cancer and brain tumors and improved patient outcomes.

1.6.1.3. Empowerment of Patients and Healthcare Providers: The platform empowers patients to take an active role in their healthcare journey by providing them with access to their medical images and analysis results. Additionally, the platform facilitates collaboration and communication between patients and healthcare providers, enabling remote consultation and collaborative decision-making.

1.6.1.4. Contribution to Medical Research and Education: The anonymized data collected through the platform has the potential to contribute valuable insights to medical research and education. Researchers can leverage the rich dataset to gain a deeper understanding of disease prevalence, progression, and treatment outcomes, while educators can utilize the platform as a teaching tool to train future generations of healthcare professionals.

1.6.2. Drawbacks:

1.6.2.1. Dependence on Technology: One of the primary drawbacks of the platform is its dependence on technology. Users must have access to an internet connection and a device capable of uploading medical images, which may pose challenges for individuals in remote or underserved areas with limited access to technology.

1.6.2.2. Potential for Misdiagnosis: While the platform aims to enhance diagnostic accuracy through the use of advanced algorithms, there is always the potential for misdiagnosis. Automated analysis results should be interpreted with caution and validated by healthcare professionals to ensure accurate diagnosis and appropriate treatment.

1.6.2.3. Privacy and Security Concerns: The collection and storage of medical images raise privacy and security concerns regarding the confidentiality and integrity of user data. It is essential to implement robust encryption protocols and stringent access controls to safeguard sensitive medical information and ensure compliance with regulatory standards.

1.6.2.4. Limited Scope of Application: The platform is designed specifically for the detection and analysis of skin cancer and brain tumors and may have limited applicability to other medical conditions. While the platform addresses critical healthcare needs, its scope may be limited for individuals seeking diagnosis or treatment for other medical conditions.

1.7. Original Key Contribution

The original key contribution of the website and desktop application for skin cancer and brain tumor detection lies in its innovative approach to accessing advanced diagnostic tools while leveraging cutting-edge technology to enhance diagnostic accuracy, efficiency, and high accuracy.

1.7.1. Features:

1.7.1.1. Seamless Image Upload: The platform offers a seamless and user-friendly interface for uploading medical images, allowing users to easily submit dermoscopic images of skin lesions or MRI scans of brain tumors. The intuitive design streamlines the process, ensuring accessibility for users of all technical proficiencies.

1.7.1.2. Advanced Algorithmic Analysis: Leveraging state-of-the-art artificial intelligence and machine learning algorithms, the platform conducts advanced analysis of uploaded images. These algorithms are trained on extensive datasets to identify patterns, features, and abnormalities indicative of skin cancer or brain tumors with high accuracy.

1.7.1.3. Automated Diagnosis: One of the standout features of the platform is its ability to provide automated diagnosis results based on the analysis of uploaded images. Users receive instant feedback on the presence of suspicious lesions or tumors, empowering them with timely information to seek further evaluation and treatment from healthcare professionals.

1.7.2. Explain the Way:

1.7.2.1. The website and desktop application revolutionize medical imaging analysis by seamlessly integrating user-friendly interfaces, advanced algorithms, and remote consultation options. Here's how it works:

1.7.2.2. User Experience: Upon accessing the platform, users are guided through a straightforward process to upload their medical images securely. The interface is designed with simplicity and intuitiveness in mind, ensuring accessibility for users of varying technical backgrounds.

1.7.2.3. Algorithmic Analysis: Once the images are uploaded, the platform employs advanced artificial intelligence and machine learning algorithms to analyze the images comprehensively. These algorithms are trained on vast datasets of annotated images, enabling them to identify subtle patterns and features indicative of skin cancer or brain tumors with remarkable accuracy.

1.7.2.4. Automated Diagnosis: Based on the analysis results, the platform provides users with instant feedback on the presence of suspicious lesions or tumors. This automated

diagnosis empowers users with timely information, enabling them to take proactive steps towards further evaluation and treatment.

1.8. Research Organization

This book consists of five chapters:

- Chapter two includes a review of the Literature Survey and related work, as well as research that clarifies change occurrences.
- Chapter three explains System Analysis and Design, which includes all of your system architecture and requirements, such as user requirements.
- Chapter four introduces the proposed system and describes in detail how each aspect of the project was completed.
- Chapter five introduces results and discussion.

CHAPTER TWO

RELATED WORK

2.1. Introduction

Recent advances in medical imaging, particularly in dermatology and neurology, have transformed lesion detection and classification through the integration of artificial intelligence (AI), specifically deep learning. Dermoscopic images are analyzed using deep learning algorithms to accurately segment and classify skin lesions, aiding in early detection of conditions like skin cancer. Similarly, deep learning techniques applied to magnetic resonance imaging (MRI) scans enable precise segmentation and characterization of brain lesions, essential for treatment planning and disease monitoring. This review explores these advancements, analyzing methodologies, findings, and implications to inform future research and improve the diagnosis and management of skin and brain disorders.

2.2. Scientific Background

2.2.1. Machine Learning in Classification:

Machine learning techniques have played a pivotal role in the classification of medical images, including those related to skin lesions and brain abnormalities. Traditional machine learning algorithms, such as support vector machines (SVM) [21] and decision trees, have been employed for feature extraction and classification based on handcrafted features. While effective in certain scenarios, these methods often rely on domain-specific expertise and may struggle to capture complex patterns present in medical images.

2.2.2. Convolutional Neural Networks (CNN):

Convolutional Neural Networks (CNNs) have emerged as a dominant paradigm in medical image analysis, revolutionizing both classification and segmentation tasks. CNNs are designed to automatically learn hierarchical representations of data, making them well-suited for processing complex and high-dimensional images. In the context of skin lesion classification [3, 12, and 17], CNNs have demonstrated remarkable accuracy in distinguishing between different types of lesions, leveraging features learned directly from raw image data.

Moreover, CNNs have also been employed for segmentation tasks, wherein the goal is to delineate regions of interest within medical images. Segmentation plays a crucial role in quantifying the extent and location of abnormalities, facilitating treatment planning, and monitoring disease progression. CNN-based segmentation approaches have shown promising results in various medical imaging modalities, including magnetic resonance imaging (MRI) and dermoscopy.

2.2.3. U-Net for Segmentation:

UNet, a convolutional neural network architecture, has gained widespread popularity for its effectiveness in semantic segmentation tasks, particularly in biomedical image analysis. The UNet architecture consists of a contracting path, which captures context and extracts features, followed by an expansive path, which enables precise localization through upsampling and concatenation of feature maps.

In medical image segmentation, UNet has been successfully applied to delineate anatomical structures, detect lesions, and segment regions of interest. Its ability to capture both local details and global context makes it particularly well-suited for tasks requiring precise delineation of boundaries and regions with intricate features.

In the context of skin lesion segmentation, UNet has shown promise in accurately delineating lesion boundaries and differentiating between lesions and surrounding healthy tissue [5 and 21]. Similarly, in brain imaging, UNet-based approaches have facilitated the segmentation of tumors, white matter, and other brain structures with high accuracy and efficiency.

2.2.4. Transfer Learning in Medical Image Analysis:

Transfer learning, a technique in machine learning where a model trained on one task is adapted for use on a different, but related task, has also found application in medical image analysis. In the context of convolutional neural networks (CNNs), transfer learning involves leveraging pre-trained models, often trained on large-scale image datasets like ImageNet, and fine-tuning them on medical image datasets for specific tasks such as classification and segmentation.

Transfer learning offers several advantages in medical image analysis. Firstly, it mitigates the need for large annotated medical image datasets, which are often scarce and time-consuming to acquire. By starting with a pre-trained model, practitioners can benefit from the general features learned during the initial training on a large dataset, and then fine-tune the model on their specific medical imaging data, which typically involves smaller datasets. This approach helps in achieving better generalization and performance on the medical image task at hand.

Moreover, transfer learning can expedite the development and deployment of deep learning models in medical imaging, as it reduces the computational resources and time required for training from scratch. Additionally, fine-tuning pre-trained models allows practitioners to capitalize on the wealth of research and advancements in deep learning for computer vision tasks, adapting these advancements to the domain of medical image analysis.

Several pre-trained CNN architectures, such as ResNet, VGG, and Inception, have been successfully applied in medical image analysis through transfer learning:

- ResNet: Residual Networks (ResNet) [20] introduce skip connections that allow gradients to flow more directly during training, mitigating the vanishing gradient problem. This architecture enables the training of very deep networks (hundreds of layers) efficiently. In medical image analysis, ResNet has been utilized for tasks such as lesion classification and segmentation, leveraging its ability to capture intricate features within the data hierarchy.
- VGG: The VGG (Visual Geometry Group) [1 and 16] network architecture is characterized by its simplicity and uniformity, consisting of repeated blocks of convolutional layers followed by max-pooling layers. VGG networks are known for their excellent generalization ability and have been widely adopted in various computer vision tasks. In medical image analysis, VGG networks have been employed for tasks such as brain tumor detection and skin lesion classification, demonstrating strong performance.
- Inception: The Inception architecture, particularly InceptionV3 and InceptionResNetV2 [8] introduces the concept of inception modules, which consist of parallel convolutional operations with different filter sizes. This allows the network to capture features at multiple scales efficiently. In medical image analysis, Inception networks have been utilized for tasks such as lung nodule detection and diabetic retinopathy diagnosis, showcasing their effectiveness in extracting relevant features from complex medical images.

By fine-tuning pre-trained ResNet, VGG, and Inception models on medical image datasets, researchers and clinicians can leverage their respective strengths in capturing features and hierarchies within the data, further enhancing the performance of deep learning models in medical image analysis tasks.

Overall, The integration of machine learning techniques, particularly deep learning paradigms, into medical image analysis continues to drive advancements in diagnostic accuracy and patient care. Future research directions include exploring novel architectures, optimizing model interpretability, and addressing challenges related to data scarcity and model robustness. By leveraging these advancements, the field of medical image analysis is poised for further innovation and impact in healthcare.

2.3. Literal Review

2.3.1. Comparative Study on Different Deep Learning Models for Skin Lesion Classification Using Transfer Learning Approach, January 2021:

2.3.1.1. introduction

The first research paper [1] delves into the domain of skin lesion classification using deep learning models, specifically focusing on a comparative study of different transfer

learning approaches. The paper addresses the critical need for early detection of skin cancer, particularly in regions with limited access to healthcare facilities.

The primary objective of the research paper is to identify the most effective deep learning model for skin lesion classification by comparing various pre-trained models using transfer learning techniques. The study employs a diverse dataset comprising different categories of skin diseases, including Actinic Keratosis, Vascular Lesions, Lentigo, Melanoma, and Dermatofibroma. The chosen pre-trained models include VGG19, Xception, DenseNet, Inception, MobileNet, NasNetMobile, and ResNet, all renowned for their efficacy in image classification tasks.

Through rigorous experimentation and performance evaluation, the research paper concludes that transfer learning methods significantly enhance the efficiency and accuracy of skin lesion classification models. Among the pre-trained models evaluated, DenseNet201 emerges as the top performer, achieving remarkable accuracy and demonstrating practical utility in real-world applications, as shown in table 2.1 and figures 2.1 and 2.2. The deployment of the DenseNet201 model on a web platform underscores its potential for facilitating accessible and efficient skin lesion analysis, particularly in resource-constrained settings.

2.3.1.2. Results

Table 2.1: Performance Analysis: Metric Comparison across Training and Testing.

	Train			Test		
	Precision	Recall	F1	Precision	Recall	F1
DenseNet201	96.9	95.5	96	90.1	86.4	87.8
MobileNetV2	97.0	95.2	95.9	83.2	77.1	79.6
InceptionResNetV2	95.9	94.9	95.3	82.9	78.0	79.6
MobileNet	96.1	93.8	94.7	78.5	75.4	76.0
Xception	96.2	94.0	94.0	74.0	71.2	72.0
NASNetMobile	92.3	90.2	91.0	79.0	72.9	75.0
InceptionV3	91.7	89.6	90.2	79.0	77.1	77.05
VGG19	77.4	68.2	67.0	69.2	65.3	61.5

Training Metrics Scores

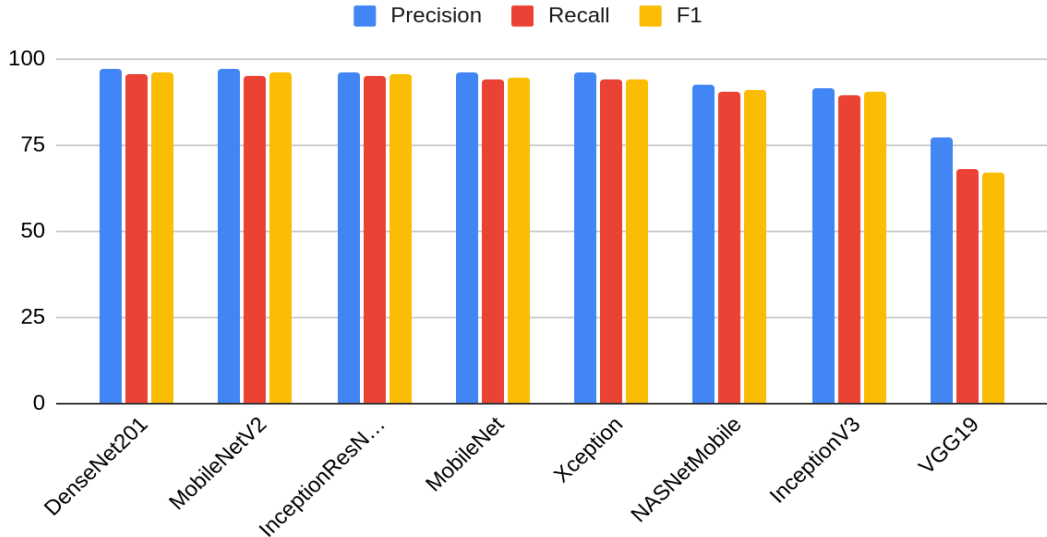


Figure 2.1: Performance Analysis: Metric Comparison across Training Algorithms.

Testing Metrics Scores

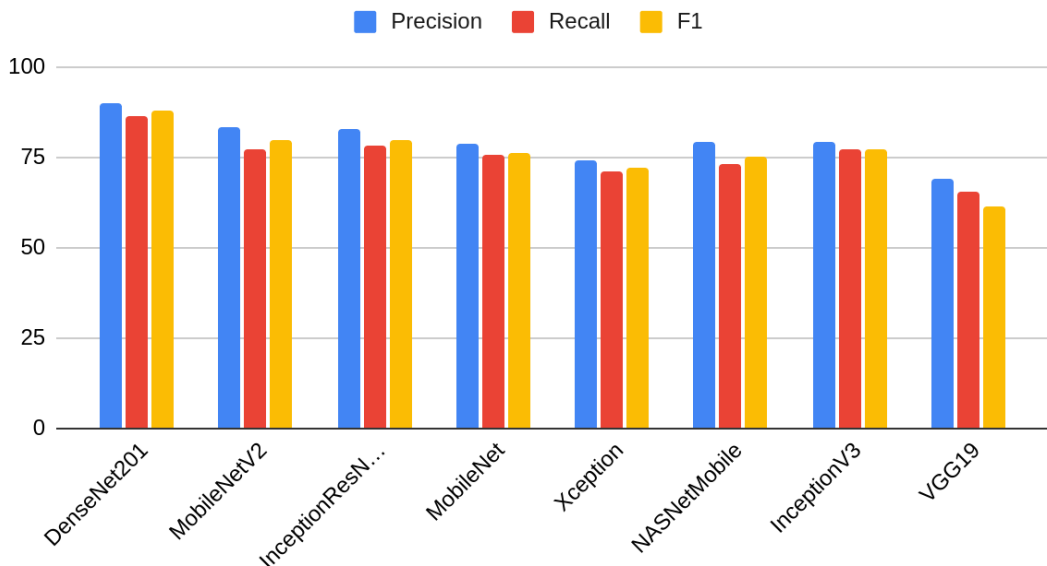


Figure 2.2: Performance Analysis: Metric Comparison across Testing Algorithms.

2.3.1.3. Strengths

- Comprehensive Dataset: The study utilizes a diverse dataset encompassing various categories of skin lesions, providing a comprehensive representation of pathological conditions encountered in clinical practice. This ensures robust model training and evaluation across a spectrum of skin diseases.
- Utilization of State-of-the-Art Models: Leveraging advanced deep learning architectures such as Xception, DenseNet201, ResNet, and others allows for sophisticated feature extraction and classification.

- Performance Evaluation Metrics: The study employs a wide range of performance metrics, including accuracy, precision, recall, and advanced measures like F-measure and G-mean. This thorough evaluation provides nuanced insights into model performance, enabling a comprehensive assessment of classifier effectiveness.
- Transfer Learning Approach: By adopting transfer learning techniques, the study capitalizes on pre-trained models' knowledge, thereby reducing the need for extensive labeled data and expediting the training process. Transfer learning has been shown to enhance model generalization and efficiency, particularly in medical image analysis tasks.
- Practical Deployment: The deployment of the DenseNet201 model on a web platform demonstrates the practical utility of the developed system for skin lesion analysis. This highlights the translational potential of the research findings, facilitating accessible and efficient skin cancer detection.

2.3.1.4. Limitations

- Dataset Imbalance: The dataset may suffer from class imbalance, wherein certain skin lesion categories are underrepresented compared to others. This imbalance can skew model performance evaluation, leading to biased results, especially for minority classes.
- Generalization to Diverse Populations: The study's findings and model performance may be influenced by the dataset's demographic characteristics, potentially limiting generalizability to populations with different skin types or geographical regions. External validation on diverse datasets is necessary to assess model robustness across varied demographics.
- Interpretability and Explainability: Deep learning models, while effective in classification tasks, often lack interpretability and explainability, making it challenging to understand the rationale behind specific predictions. This hinders the clinical adoption of the models, as healthcare practitioners may require transparent decision-making processes.
- Resource Intensiveness: Training and deploying deep learning models, particularly those with complex architectures like DenseNet201, can be resource-intensive in terms of computational power and time. This may pose practical challenges, especially in resource-constrained settings where access to high-performance computing infrastructure is limited.
- Evaluation Metrics Limitations: While the study employs a comprehensive set of performance metrics, certain metrics like accuracy may not adequately capture model performance, especially in the presence of class imbalance.

2.3.2. Multi-Class Skin Lesion Classification Using a Lightweight Dynamic Kernel Deep-Learning-Based Convolutional Neural Network, August 2022:

2.3.2.1. introduction

The second research paper [2] presents a novel approach to multi-class skin lesion classification using a lightweight dynamic kernel deep-learning-based convolutional neural network (CNN). The paper addresses the imperative for accurate and timely diagnosis of skin diseases, emphasizing the role of automated classification systems in improving diagnostic precision and healthcare outcomes. Through the integration of dynamic-sized kernels and activation functions, the research aims to develop a highly efficient and effective model for skin lesion classification.

The primary objective of the research paper is to propose a lightweight CNN architecture capable of accurately classifying skin lesions across multiple diagnostic categories. The model architecture incorporates dynamic-sized kernels and employs both ReLU and leakyReLU activation functions to extract discriminative features from dermoscopic images. The study evaluates the proposed approach on the HAM10000 dataset, a widely used benchmark dataset in dermatology, through extensive experimentation and performance analysis.

The research paper demonstrates the effectiveness of the proposed approach in achieving impressive overall accuracy on the HAM10000 dataset, surpassing several existing state-of-the-art models while maintaining computational efficiency. By leveraging dynamic-sized kernels and activation functions, the model achieves superior performance in multi-class skin lesion classification, offering promising prospects for real-world applications in dermatology. The study emphasizes the significance of robust evaluation metrics and data preprocessing techniques in developing CAD systems for medical image analysis, as shown in table 2.2.

2.3.2.2. Results

Table 2.2: Performance Analysis: Metric Comparison across data classes.

Label	ACC	PRE	REC	F1-Score
nv	0.87	1.00	0.87	0.93
mel	0.98	0.94	1.00	0.97
bkl	0.99	0.94	0.99	0.97
bcc	1.00	0.99	1.00	0.99
akiec	1.00	1.00	1.00	1.00
vasc	1.00	1.00	1.00	1.00
df	1.00	1.00	1.00	1.00
Average	0.978	0.981	0.98	0.98

2.3.2.3. Strengths

- High Accuracy: The proposed model achieves an impressive overall accuracy of 97.85% on the HAM10000 dataset, indicating its efficacy in accurately classifying skin lesions from dermoscopic images.

- Efficient Architecture: Leveraging a lightweight architecture, the model demonstrates computational efficiency without compromising performance, making it suitable for real-world applications where computational resources may be limited.
- Dynamic Kernel Integration: Incorporating dynamic-sized kernels enables the model to adaptively adjust the receptive field size based on the spatial context of input images, enhancing its ability to capture multi-scale features and discriminate between different types of skin lesions.
- Effective Feature Extraction: By integrating both ReLU and leakyReLU activation functions, the model enhances feature representation and facilitates more effective learning of complex patterns within the data, contributing to its high classification accuracy.
- Comprehensive Evaluation: The methodology employs a suite of evaluation metrics, including accuracy, precision, recall, F1 score, and confusion matrix analysis, providing a thorough assessment of the model's performance across different classes of skin lesions.

2.3.2.4. Limitations

- Imbalanced Dataset: Despite employing data balancing techniques, the HAM10000 dataset exhibits imbalanced class distributions, which may lead to biased predictions and suboptimal performance, particularly in minority classes with fewer instances.
- Generalization to External Datasets: While achieving high accuracy on the HAM10000 dataset, the model's performance on unseen external datasets remains to be evaluated. Generalization to diverse datasets with varying imaging conditions and lesion characteristics is essential to assess its robustness in real-world clinical settings.
- Interpretability: Deep learning models, including the proposed CNN architecture, often lack interpretability, making it challenging to understand the underlying rationale behind classification decisions. Interpretable models or visualization techniques may be required to enhance the model's transparency and facilitate clinical decision-making.
- Computational Resource Requirements: While the model exhibits computational efficiency compared to more complex architectures, training and inference may still require significant computational resources, limiting its accessibility in resource-constrained environments, such as low-resource healthcare settings.

2.4. Synthesis and Comparison:

Table 2.3: Synthesis and Comparison for two papers

Aspect	Research Paper 1	Research Paper 2
Common Themes	Both papers aim to advance skin lesion classification using deep learning, emphasizing early and accurate diagnosis. They utilize transfer learning and innovative architectures.	Both papers highlight the importance of automated classification systems in dermatology, focusing on improving diagnostic precision. They employ transfer learning and novel CNN architecture.
Methodological Comparison	Research Paper 1 conducts a comparative study of pre-trained models on a diverse dataset for performance evaluation.	Research Paper 2 proposes a novel CNN architecture with dynamic-sized kernels, emphasizing computational efficiency and multi-class classification.
Findings and Conclusions	Research Paper 1 identifies DenseNet201 as a top performer, showcasing practical utility.	Research Paper 2 introduces a lightweight CNN architecture that surpasses existing models in accuracy and efficiency.
Strengths and Limitations	Research Paper 1 offers comprehensive model comparison and practical deployment insights. Acknowledges dataset limitations.	Research Paper 2 innovates with lightweight CNN architecture but requires further validation in clinical settings.
Overall Comparison	Both papers contribute significantly to skin lesion classification but via different approaches.	Research Paper 1 emphasizes model comparison and practical deployment, while Research Paper 2 introduces a novel CNN architecture with enhanced feature representation.
Future Directions	Both studies highlight the need for addressing dataset limitations and validating findings in clinical settings.	Future research should focus on refining models, validating in clinical settings, and utilizing larger, diverse datasets to improve skin lesion classification further.

2.5. Implications and Future Directions:

2.5.1. Implications of Collective Findings: The collective findings of both research papers underscore the significance of deep learning in revolutionizing skin lesion classification. The development of accurate and efficient classification models holds profound implications for dermatology, facilitating early detection, diagnosis, and treatment of various skin conditions, including potentially life-threatening diseases like melanoma. Moreover, the practical deployment of these models, as demonstrated in Research Paper 1, has the potential to extend access to timely healthcare interventions, particularly in underserved regions with limited medical resources.

2.5.2. Contributions to Existing Knowledge: By synthesizing the findings of both papers, we contribute to the existing knowledge on skin lesion classification methodologies and their applications. Research Paper 1 enriches our understanding of the performance characteristics of different pre-trained models and highlights the effectiveness of transfer learning in medical image analysis. On the other hand, Research Paper 2 introduces a novel CNN architecture, expanding the repertoire of model architectures optimized for skin lesion classification. Together, these contributions pave the way for continued advancements in automated dermatological diagnosis and inform the development of more accurate and efficient classification systems.

2.5.3. Identified Areas for Further Research: Despite the advancements presented in the two research papers, several areas warrant further investigation to address existing challenges and enhance the practical applicability of skin lesion classification models. Future research efforts could focus on:

Dataset Diversity and Generalization: Expanding the diversity of datasets used for model training and validation.

Real-world Validation and Clinical Integration: Conducting rigorous validation studies in clinical settings to evaluate the performance of classification models in real-world scenarios and assess their impact on clinical decision-making processes and patient outcomes.

Interpretability and Explainability: Enhancing the interpretability and explainability of classification models to facilitate trust and acceptance among healthcare providers, patients, and regulatory bodies. Methods for interpreting model predictions and generating clinically actionable insights should be explored further.

2.6. Conclusion:

In this literature survey, we explored advancements in skin lesion classification using deep learning through two key research papers. The first paper examined transfer learning's effectiveness in classifying skin lesions, emphasizing its practical application in resource-limited settings. The second paper introduced a dynamic kernel CNN architecture tailored for efficient multi-class classification, emphasizing model interpretability and scalability in healthcare AI. Both studies underscored the importance of diverse datasets, interpretable models, and ethical considerations in AI-driven healthcare. They contribute to improving automated dermatological diagnosis, with implications for early detection and personalized treatment. However, addressing challenges and ensuring equitable AI integration requires collaboration across disciplines and a commitment to ethical principles.

Chapter Three

SYSTEM ANALYSIS & DESIGN

3.1. Introduction

System Analysis and Design (SAD) is a foundational discipline in the realm of information technology and software engineering. It serves as the initial phase in the development lifecycle of information systems, encompassing activities such as requirements gathering, feasibility analysis, and system specification. During the analysis phase, SAD professionals work closely with stakeholders to understand their needs, objectives, and constraints. This involves conducting interviews, surveys, and workshops to elicit requirements and gain insights into existing processes. Subsequently, in the design phase, SAD focuses on translating these requirements into a conceptual blueprint for the system. This includes defining system architecture, data models, user interfaces, and interaction flows. By meticulously analyzing and designing systems, SAD lays the groundwork for the successful implementation and deployment of information systems that effectively meet organizational needs.

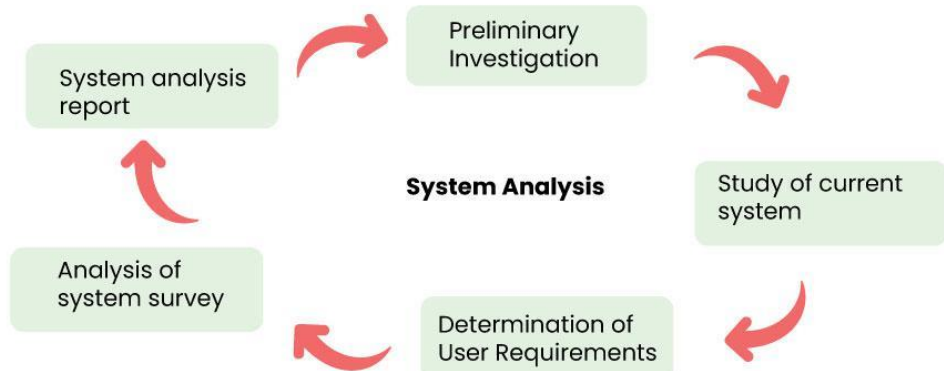


Figure 3.1: system analysis

System analysis and design are critical for assuring the efficiency and effectiveness of information systems. SAD professionals use systematic analysis to find opportunities for process improvement and optimization inside enterprises. Understanding corporate processes and workflows allows SAD to streamline operations, reduce redundancies, and increase efficiency. Furthermore, SAD promotes the identification and integration of emerging technologies and best practices, allowing firms to remain at the forefront of innovation. By developing systems that are in line with corporate objectives and technology capabilities, SAD ensures that businesses may use information systems as strategic assets to promote growth and competitive advantage. In essence, system analysis and design provide a framework for companies looking to leverage the power of technology to achieve their goals and objectives.

3.2. The Role of System Analysis and Design

System Analysis and Design (SAD) is crucial in IT and software engineering, involving understanding, designing, and implementing information systems. Here's why it's important:

3.2.1. Requirement Understanding: SAD gathers and analyzes stakeholder requirements to align the developed system with user needs, business processes, and organizational goals.

3.2.2. Efficient Design: SAD enables the design of efficient systems by defining architecture, data models, and user interfaces for optimal performance and usability.

3.2.3. Cost Reduction: Proper analysis and design upfront lead to long-term cost savings by avoiding rework and modifications later.

3.2.4. Risk Management: SAD assesses and mitigates risks like security vulnerabilities and scalability issues, ensuring system reliability and security.

3.2.5. Improved Communication: SAD facilitates clear communication between stakeholders, developers, and users through workshops, prototyping, and documentation.

3.2.6. Quality Assurance: SAD emphasizes quality by defining clear requirements, designing robust architectures, and conducting thorough testing.

3.2.7. Adaptability and Scalability: Systems designed with SAD principles are adaptable and scalable, accommodating future growth and changing requirements.

3.2.8. Competitive Advantage: Well-designed systems from SAD streamline processes, enhance efficiency, and foster innovation, providing organizations with a competitive edge.

3.3. The context diagram

The context diagram, also known as a system context diagram or level 0 DFD (Data Flow Diagram), is a high-level visual representation that illustrates the scope and boundaries of a system and its interactions with external entities. It provides a broad overview of the system, showing its relationships with external entities without delving into the internal workings or details of the system.

The main components of a context diagram:

3.3.1. System: Represents the subject of analysis or design, like a software app or business process.

3.3.2. External Entities: Interact with the system, like users, systems, databases, or sensors.

3.3.3. Data Flows: Arrows showing data movement between the system and external entities, indicating inputs and outputs.

A context diagram gives a brief, clear snapshot of a system and its surroundings. It helps stakeholders grasp the system's function and its interactions. It's a vital tool in early system analysis, fostering shared understanding among stakeholders about the system's scope. Typically, it precedes more detailed diagrams like level 1 DFDs, which delve into specific processes and data flows.

Users interact with the platform by uploading a variety of images, ranging from X-rays and scans to standard jpg images. These images, along with accompanying details provided by the users, are then processed by the website, utilizing advanced analysis techniques to identify potential indications of cancer. The results presented to users following this analysis offer valuable insights, potentially including detailed reports specifying the type of cancer suspected or providing additional pertinent information crucial for understanding their health condition.

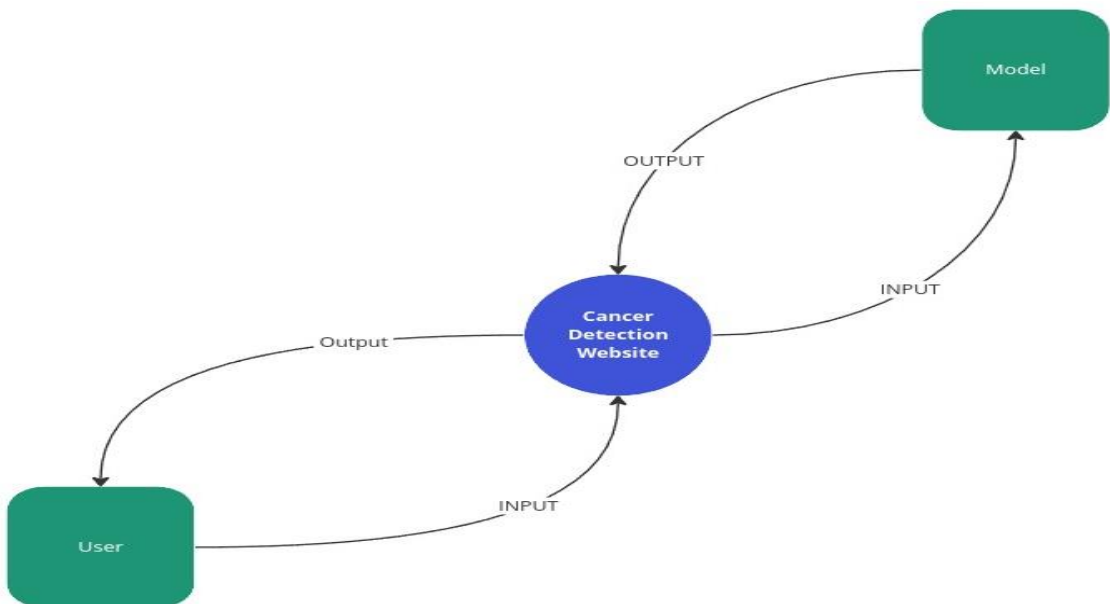


Figure 3.2: Context Diagram.

3.4. The class diagram

The class diagram is one of the most widely used modeling techniques in object-oriented software development. It's a static structural diagram that represents the structure of a system by showing the classes of the system, their attributes, methods, and the relationships between them.

The main components of a class diagram:

3.4.1. Class: Blueprint for object creation, featuring properties (attributes) and behaviors (methods). Depicted as rectangles with sections for name, attributes, and methods.

3.4.2. Attributes: Data elements describing the state of a class, depicted as name:type pairs within class rectangles.

3.4.3. Methods: Define class behaviors and interactions, depicted as name(parameters):returnType within class rectangles.

3.4.4. Relationships: Relationships between classes describe how classes are connected or associated with each other. There are several types of relationships in class diagrams:

- Association: Bi-directional connection between classes, indicated by lines with optional multiplicity.
- Aggregation: "Whole-part" relationship, shown as a line with a diamond on the containing class end.
- Composition: Stronger version of aggregation, parts cannot exist independently, depicted with a filled diamond.
- Inheritance: "Is-a" relationship, subclass inherits attributes and methods from superclass, shown with a line and hollow arrowhead.

3.4.5. Multiplicity: Indicates instances related in an association, represented as a range or specific values.

Class diagrams are valuable tools for designing and documenting the structure of object-oriented systems. They help developers visualize the relationships between classes, understand the system's architecture, and communicate design decisions to stakeholders.

The "User" class serves as a representation of the system's users, storing essential credentials necessary for logging into the system. These credentials include the UserID, serving as the primary key for user identification, along with UserName, Email, and Password fields. These details collectively enable seamless access and interaction within the system.

On the other hand, the "Image" class encapsulates the medical images uploaded by users, crucial for brain cancer prediction. Each image instance is characterized by attributes such as ImageID, functioning as the primary key for image identification, as well as details like Type (e.g., MRI), Upload Time, and ImagePath, providing pertinent information about the image's origin and storage location.

Further, the system implements distinct prediction models for skin and brain cancer, represented by the "SkinPrediction" and "BrainPrediction" classes, respectively. These classes house attributes specific to each prediction, including PredictionID for unique identification, ImageID as a foreign key linking predictions to their corresponding images, Prediction (providing textual descriptions such as "malignant" or "benign"), and Confidence, denoting the level of certainty associated with the prediction.

Establishing the relationships between these classes, a one-to-many relationship exists between "User" and "Image," allowing a single user to upload multiple images while ensuring each image is associated with only one user. Similarly, a one-to-many relationship is between "Image" and both "SkinPrediction" and "BrainPrediction," facilitating the association of multiple predictions with a single image while maintaining the integrity of each prediction's linkage to its respective image.

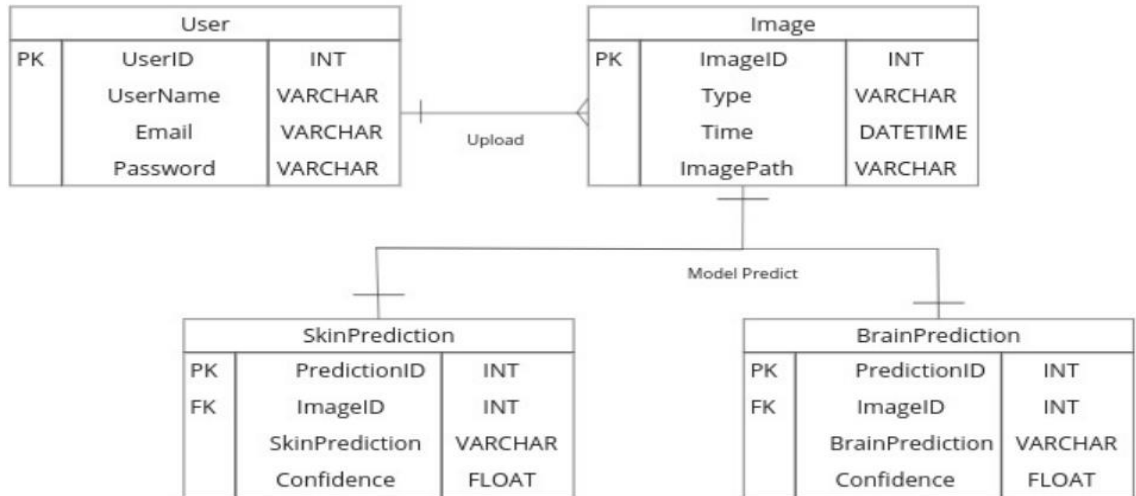


Figure 3.3: Class Diagram.

3.5. An Entity-Relationship Diagram (ERD)

An Entity-Relationship Diagram (ERD) is a visual representation used to model the data or information within a system or organization. ERDs are particularly useful in database design as they illustrate the relationships between different entities or data objects and the attributes associated with each entity.

The main components of an ERD:

3.5.1. Entities: Represent main database objects, like Student or Course. Attributes describe entity properties, like StudentID or Name.

3.5.2. Attributes: Characteristics of entities, depicted as ovals. For example, Student attributes could include StudentID, Name, and DateOfBirth.

3.5.3. Relationships: Show connections between entities. Depicted as lines with verb phrase labels. For instance, "Enrolls In" between Student and Course.

3.5.4. Cardinality: Defines how many instances of one entity can link to another. Represented as symbols like "1" for one, "M" for many. Example: "1:N" between Student and Course.

3.5.5. Primary Keys and Foreign Keys: Primary keys uniquely identify records, shown by underlining attributes. Foreign keys establish relationships by referencing primary keys of other entities, shown with dashed lines.

The "User" entity embodies the representation of the system's users, encompassing essential attributes vital for user identification and interaction within the system. These attributes include UserID, serving as the primary key for user identification, along with Name, Email, and Password, facilitating seamless authentication and user management processes.

The "Image" entity stands as a representation of the medical images contributed by users for brain cancer prediction. This entity captures pertinent details associated with each uploaded image, including ImageID, serving as the primary key for image identification, Path denoting the file path where the image is stored, Time indicating the date and time of image upload, and Type specifying the nature of the image (e.g., MRI).

The process, the "Prediction" entity likely signifies the outcome of brain cancer predictions generated by the system's analysis. It incorporates attributes such as PredictionID for unique identification, ImageID as a foreign key linking predictions to their respective images, Confidence representing the system's confidence level in its prediction (a numerical value ranging between 0 and 1), BrainPrediction providing a textual description of the brain tissue prediction (e.g., "malignant" or "benign"), and SkinPrediction offering a textual description of the skin tissue prediction (e.g., "NV" or "BCC").

Regarding their relationships, "User" and "Image" have a one-to-many relationship, allowing a single user to upload multiple images while ensuring that each image is associated with only one user. Furthermore, a one-to-one relationship is between "Image" and "Prediction," indicating that each image has a unique prediction associated with it, and that each prediction is derived from one image, ensuring a direct linkage between the two entities for accurate analysis and interpretation.

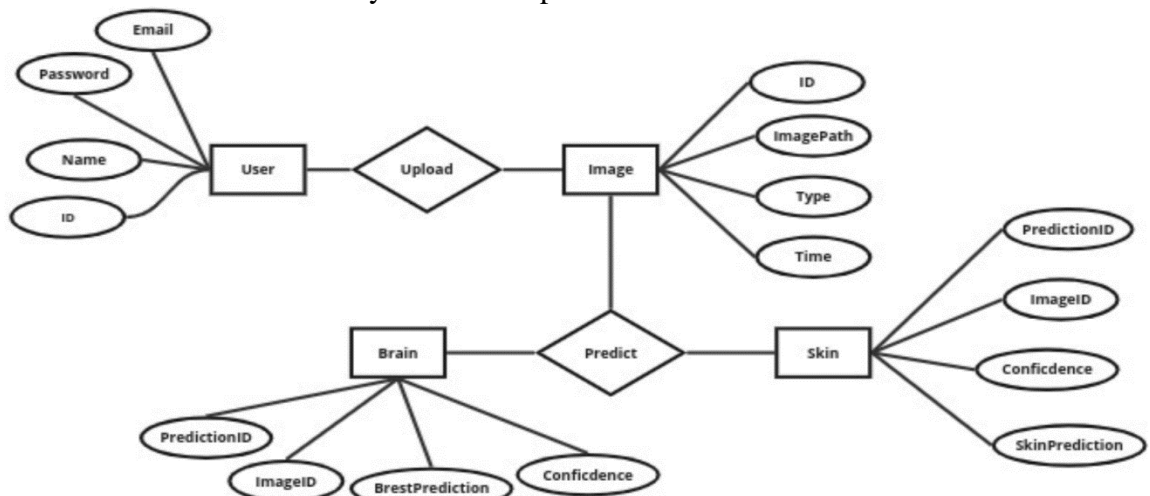


Figure 3.4: ERD.

3.6. State Chart:

A State Chart, also known as a State Machine Diagram, is a visual representation used to model the behavior of a system or an object over time. It illustrates the various states that an object can be in and the transitions between those states in response to events or actions.

The main components of a State Chart:

3.6.1. State: A state signifies the condition of an object/system at a specific time. Represented by rounded rectangles with names (e.g., "Idle," "Waiting for Coin").

3.6.2. Transition: A transition denotes a state change triggered by an event/action. It's shown as arrows between states, labeled with the triggering event (e.g., transition from "Idle" to "Waiting for Coin" triggered by "Insert Coin").

3.6.3. Event: An event initiates state transitions. It can be an external input, internal condition, or user/system action, depicted near triggering transitions.

3.6.4. Actions: Actions are tasks executed during transitions, representing system behavior (e.g., computations, outputs).

3.6.5. Initial State: The starting point of the State Chart, indicated by an arrow from outside the diagram.

3.6.6. Final State: The endpoint of the State Chart, depicted as a rounded rectangle with concentric circles, usually labeled "End" or "Final."

The process begins with the "Uploaded Image" state, wherein a user uploads an image into the system, initiating the cancer prediction workflow. Subsequently, the image progresses to the "Data Preprocessing" state, where essential preprocessing tasks such as resizing or noise reduction are performed to optimize the image for analysis. Once the preprocessing stage concludes, the system advances the image to the "Type Selection" state.

Within the "Type Selection" state, the system identifies the type of image uploaded, discerning whether it pertains to brain or skin tissue. This determination dictates the subsequent course of action, guiding the system to transition either to the "Brain Prediction" or "Skin Prediction" state accordingly.

Upon entering the "Model Prediction" state, the system executes the prediction analysis utilizing the appropriate model for the identified tissue type. Following the completion of the prediction process, the system proceeds to the "Generate Report" state, where it compiles a comprehensive report summarizing the analysis results.

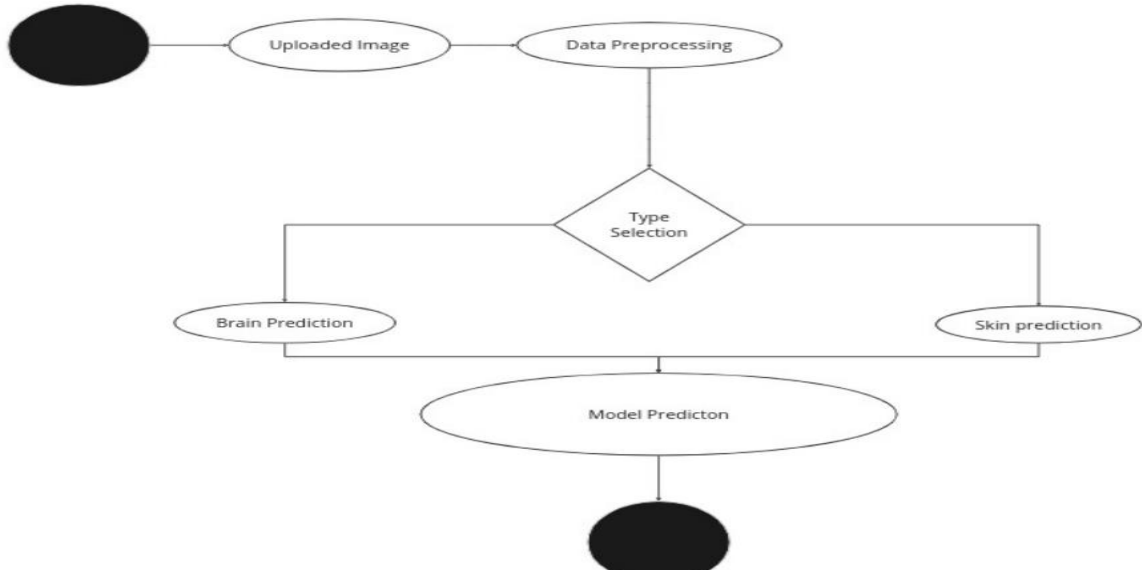


Figure 3.5: State Chart.

3.7. Use Case Diagram

A Use Case Diagram is a visual representation used to illustrate the interactions between actors (users or external systems) and a system under consideration. It depicts the various ways in which users interact with the system to accomplish specific goals or tasks. Use Case Diagrams are widely used in software engineering to capture and communicate the functional requirements of a system.

The main components of a Use Case Diagram:

3.7.1. Actor: Represents users, roles, or external systems interacting with the system. Depicted as stick figures or icons outside the system boundary. Examples: "Customer," "Bank Teller," "ATM."

3.7.2. Use Case: Describes specific system functionalities or behaviors. Shows interactions between the system and actors to achieve goals. Depicted as ovals within the system boundary. Examples: "Withdraw Money," "Deposit Funds," "Check Account Balance."

3.7.3. Relationships: Interactions between actors and use cases.

- Association: Communication or interaction between actor and use case, shown as solid lines.
- Generalization (Inheritance): Specialization relationship between actors or use cases, depicted as solid lines with a triangle arrowhead pointing from specialized (child) to general (parent) actor or use case.

3.7.4. System Boundary: Defines the system's scope, separating it from external actors. Contains all actors and use cases, illustrating their interactions with the system.

Use Case Diagrams are valuable tools for capturing and documenting the functional requirements of a system from a user's perspective. They help stakeholders understand the system's behavior, identify the various use cases supported by the system, and clarify the roles and responsibilities of different actors.

In response to the user's actions, the system activates the "Brain and Skin Cancer Detection" use case, designed to analyze the uploaded image comprehensively. Following successful login and image upload, the system initiates the analysis phase, scrutinizing the uploaded image to identify potential indications of brain or skin cancer.

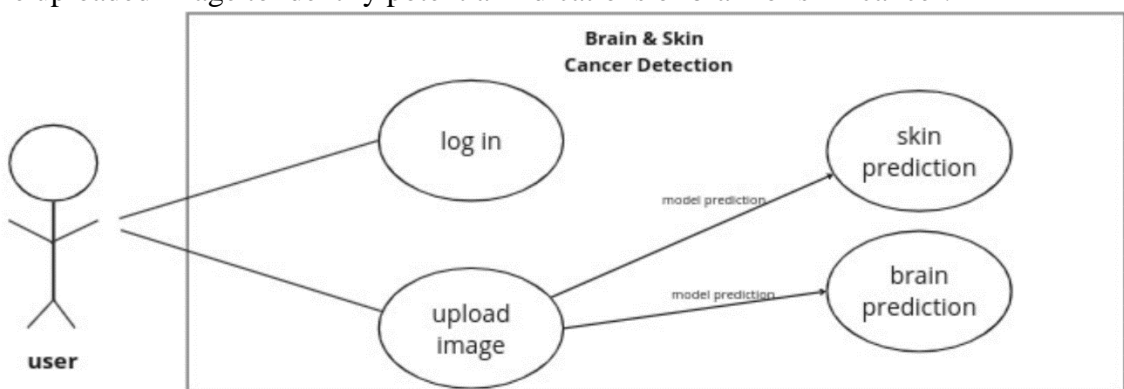


Figure 3.6: Use Case Diagram.

3.8. A Data Flow Diagram (DFD)

A Data Flow Diagram (DFD) is a graphical representation that illustrates the flow of data within a system or organization. It's a widely used modeling technique in software engineering and business analysis for visualizing the processes involved in a system and the data that flows between them.

The main components of a Data Flow Diagram:

3.8.1. Processes: Functions within the system that transform input data into output data through operations or computations, depicted as shapes connected by data flow arrows in DFDs.

3.8.2. Data Flows: Represent the movement of data between processes, data stores, and external entities, illustrated by arrows indicating input, processing, and output of data, each labeled to describe the data type.

3.8.3. Data Stores: Repositories or storage locations, physical or virtual, where system data is held, depicted as open-ended rectangles connected to processes or data flows.

3.8.4. External Entities: Sources or destinations of data outside the system boundary, such as users, systems, or hardware devices, interacting with the system through input and output data exchange.

3.8.5. Data Flow Labels: Describe the nature or contents of data transferred between system components, providing clarity on data processing and flow purposes.

The "User" data source represents the individuals utilizing the system, who have the capability to upload medical images for analysis. These users serve as the primary initiators of the data flow process, providing essential input to the system.

The "Image" data store functions as a centralized repository for storing the medical images uploaded by users.

The data flows within the system orchestrate the movement of information between various components, ensuring a seamless progression of tasks. The "Upload Image" data flow signifies users uploading medical images to the system, with the image data flowing from the "User" data source to the "Image Repository" data store, initiating the analysis pipeline.

Subsequently, the "Preprocess Image Data" data flow denotes the preparation of uploaded images for analysis, as the image data moves from the "Image Repository" to the "Brain Cancer Prediction" model. Here, preprocessing tasks such as normalization or noise reduction are performed to optimize the data for accurate analysis.

The "Brain Cancer Prediction" data flow represents the pivotal analysis phase, where the preprocessed image data undergoes thorough examination by the Brain Cancer Prediction model. This model utilizes advanced algorithms to analyze the data and predict the likelihood of brain cancer based on identified patterns and features.

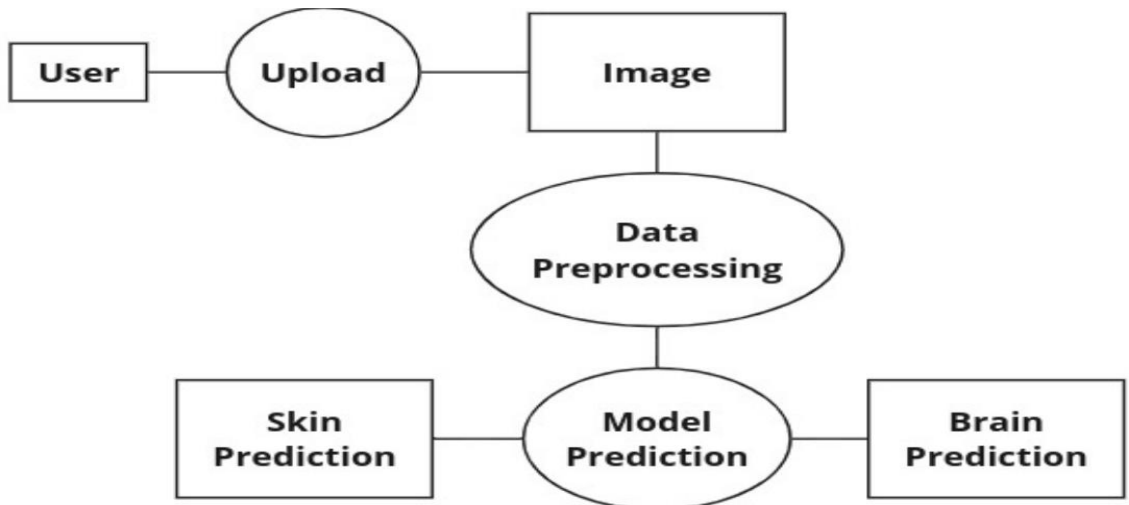


Figure 3.7: Data Flow Diagram.

3.9. Process Model Diagram

A Process Model Diagram, also known as a Process Flow Diagram (PFD) or a Process Map, is a visual representation used to illustrate the steps or stages involved in a process or workflow. It provides a high-level overview of how activities are performed, the sequence in which they occur, and the interactions between different components of the process.

The main components of a Process Model Diagram:

3.9.1. Activities: Tasks in the process, like "Assemble Components" in manufacturing.

3.9.2. Sequence Flows: Control flow between activities, showing order with arrows.

3.9.3. Decisions: Points where the process branches based on conditions, shown as diamonds.

3.9.4. Start and End Events: Process start and end points, depicted as circles.

3.9.5. Annotations and Notes: Additional info about elements in the model, clarifying purpose or providing instructions.

The process initiates with the "Start" step, marking the commencement of user interaction within the system. At this stage, the system initiates a pivotal check to ascertain whether the user possesses a registered account.

Upon confirming the user's registration status, two divergent paths emerge:

- If the user is registered, denoted by a "Yes" response, the process seamlessly progresses to the "Login" step (step 4), where the user can securely access their account by providing their credentials.
- Conversely, if the user is not registered, denoted by a "No" response, the process branches into two distinct routes:

- "Signup": Here, the user has the option to create a new account by completing the signup process, typically involving the creation of a username and password. Upon successful registration, the process loops back to the initial step (step 1), now recognizing the user as registered within the system.
- "Anonymous": Alternatively, the user can opt to proceed anonymously without creating an account, bypassing the registration process and proceeding directly to the "Login" step (step 4).

Following the user authentication process, the "Upload Image" step ensues, enabling the user to upload a medical image, such as an X-ray, MRI, or other relevant scan, crucial for cancer detection analysis.

Subsequently, the uploaded image undergoes analysis by a cancer detection model in the "Model Prediction" step, where advanced algorithms meticulously scrutinize the image to predict the likelihood of cancer presence.

Upon completion of the analysis, the system proceeds to deliver the prediction results to the user in the "Send Prediction to User" step, ensuring prompt dissemination of critical information regarding the cancer prediction outcome.

Finally, the process culminates with the "End" step, signifying the successful completion of the entire process, thus concluding the user interaction within the system.

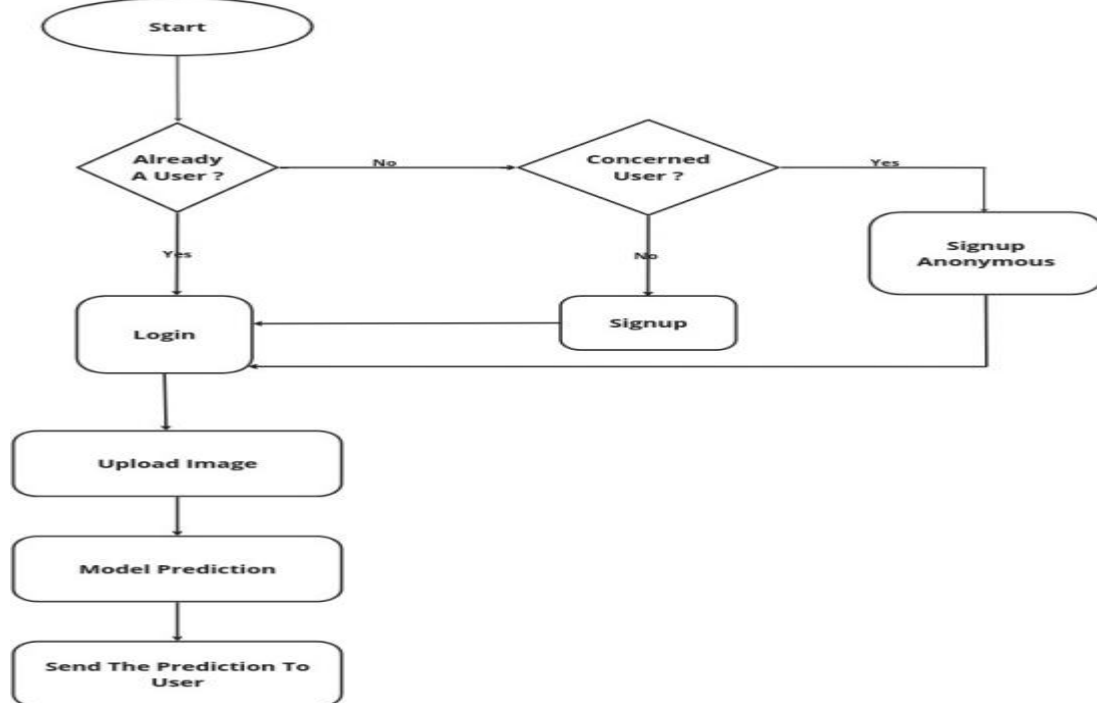


Figure 3.8: Process Model Diagram.

3.10. Sequence Diagram

A Sequence Diagram is a type of interaction diagram in Unified Modeling Language (UML) that illustrates how objects interact in a particular scenario of a system. It depicts the sequence of messages exchanged between objects over time to accomplish a specific task or scenario.

The main components of a Sequence Diagram:

3.10.1. Objects: Instances of classes or components in interaction, shown as vertical dashed lines with names/identifiers at the top, arranged according to roles.

3.10.2. Lifelines: Represent object existence over time, aiding in tracking message sequence. Depicted as vertical lines extending downward from object representations.

3.10.3. Messages: Object communication depicted as arrows/horizontal lines between lifelines, synchronous/asynchronous, with labels showing message details.

3.10.4. Activation Boxes: Represent periods of active message processing by objects, shown as rectangles on lifelines, indicating activity duration.

3.10.5. Return Messages: Show object responses/return values after message processing, depicted as arrows/horizontal lines with dashed return path and labels for return values.

3.10.6. Optional and Conditional Messages: Represent alternate paths or optional interactions, indicating branching/decision points. Depicted with different notation/labels for conditional nature.

The interaction between the system's administrator ("Admin") and the database unfolds through a series of steps, facilitating efficient data management and administration within the system.

Login: The process starts with the user logging in to the website. By entering a username and password.

Image Upload: After successful login, the user uploads an image to the system.

Model Prediction: If the image is valid, it's sent for analysis by a pre-trained model, using the models that are trained to detect these specific cancers in images. The models then generates a prediction based on the image content.

Store Results: The system stores the prediction results in a database, along with the uploaded image for future reference.

Send Prediction: The system sends the prediction to the user.

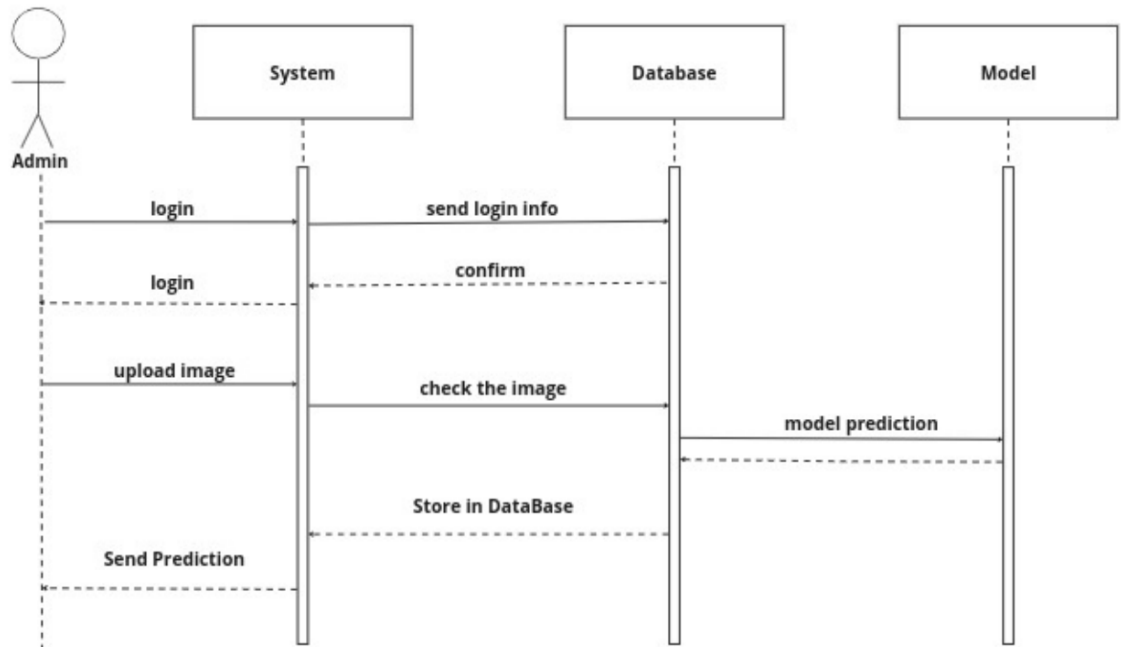


Figure 3.9: Sequence Diagram.

Chapter Four

IMPLEMENTATION

4.1. Introduction

In medical imaging, advanced technologies combined with deep learning are revolutionizing diagnosis, enhancing patient care. This chapter explores computer vision's role, focusing on the Proposed System—a project aiming to improve skin cancer and brain tumor diagnosis through advanced classification and segmentation. The Proposed System utilizes convolutional neural networks (CNNs) across web-based platforms—a website, desktop, and streamlit app enabling precise medical image analysis. It integrates skin cancer classification and brain tumor segmentation, leveraging top-tier models and preprocessing techniques to decode complex biomedical imaging data. The Proposed System stands out for its capabilities in skin cancer and brain tumor analysis, showcasing AI's potential in healthcare's evolution toward personalized medicine and patient-centric care.

4.2. Definitions:

4.2.1. Supervised Learning: Supervised learning is a core aspect of modern machine learning, where algorithms learn from labeled data to make predictions. The process involves stages like data curation, training, and evaluation using sets of labeled data. Various algorithms are used, ranging from simple ones like linear regression to complex neural networks. Supervised learning is valued for its ability to generalize patterns to new data, making it useful across many applications.

4.2.2. Computer Vision: Computer vision combines computer science and artificial intelligence, to help machines understand visual information. It involves tasks like image processing and scene understanding, aiming to replicate human visual cognition using computational methods. With techniques like deep learning, especially convolutional neural networks (CNNs), computer vision has made significant progress, impacting areas like autonomous vehicles, surveillance, medical imaging, robotics, and augmented reality.

4.2.3. Image Classification: Image classification is crucial in computer vision, assigning labels to images. It's vital in various fields like autonomous driving, healthcare, e-commerce, and security. The process involves training a model to recognize patterns in images to categorize them. Initially, a dataset with labeled images is gathered and split into training and test sets. During training, the model learns to associate features with class labels using optimization algorithms like stochastic gradient descent. Convolutional Neural Networks (CNNs) are commonly used for image classification due to their ability to learn hierarchical features from raw pixel data. CNNs consist of layers like convolutional, activation, pooling, and fully connected layers, enabling them to extract abstract features and classify images accurately. Image classification has broad

applications, from identifying objects in natural scenes to medical anomaly detection and e-commerce product classification.

4.2.4. Image Segmentation: Image segmentation divides an image into meaningful segments based on criteria like color or texture. It's crucial in various fields like medicine and autonomous navigation. Traditional methods use rules, while deep learning, especially CNNs, has become popular for its accuracy. There are different types like semantic segmentation (assigning labels to pixels), instance segmentation (differentiating between instances of the same class), and panoptic segmentation (combining semantic and instance segmentation).

4.2.5. Convolutional Neural Networks (CNNs): CNNs are specialized deep neural networks for processing grid-like data like images, excelling in computer vision tasks. They use convolutional layers with learnable filters to extract features and patterns efficiently. Components like activation functions, normalization layers, and pooling layers enhance the network's ability to capture complex visual information. Their hierarchical structure allows them to automatically learn representations of visual features, starting from basic elements like edges and textures and progressing to higher-level abstractions.

4.2.6. Pooling Layers: Pooling layers are vital in Convolutional Neural Networks (CNNs), reducing feature map dimensions while retaining key information. Max pooling and average pooling are common operations, reducing computational load and enhancing robustness to spatial variations. They sit between convolutional layers, progressively shrinking feature maps while boosting feature abstraction. However, criticisms highlight potential loss of spatial information. Alternatives like dilated convolutions and global average pooling offer options for specific needs. Despite debates, pooling layers remain essential for efficient CNNs in various computer vision tasks.

4.2.7. Transfer learning: Transfer learning is a potent method in machine learning, using knowledge from one task to enhance performance on another related task. Instead of starting from scratch, it transfers learned features from a pre-trained model to expedite training and improve generalization, especially with limited labeled data for the new task.

It involves three stages:

- Pre-training: Initially, a model is trained on a large dataset for a similar task, learning generic features.
- Transfer: Knowledge from the pre-trained model is adapted to the new task by further training on a smaller dataset.
- Fine-tuning: The model is refined on the target dataset to optimize performance, adjusting parameters with a lower learning rate.

Transfer learning applies to various domains like image classification, NLP, and speech recognition. For instance, pre-trained CNNs serve as feature extractors in computer vision tasks.

4.2.8. Data preprocessing: is essential in machine learning, involving cleaning, transforming, and normalizing raw data for analysis and model training. Techniques

include handling missing values, outliers, and errors (data cleaning), converting data into suitable formats (data transformation), creating or modifying features (feature engineering), and dividing data into training, validation, and test sets (data splitting). Normalizing and standardizing features ensures uniformity for better model performance. Overall, data preprocessing is vital for building accurate and reliable machine learning models by addressing common challenges and biases in datasets.

4.2.9. Data Augmentation: Data augmentation enhances datasets by applying various transformations to existing samples, commonly used in computer vision tasks. It aims to increase dataset size and diversity, crucial for training robust models, especially with limited or imbalanced data. Common transformations include rotation, flipping, scaling, translation, shearing, and brightness/contrast adjustment. These variations simulate real-world scenarios, improving model exposure to diverse examples. By augmenting datasets with transformed samples, data augmentation prevents overfitting, improves generalization, and addresses class imbalance. However, it should be applied judiciously to avoid unrealistic distortions that may hinder model performance.

4.2.10. U-Net: U-Net is a convolutional neural network architecture designed for biomedical image segmentation tasks. The U-Net architecture consists of a contracting path, which captures context and spatial information through convolutional and pooling layers, followed by an expansive path, which enables precise localization and segmentation using upsampling and concatenation operations. The contracting path resembles a typical convolutional neural network, while the expansive path involves upsampling the feature maps and concatenating them with feature maps from the contracting path to refine segmentation boundaries. U-Net's architecture facilitates end-to-end learning of segmentation tasks and has been successfully applied to various medical imaging tasks, including cell segmentation, organ segmentation, and tumor detection.

4.3. Proposed System

Figure 4.1, The process begins with input images. Preprocessing follows to prepare the images for CNN analysis. Segmentation isolates the mole from the background, which is essential for focused analysis. Feature extraction follows, during which the CNN identifies mole characteristics such as size, shape, color, and border. These features inform classification, where the CNN determines if the mole is benign or malignant by comparing extracted features to a database. The final step presents the diagnosis, indicating the benign or malignant status.

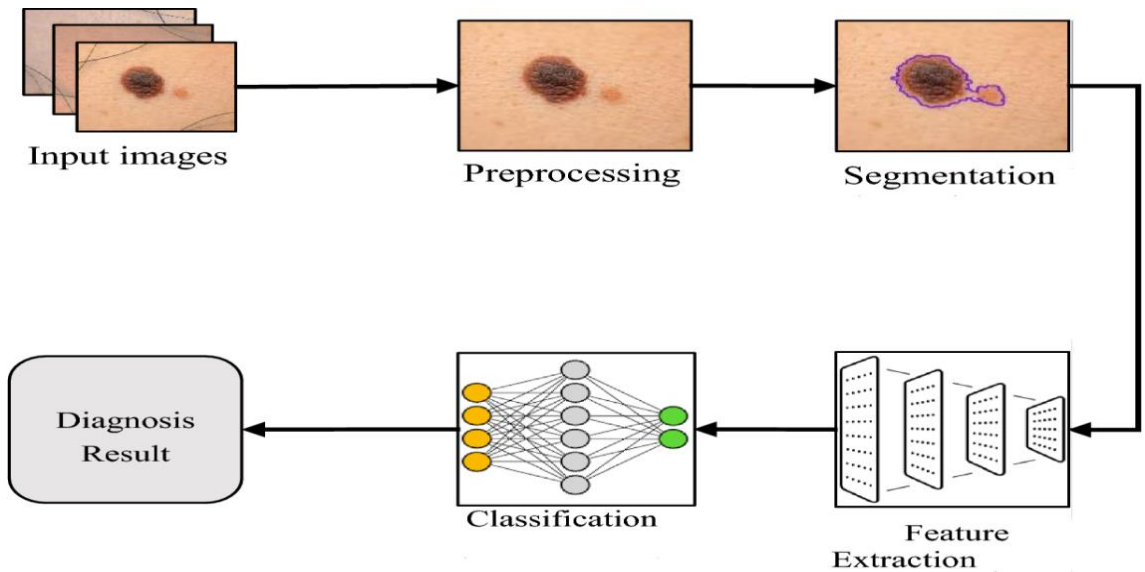


Figure 4.1: Proposed System for Skin Cancer.

Figure 4.2, The data processing pipeline begins with data collection, followed by preprocessing to ensure data quality through tasks like cleaning and formatting. Then, the model is applied to the training data to identify patterns. After implementation, the model is evaluated using testing data to assess its performance on unseen data.

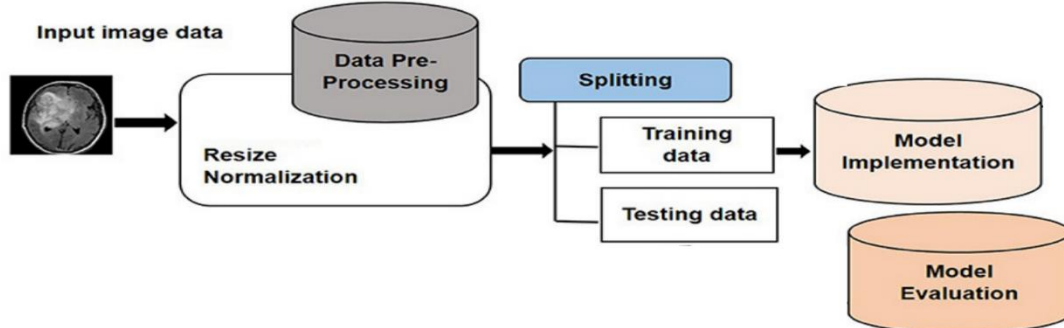


Figure 4.2: Proposed System for Brain Tumor.

4.4. Methodology

4.4.1. Data Collection

The datasets employed in this research are the "HAM10000" dataset and the "PH2" dataset. The "HAM10000" dataset comprises skin cancer images depicting various skin lesions. This dataset comprises a total of 10,015 images, each with dimensions (450, 600, 3). Each image is linked to a specific diagnosis, categorized into seven classes: Melanocytic nevi (nv), Melanoma (mel), Benign keratosis-like lesions (bkl), Basal cell carcinoma (bcc), Actinic keratoses (akiec), Vascular lesions (vasc), and Dermatofibroma (df). The dataset also provides additional information for each image, including diagnosis and age. The "PH2" dataset is another dataset used in this research, which consists of skin lesion images as well. It includes a total of 200 images, with dimensions of 768×560 pixels. These images were acquired in RGB color as BMP files.

4.4.2. Data Preprocessing

HAM10000: Following the retrieval of image files, all images were resized from 450x600 pixels to 28x28 pixels. Subsequently, the dataset was partitioned into training and testing sets, with 80% of the data allocated to the training set and the remaining 20% to the test set. Both the training and test sets were normalized to ensure consistency in the data distribution. Additionally, a label mapping was created, consisting of a dictionary that associates the names of the seven classes with key values ranging from 0 to 6, facilitating classification tasks.

PH2: All images were resized from 768x560 pixels to 224x224 pixels. Subsequently, the dataset was partitioned into training and testing sets, with 80% of the data allocated to the training set and the remaining 20% to the test set, ensuring a balanced distribution for training and evaluation. This resizing process enables compatibility with models that expect input images of uniform dimensions.

The Brain LGG (Low-Grade Glioma) dataset: MRI images and masks undergo resizing to a consistent resolution of (256, 256) pixels. Intensity normalization follows, standardizing pixel values within the images and masks by rescaling them to the range [0, 1] through division by 255. Subsequently, binary mask thresholding is applied, where mask pixel values are dichotomized: those surpassing 0.5 signify tumor presence (set to 1), while those equal to or below 0.5 represent background (set to 0).

4.4.3. Data Augmentation

HAM10000: To address the class imbalance and augment the training dataset, various methods were employed. Skin images were augmented using transformations such as rotation, width shift, height shift, shear, horizontal flip, and vertical flip. This augmentation strategy increased the number of images from 10,015 to 45,756, while preserving identical dimensions of twenty-eight pixels in width, twenty-eight pixels in height, and three-color channels. By introducing variability into the training set, this augmentation approach enhances the model's generalization and robustness to different skin lesion variations.

PH2: Random rotation and horizontal flipping were applied to augment the PH2 dataset. These transformations introduce variations in the dataset, which helps in improving the model's ability to generalize to unseen data and enhances its robustness. This augmentation strategy diversifies the dataset while maintaining consistency in dimensions, facilitating more effective training of the model.

The Brain LGG (Low-Grade Glioma) dataset: To enhance the diversity of the training dataset and bolster model generalization and robustness, data augmentation techniques are implemented on both MRI images and their corresponding masks. Various strategies are employed: random rotation within specified ranges to emulate spatial orientation variations, horizontal and vertical flips for mirror reflections, random zooming to simulate scale and perspective changes, and random shifts in both horizontal and vertical positions. Furthermore, brightness and contrast adjustments are randomly applied to

mimic varying illumination conditions, collectively enriching the dataset and augmenting its variability for improved model performance.

4.4.4. Model Architecture:

Classification using the HAM10000 dataset: The model consists of twelve layers. The model initiates with convolutional layers, proficient at capturing intricate patterns within images. The initial layer deploys sixteen filters, followed by a max-pooling layer strategically down-sampling spatial dimensions. This pattern iterates, progressively escalating complexity with 32, 64, and 128 filters in subsequent convolutional layers. The corresponding max-pooling layers strike a balance between preserving crucial features and reducing spatial dimensions, culminating in a final convolutional layer followed by a flattening operation. This transition readies the data for the fully connected layers, establishing a connection between spatial hierarchies and the dense layers. The subsequent dense layers, featuring 64 and 32 neurons, act as a potent feature extractor, refining the learned representations. The output is realized through a dense layer with seven neurons, each representing a distinct class in the present classification task. The SoftMax activation function ensures the model provides well-calibrated probabilities for each class, facilitating confident predictions. This comprehensive architecture carefully considers both spatial intricacies and hierarchical feature extraction, contributing to the model's robust performance in computer vision tasks. Figure 4.3 shows the used classification model architecture. Table 4.1 shows the hyperparameters for Classification Methodology.

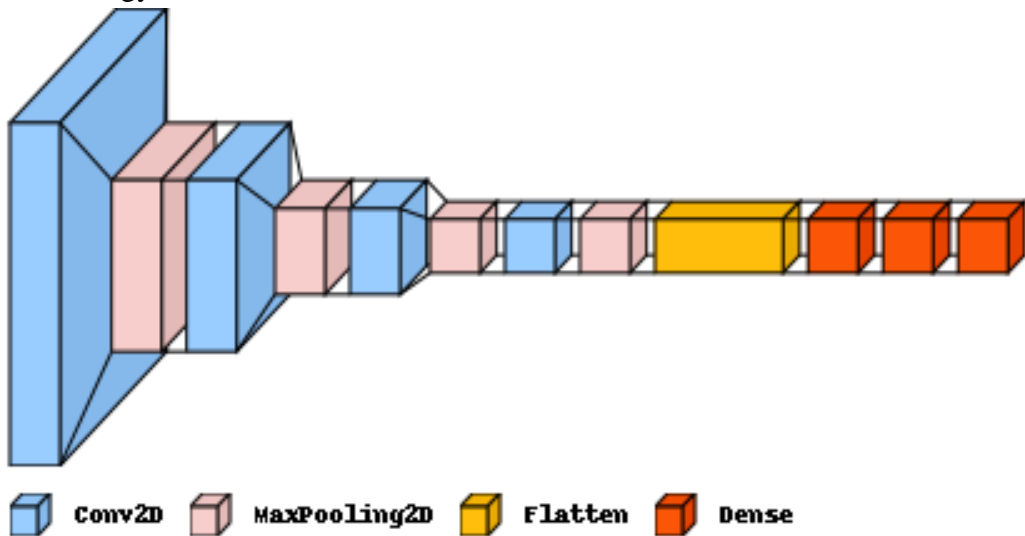


Figure 4.3: Proposed Classification Model Architectural Framework.

Table 4.1: Hyperparameters for Skin Classification process.

Hyperparameter	Value	Description
Learning Rate	0.001	The rate at which the model adjusts its weights during training.
Rotation Range	10	Range (in degrees) for random rotations applied to the images.
Width Shift Range	0.2	Range for random horizontal shifts applied to the images.
Height Shift Range	0.2	Range for random vertical shifts applied to the images.
Shear Range	0.2	Shear intensity (in radians) for geometric transformations.
Horizontal Flip	TRUE	Randomly flip images horizontally during training.
Vertical Flip	TRUE	Randomly flip images vertically during training.
Batch Size	64	Number of samples processed per gradient update during training.
Epochs	20	Number of complete passes through the entire training dataset.

Segmentation using the PH2 dataset: The model architecture includes one encoder and one decoder pathway. The encoder pathway initiates with four convolutional layers, followed by max-pooling layers for down-sampling, progressively increasing the complexity with deeper layers. Each convolutional block is composed of two convolutional layers with batch normalization and ReLU activation, ensuring effective feature extraction while mitigating the risk of overfitting. Additionally, spatial dropout is incorporated to enhance the model's robustness by introducing randomness during training.

The decoder pathway mirrors the encoder in terms of the number of layers, with four transposed convolutional layers for up-sampling. These layers are used to sample the feature maps to the original image resolution. This symmetric architecture facilitates the precise localization of skin lesion boundaries. Furthermore, the final layer employs a 1x1 convolution followed by a sigmoid activation function. Figure 4.4 shows the used Segmentation model architecture.

The Jaccard distance loss function is used to train the model by calculating the difference between predicted and ground truth segmentation masks. The segmentation model is trained for 100 epochs with the Adam optimizer and a learning rate of 0.003. Throughout the training process, different evaluation measures such as Intersection over Union (IoU), Dice coefficient, precision, recall, and accuracy are tracked to assess the model's performance on both the training and validation sets. Table 4.2 shows the hyperparameters for Segmentation Methodology.

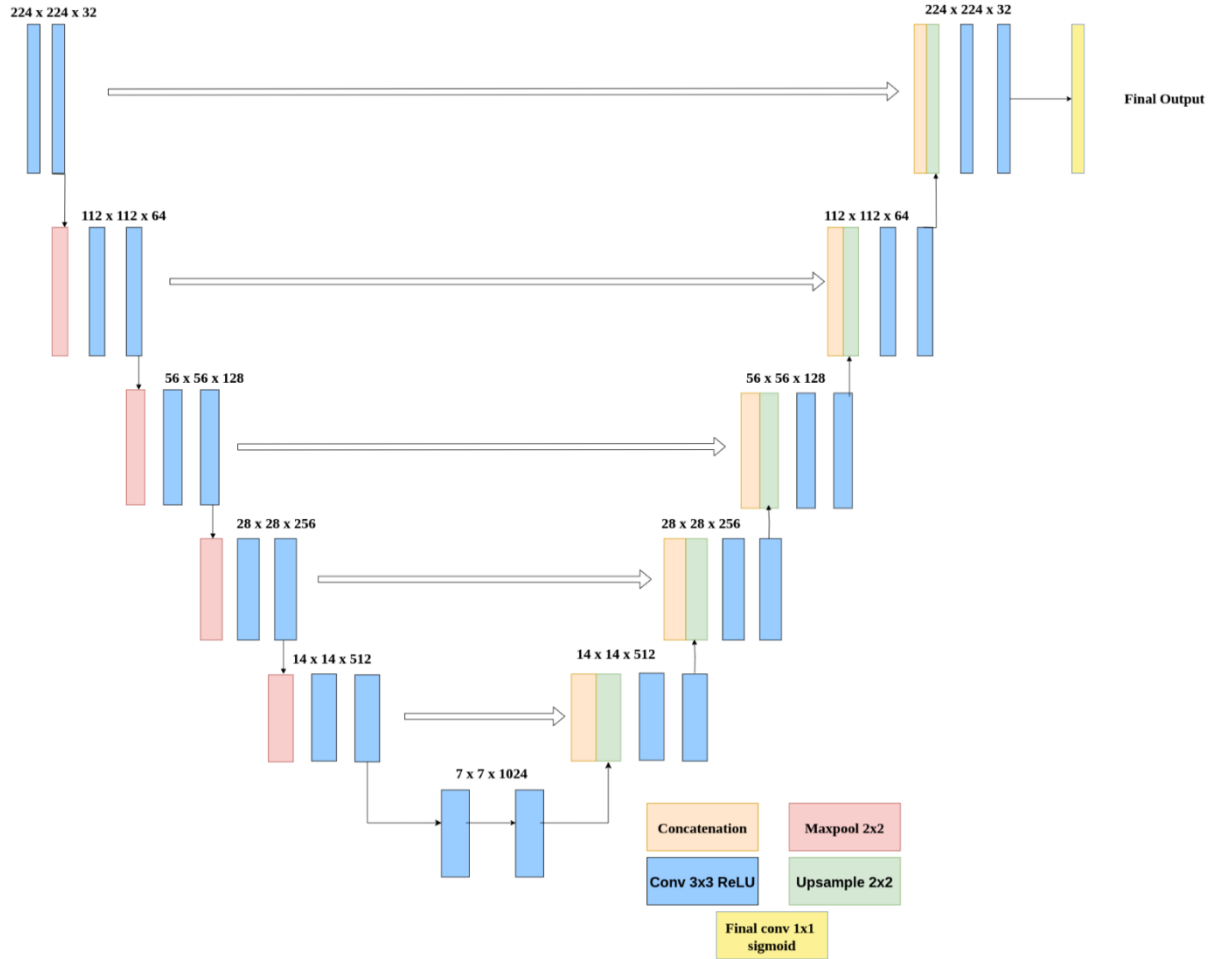


Figure 4.4: Segmentation Model Architectural Framework.

Table 4.2: Hyperparameters for Skin Segmentation process.

Hyperparameter	Value	Description
Rotation Range	-40 to 40	Range (in degrees) for random rotations applied to the images.
Horizontal Flip	TRUE	Randomly flip images horizontally during training.
Dropout	0.4	Dropout rate for spatial dropout applied to convolutional layers.
Learning Rate	0.003	The rate at which the model adjusts its weights during training.
Optimizer	Adam	Optimizer algorithm used for training the model.
Batch Size	16	Number of samples processed per gradient update during training.
Epochs	100	Number of complete passes through the entire training dataset.

Segmentation using the LGG dataset: The model architecture is based on a U-Net structure as shown in figure 4.5, and it includes an encoder-decoder framework with skip connections to facilitate the propagation of detailed information from earlier to later layers. The encoder section uses a series of convolutional layers, followed by batch normalization and rectified linear unit activation functions. This sequence extracts hierarchical features from the input images while gradually capturing abstract representations. The spatial dimensions are then downsampled using max-pooling layers, which improves the model's receptive field while reducing computational complexity.

In contrast, the decoder section employs transposed convolutions to gradually recover the spatial resolution of the feature maps. These upsampled features are concatenated with the encoder's feature maps via skip connections, allowing the decoder to refine segmentation boundaries with fine-grained detail. Batch normalization and ReLU activation functions are used again to stabilize training and introduce nonlinearity, respectively. The final layer uses a sigmoid activation function to generate pixel-level predictions, resulting in a binary segmentation mask. This comprehensive architecture, which combines deep feature extraction and precise localization capabilities, serves as the model's backbone, allowing for accurate and robust segmentation. Table 4.3 shows the hyperparameters for Segmentation Methodology.

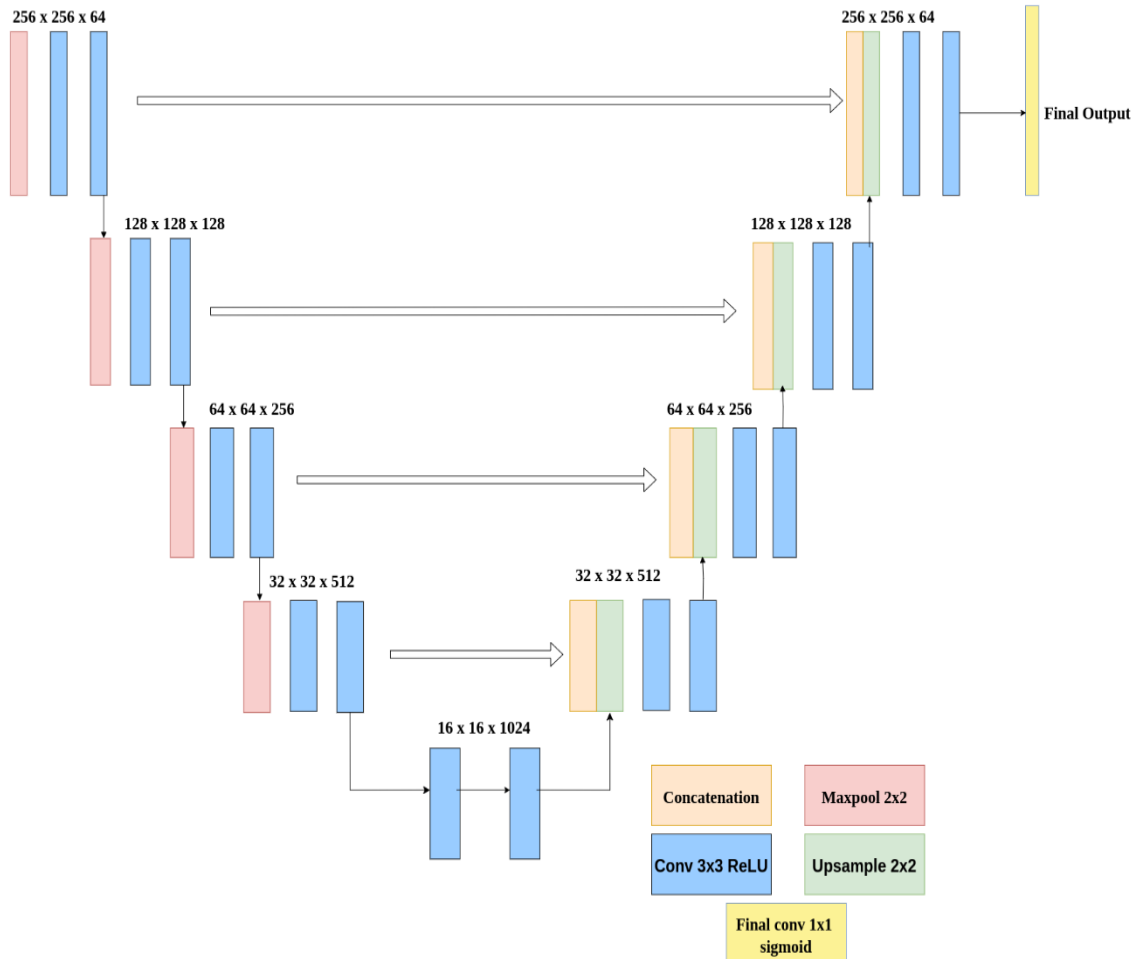


Figure 4.5: Segmentation Model Architectural Framework.

Table 4.3: Hyperparameters for Brain Segmentation process.

Hyperparameter	Value	Description
Smooth Value	100	A small constant added to the denominator in the dice coefficient and intersection over union calculations to prevent division by zero.
Shear Range	0.05	Random shearing transformations applied to the images during data augmentation.
Zoom Range	0.05	zoom applied to the images during data augmentation.
Rotation Range	0.2	Range (in degrees) for random rotations applied to the images.
Horizontal Flip	TRUE	Randomly flip images horizontally during training.
Learning Rate	Adam	The rate at which the model adjusts its weights during training.
Optimizer	32	Optimizer algorithm used for training the model.
Batch Size	150	Number of samples processed per gradient update during training.
Epochs	100	Number of complete passes through the entire training dataset.

4.5. Tools Used:

1. Python: A versatile programming language widely used in machine learning and data science for its simplicity, readability, and vast ecosystem of libraries.
2. Kaggle: An online platform that hosts machine learning competitions and provides datasets, kernels (code notebooks), and discussion forums for data scientists to collaborate and learn.
3. Anaconda: A distribution of Python and R programming languages for scientific computing, offering pre-installed libraries and tools useful for data analysis, machine learning, and visualization.
4. TensorFlow: An open-source machine learning framework developed by Google, known for its flexibility and scalability, widely used for building and training neural networks.
5. GitHub: A platform for version control and collaboration in software development, enabling sharing and collaboration on code projects, including machine learning models and datasets.

6. OpenCV (Open Source Computer Vision Library): A library of programming functions mainly aimed at real-time computer vision, offering tools for image and video analysis, manipulation, and processing.
7. Keras: A high-level neural networks API, built on top of TensorFlow, designed for fast experimentation and prototyping of deep learning models.
8. Visual Studio Code: A lightweight and customizable code editor developed by Microsoft, widely used for coding in various programming languages including Python and JavaScript, with support for extensions and debugging tools.
9. HTML (Hypertext Markup Language): The standard markup language for creating web pages and web applications, used for structuring content and defining its layout.
10. SQL (Structured Query Language): A domain-specific language used in programming and designed for managing and querying relational databases, essential for storing and retrieving data in many applications.
11. CSS (Cascading Style Sheets): A style sheet language used for describing the presentation of a document written in HTML, defining the layout, colors, fonts, and other visual aspects of web pages.
12. JavaScript: A programming language commonly used for web development, enabling interactive and dynamic features on web pages, often used in conjunction with HTML and CSS.
13. PySimpleGUI: A Python library for creating simple and intuitive graphical user interfaces (GUIs).
14. Streamlit: An open-source app framework for building data-driven web applications.

Chapter Five

TESTING & RESULTS

5.1. introduction

In the field of medical imaging, advances in computer vision and machine learning have created new opportunities for precise localization and classification of life-threatening conditions. In this chapter, we look at the findings from our research on skin cancer localization and classification, as well as brain tumor segmentation. We present a comprehensive exploration of our findings using advanced algorithms and cutting-edge imaging techniques.

5.2. Datasets Used

5.2.1. Skin Cancer Classification Dataset

The HAM10000 dataset [23], also known as the Human Against Machine with ten thousand training images dataset, features high-quality images of skin lesions. It encompasses several types of skin lesions, ranging from benign to malignant. The lesions are categorized into seven distinct classes. However, there is an imbalance among the classes in the dataset, as illustrated in Table 5.1 and Figure 5.1.

Table 5.1: Class Distribution Analysis of the dataset.

Class	Counts
Melanocytic nevi (nv)	6705
Melanoma (mel)	1113
Benign keratosis-like lesions (bkl)	1099
Basal cell carcinoma (bcc)	514
Actinic keratoses and intraepithelial carcinoma (akiec)	327
Vascular lesions (vasc)	142
Dermatofibroma (df)	115

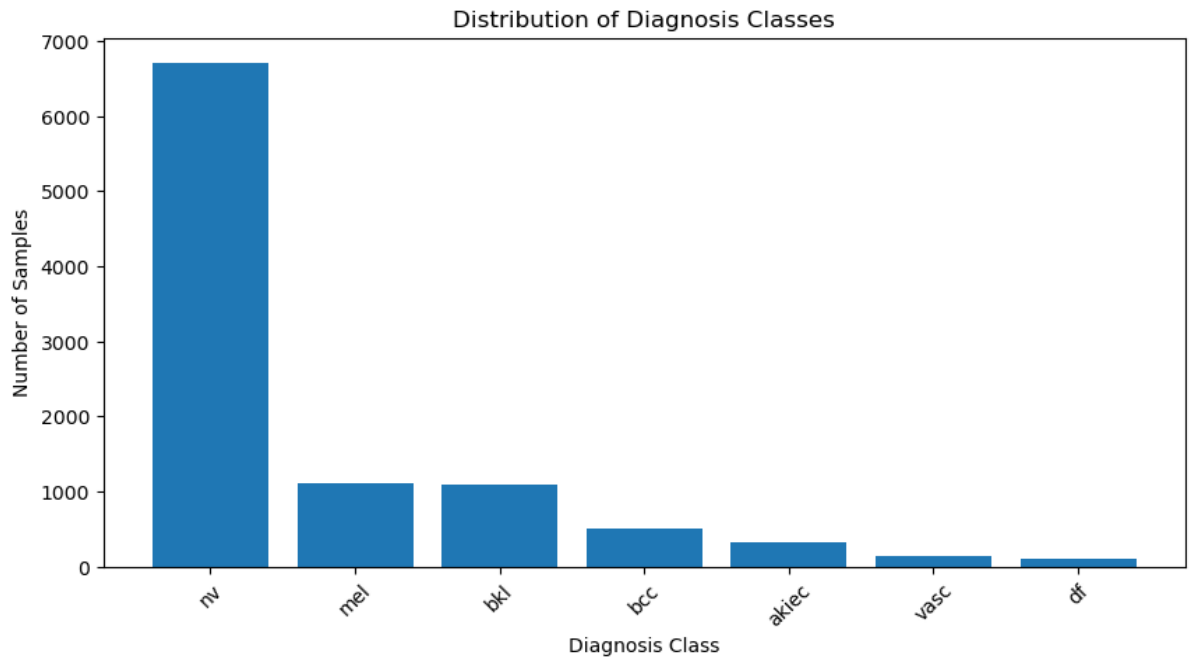


Figure 5.1: Class Distribution Analysis of the dataset.

To address the challenge of an unbalanced dataset within the HAM1000 dataset, a strategy of duplicating images was employed for augmentation purposes. This duplication process did not result in any new augmentation transformations, and to preserve the NV class's integrity in the HAM1000 dataset, no augmentation techniques were used. During data preparation for training and testing, augmentation transformations such as rotation, shifting, and flipping were applied to the training set only, leaving the original dataset unchanged.

Table 5.2 and Figure 5.2 summarize the data augmentation strategies used to address the unbalanced dataset in HAM1000. The approach involved duplicating images for augmentation without introducing new transformations, while maintaining the integrity of the NV class. Augmentation techniques such as rotation, shifting, and flipping were exclusively applied to the training set.

Table 5.2: Class Distribution after using the factor.

Class	Counts	Factor used	Counts + (Counts*factor) + Counts
Melanoma (mel)	1113	4	6678
Benign keratosis-like lesions (bkl)	1099	4	6594
Basal cell carcinoma (bcc)	514	11	6682
Actinic keratoses and intraepithelial carcinoma (akiec)	327	17	6213
Vascular lesions (vasc)	142	45	6674
Dermatofibroma (df)	115	52	6210

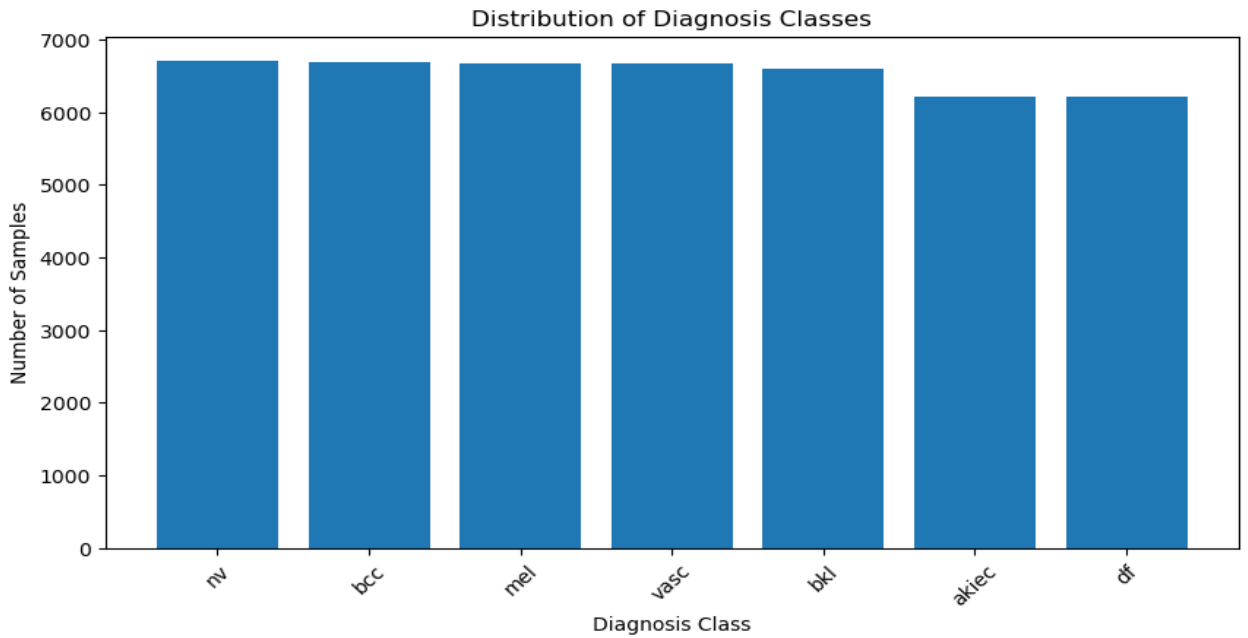


Figure 5.2: All Class Distribution after using the factor.

5.2.2. Skin Cancer Segmentation Dataset

The PH2 dataset [20] is a well-known dataset in the field of dermatology and medical image analysis. It consists of 200 high-resolution images acquired in RGB color format as BMP files, with dimensions of 768×560 pixels.

5.2.3. Brain Tumor Segmentation Dataset

The Brain LGG (Low-Grade Glioma) dataset: which is commonly employed for brain tumor segmentation tasks. The Brain LGG dataset comprises magnetic resonance imaging (MRI) scans of patients diagnosed with low-grade gliomas. These MRI scans provide detailed information about the internal structure of the brain, including the presence and location of tumors.

5.3. Evaluation Metrics for both classification and segmentation

Before we delve into the results obtained from training various deep learning algorithms on the HAM10000 and PH2 datasets for predicting skin cancer, it is essential to understand the significance of each metric used in the evaluation process. Accuracy, precision, and recall for classification and Jaccard Distance, Intersection over Union (IoU), Dice Coefficient, precision, recall, and Accuracy for segmentation.

5.3.1. Accuracy [24]

Definition: Accuracy is a measure of the overall correctness of the model. It calculates the ratio of correctly predicted instances to the total instances.

$$\text{Accuracy} = \frac{\text{True Positives} + \text{True Negatives}}{\text{Total Predictions}} \quad (1)$$

Usefulness: While accuracy provides a general sense of how well the model is performing, it might not be the best metric for imbalanced datasets. In the case of skin

cancer classification, where the occurrence of malignant cases might be significantly lower than benign cases, accuracy alone may not provide a complete picture.

5.3.2. Precision [24]

Definition: Precision measures the accuracy of positive predictions. It calculates the ratio of true positives to the total predicted positives.

$$Precision = \frac{\text{True Positives}}{\text{True Positives} + \text{False Positives}} \quad (2)$$

Usefulness: Precision is crucial in scenarios where false positives are costly. In skin cancer classification, high precision means that when the model predicts a sample as malignant, it is likely to be correct. It is particularly important in medical contexts where misdiagnosing benign cases as malignant could lead to unnecessary treatments.

5.3.3. Recall [24]

Definition: Recall measures the ability of the model to capture all the relevant instances. It calculates the ratio of true positives to the total actual positives.

Equation:

$$Recall = \frac{\text{TruePositives}}{\text{TruePositives} + \text{FalseNegatives}} \quad (3)$$

Usefulness: Recall is vital when the cost of false negatives is high. In the context of skin cancer classification, high recall indicates that the model is effective in identifying malignant cases, minimizing the chances of missing potentially dangerous lesions.

5.3.4. Jaccard Distance [25]

Definition: The Jaccard distance, also known as the Intersection over Union (IoU), quantifies the dissimilarity between the predicted and ground truth segmentation masks. It measures the ratio of the intersection to the union of the two masks. A lower Jaccard distance indicates better segmentation accuracy.

$$JaccardIndex = \frac{|A \cap B|}{|A \cup B|} \quad (4)$$

$$JaccardDistance = 1 - JaccardIndex \quad (5)$$

Where:

- A and B are the ground truth and predicted segmentation masks, respectively.
- $|A \cap B|$ denotes the number of pixels common to both masks.
- $|A \cup B|$ represents the total number of pixels in both masks.

Usefulness: Jaccard distance is useful for evaluating the similarity between two segmentation masks. It provides a measure of how well the predicted segmentation aligns with the ground truth. A lower Jaccard distance indicates better segmentation accuracy.

5.3.5. Intersection over Union (IoU) [25]

Definition: IoU is a measure of the overlap between the predicted and ground truth segmentation masks. It calculates the ratio of the intersection to the union of the two masks, providing insights into the model's ability to accurately delineate skin lesion boundaries. Higher IoU values signify better segmentation performance.

$$IoU(A, B) = \frac{|A \cap B|}{|A \cup B|} \quad (6)$$

Where:

- A and B are the ground truth and predicted segmentation masks, respectively.
- $|A \cap B|$ denotes the number of pixels common to both masks.

- $|A \cup B|$ represents the total number of pixels in both masks.

Usefulness: IoU is commonly used in image segmentation tasks to assess the quality of segmentation results. Higher IoU values indicate better agreement between the predicted and ground truth segmentation masks, reflecting improved segmentation accuracy.

5.3.6. Dice Coefficient [25]

Definition: The Dice coefficient assesses the similarity between the predicted and ground truth segmentation masks. It computes the ratio of twice the intersection to the sum of the volumes of the two masks. A higher Dice coefficient indicates greater overlap and similarity between the predicted and ground truth masks.

Equation:

$$Dice(A, B) = \frac{2|A \cap B|}{|A| + |B|} \quad (7)$$

Where:

- A and B are the ground truth and predicted segmentation masks, respectively.
- $|A \cap B|$ denotes the number of pixels common to both masks.
- $|A|$ and $|B|$ denote the total number of pixels in each mask.

Usefulness: The Dice coefficient is particularly useful in evaluating the performance of segmentation models. It provides a robust measure of segmentation accuracy, especially in scenarios with class imbalance, where accurately capturing small structures is essential.

5.4. Results

5.4.1. Results for Skin Cancer Classification

As shown in Table 5.3 and Figure 5.3, DeepConvNet achieved the highest accuracy, precision, and recall scores, indicating its effectiveness in accurately classifying skin cancer lesions. Auto Encoder, while having a relatively high precision score, exhibited lower accuracy and recall scores compared to DeepConvNet, suggesting that it may have struggled with correctly identifying some instances of skin cancer. CNN decay lr, VGG16, ResNet50, InceptionV3, and Xception all demonstrated varying degrees of performance, with accuracy, precision, and recall scores falling below those of DeepConvNet but still showcasing some level of effectiveness in skin cancer classification.

Table 5.3: Performance Analysis: Metric Comparison across Training Algorithms.

Training Metrics			
Model Name	Accuracy	Precision	Recall
DeepConvNet	99.5	99.5	99.5
Auto Encoder	70.17	82.26	58.09
CNN with decay lr	81.23	89.72	73.28
VGG16	67.13	84.03	54.65
ResNet50	66.99	66.99	66.99
InceptionV3	66.97	85.86	54.2
Xception	66.8	85.92	54.31

Training Metrics Scores

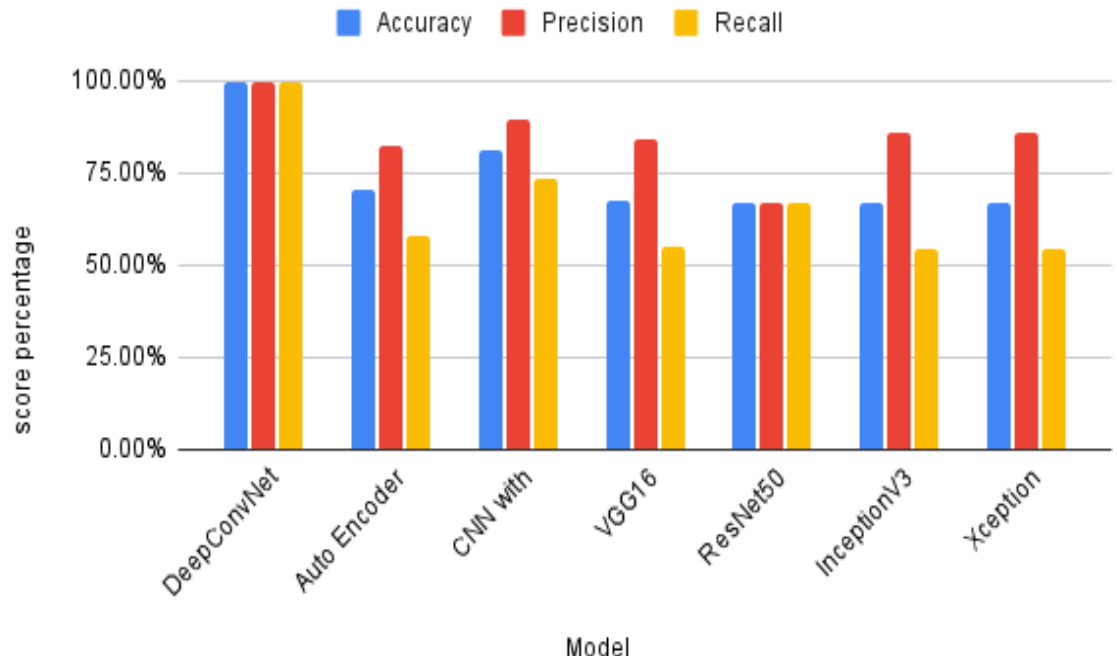


Figure 5.3: Performance Analysis: Metric Comparison across Training Algorithms.

Table 5.4 and Figure 5.4 show that the DeepConvNet outperformed all other testing algorithms in terms of accuracy, precision, and recall, demonstrating its ability to accurately categorize skin cancer lesions.

Table 5.4: Performance Analysis: Metric Comparison across Testing Algorithms.

Testing Metrics			
Model Name	Accuracy	Precision	Recall
DeepConvNet	97.204	97.5	97.2
Auto Encoder	70.17	82.49	58.17
CNN with decay lr	73.64	81.1	67.9
VGG16	66.99	83.52	60.03
ResNet50	66.83	66.83	66.83
InceptionV3	66.89	85.19	60.58
Xception	66.73	83.29	61.04

Testing Metrics Scores

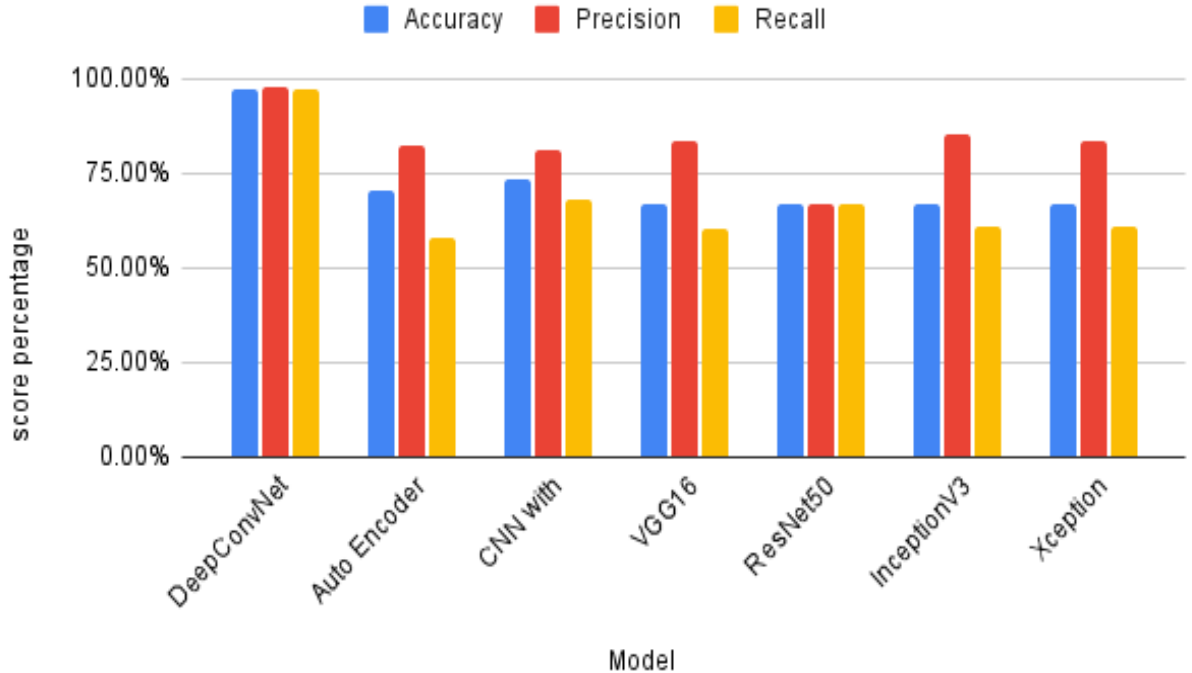


Figure 5.4: Performance Analysis: Metric Comparison across Testing Algorithms.

Figure 5.5 illustrates the progressive enhancement in accuracy and a concurrent decline in loss over time. This visual representation underscores the iterative refinement and optimization of the model, displaying a positive trend in performance as training progresses.

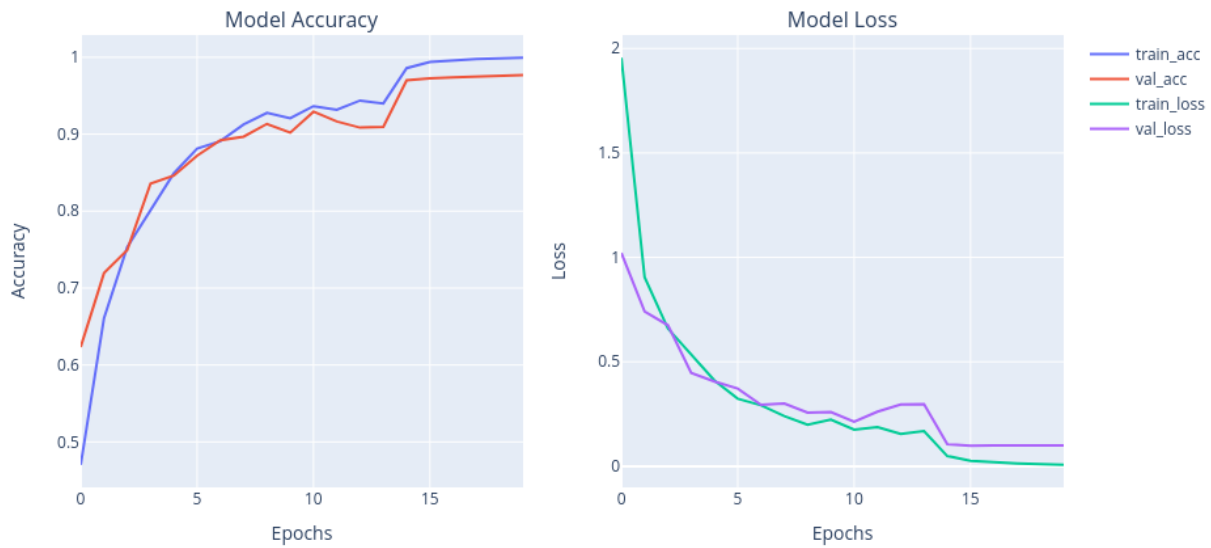


Figure 5.5: Tracking Progress: Evaluation of Accuracy and Loss for Proposed Model Architecture.

Figure 5.6 provides a visual representation of the model's performance through a confusion matrix graph for each class of data on the test set, including its performance on the unbalanced classes, as presented in Table and Figure 3. Each row in the confusion

matrix corresponds to the actual class labels, while each column represents the predicted class labels. The values in the cells of the matrix indicate the number of instances that were classified into each class.

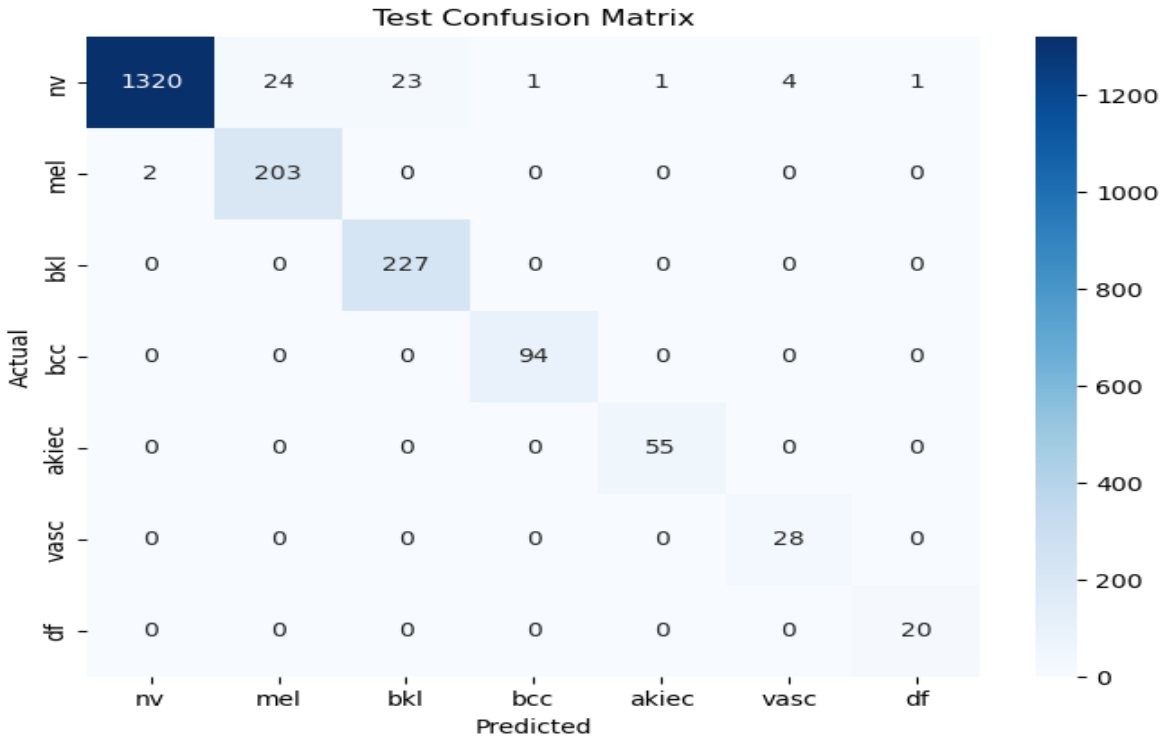


Figure 5.6: Visualizing Model Performance: Confusion Matrix Graph for Test Data.

This research paper provides a comprehensive overview of recent advances in skin lesion classification using deep learning models. The complexities of improving diagnostic accuracy and efficiency in skin disease detection are examined in detail using a variety of methodologies demonstrated by leading researchers, including transfer learning, knowledge distillation, and innovative network architectures.

- **S Panda et al. [1]:** The research paper on skin lesion classification utilizing Deep Learning models employed various methods to achieve its objectives. The study utilized transfer learning with pre-trained models such as VGG16, ResNet50, InceptionV3, and Xception to classify skin lesions into different categories. The models were trained on a dataset consisting of images of various skin diseases, including melanoma, nevus, and seborrheic keratosis. The training process involved 30 epochs with a batch size of 16 for training and 10 for validation.
- **Y Wang et al. [2]:** In a comparative study of skin lesion classification methods, deep learning models, traditional machine learning algorithms, and knowledge distillation techniques have been evaluated for their effectiveness in improving diagnostic accuracy. Deep learning models have shown promise in achieving higher accuracy rates due to their ability to learn complex patterns. Knowledge distillation techniques aim to enhance the performance of lightweight models by transferring knowledge from larger models. These methods have demonstrated improvements in accuracy, sensitivity, and specificity in skin lesion classification tasks. Leveraging advanced techniques like knowledge distillation can enhance the diagnostic accuracy of skin disease classification, contributing to more efficient diagnostic tools for skin diseases.
- **TH Aldhyani et al. [4]:** The study focuses on the development and implementation of a lightweight dynamic kernel deep-learning-based convolutional neural network for multi-class skin lesion classification. The methodology employed in the research includes the use of variable size kernels and activation functions in the network, with a strategic allocation of fewer kernels in the initial

layers for efficient utilization. Additionally, class-wise data balancing was performed to ensure unbiased training.

- S Maqsood & R Damaševičius [5]: In this study on multiclass skin lesion localization and classification using deep learning, a novel approach was developed to enhance the accuracy and efficiency of skin cancer detection. The methodology involved the utilization of a customized Convolutional Neural Network (CNN) for automatic feature extraction, incorporating well-known networks such as Xception, ResNet-50, ResNet-101, and VGG16 to reduce computation time. The feature selection process was optimized using a unique Univariate Measurement of Pairwise Dependence (UMPD) approach, which effectively selected the best features for recognition.
- B Shetty et al. [7]: In this research study on skin lesion classification, a variety of methods were employed to enhance the accuracy of the classification models. Machine learning models including Decision Tree, Random Forest, Support Vector Machine, K-Nearest Neighbor, Logistic Regression, Gaussian Naïve Bayes, and Linear Discriminant Analysis were evaluated, with Random Forest exhibiting the highest accuracy among them.
- MS Ali et al. [8]: The research focuses on utilizing a deep convolutional neural network (DCNN) model combined with transfer learning techniques to enhance the classification of skin cancer based on dermoscopy images. The proposed DCNN model was developed to accurately classify skin lesions, particularly in the early stages of cancer. By training the model on a large dataset and fine-tuning it over multiple epochs, the researchers achieved significant improvements in classification accuracy compared to existing deep learning models. The results demonstrated that the DCNN model outperformed traditional transfer learning models such as AlexNet, ResNet, VGG-16, DenseNet, and MobileNet in terms of accuracy and execution time. Through a comprehensive evaluation on the HAM10000 dataset, the DCNN model showed superior performance in distinguishing between benign and malignant skin lesions, with promising implications for early detection and treatment of skin cancer.
- V Anand et al. [15]: The research focuses on enhancing the classification of skin cancer through a transfer learning approach using the VGG16 architecture. The proposed model incorporates additional layers, including a flatten layer and dense layers with LeakyReLU and sigmoid activation functions, to improve accuracy. Data augmentation techniques are employed during pre-processing to increase dataset randomness and stability.
- TM Alam et al. [16]: In their study of an Efficient Deep Learning-Based Skin Cancer Classifier for an Imbalanced Dataset, Alam et al. used a comprehensive methodology to address the challenges posed by imbalanced data.
- S Aladhadh et al. [17]: In their research employed a two-tier framework to address the challenges associated with accurate skin cancer classification. The first stage involved data augmentation techniques to enhance the training dataset, mitigating issues related to insufficient labeled data. Subsequently, they developed a Medical Vision Transformer (MVT)-based classification model for skin cancer. This innovative approach involved splitting input images into patches and feeding them to the transformer in a sequence structure, akin to word embedding. The final classification was performed using a Multi-Layer Perceptron (MLP). The experimental results, conducted on the Human Against Machine (HAM10000) dataset, demonstrated the superiority of the proposed MVT-based model over existing state-of-the-art techniques.
- RD Seeja & A Suresh [21]: The study focuses on utilizing deep learning technology for skin lesion segmentation and classification of melanoma. The methodology employed in this research involves the initial segmentation of dermoscopy images using a Convolutional Neural Network (CNN) based U-net algorithm. Subsequently, color, texture, and shape features are extracted from the segmented images using techniques such as Local Binary Pattern (LBP), Edge Histogram (EH), Histogram of Oriented Gradients (HOG), and Gabor method. These extracted features are then fed into various classifiers including Support Vector Machine (SVM), Random Forest (RF), K-Nearest Neighbor (KNN), and Naïve Bayes (NB) for the diagnosis of melanoma or benign lesions.

- A Tajerian et al. [22]: In this study, we employed a methodological approach that leveraged dermoscopy images from the HAM10000 dataset to develop a machine-learning-based diagnostic tool for the classification of dermatoscopic skin cancer images. The process involved image pre-processing techniques such as labeling, resizing, and data augmentation to enhance the dataset. Transfer learning was utilized to create a model architecture based on EfficientNET-B1, incorporating a global average pooling 2D layer and a softmax layer with 7 nodes for classification.

Table 5.5 and Figure 5.7 present a comparison between the proposed method, implemented through the DeepConvNet architecture, and several previous research papers. Various training metrics, including accuracy, precision, and recall, are used for each model.

Table 5.5: Comparison between the proposed method and the other papers.

Training Metrics			
Paper	Accuracy	Precision	Recall
S Panda et al. [1]	-	97	95.2
Y Wang et al. [2]	84.6	-	-
TH Aldhyani et al. [4]	97.8	98.1	98
S Maqsood & R Damaševičius [5]	98.57	-	-
B Shetty et al. [7]	91.77	-	-
MS Ali et al. [8]	93.16	96.57	93.66
V Anand et al. [15]	89.09	-	-
TM Alam et al. [16]	91	-	-
S Aladhadh et al. [17]	96.14	96	96.50
RD Seeja & A Suresh [21]	85.19	42.59	50
A Tajerian et al. [22]	94	88	85
Current Proposed Method DeepConvNet	99.5	99.5	99.5

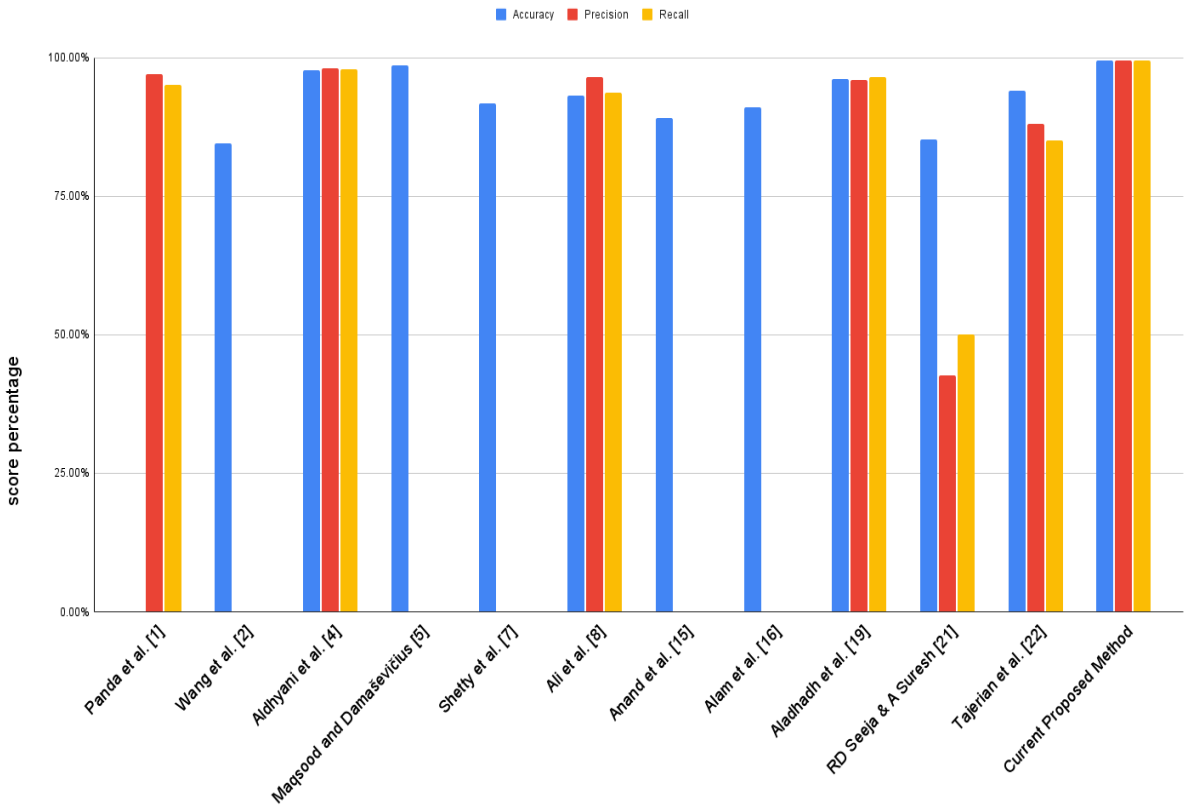


Figure 5.7: Benchmarking Proposed Method Against Existing Papers: A Comparative Study.

5.4.2. Results for Skin Cancer Segmentation

In Table 5.6 and Fig 5.8, the U-Net model's performance metrics are examined across both training and testing datasets. The U-Net model achieves high accuracy, precision, recall, Dice Coefficient, and IoU scores, underscoring its efficacy in accurately segmenting skin cancer lesions.

Table 5.6: Performance Analysis: Metric Comparison across Training and Testing Sets.

Training Metrics					
Model Name	Accuracy	Precision	Recall	Dice Coefficient	IoU
U-NET	96.68	95.39	94.24	93.58	97.09
Testing Metrics					
Model Name	Accuracy	Precision	Recall	Dice Coefficient	IoU
U-NET	96.14	93.44	94.09	92.55	96.43

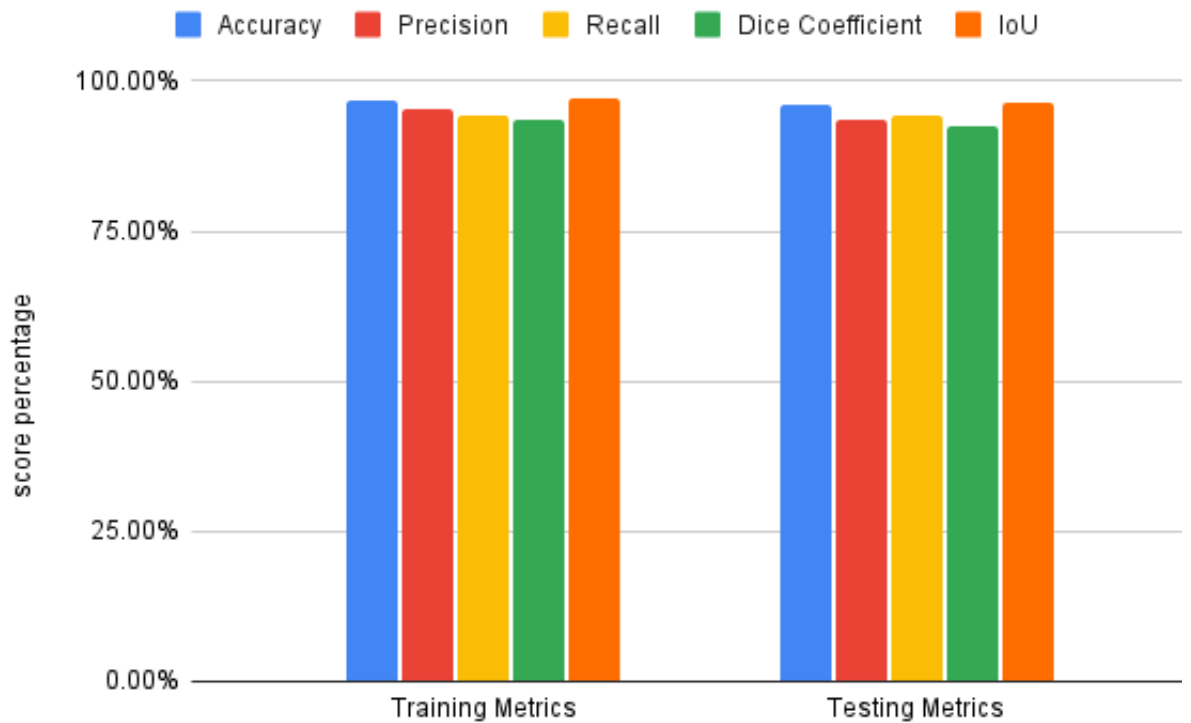


Figure 5.8: Performance Analysis: Metric Comparison across Training and Testing Sets.

Figures 5.9, 5.10, and 5.11 illustrate the progressive enhancement in accuracy, accompanied by a concurrent decline in Jaccard loss and improvement in Dice Coefficient, IoU, precision, and recall over time. These visuals represent the iterative refinement and optimization of the model, showcasing a positive trend in performance as training progresses.

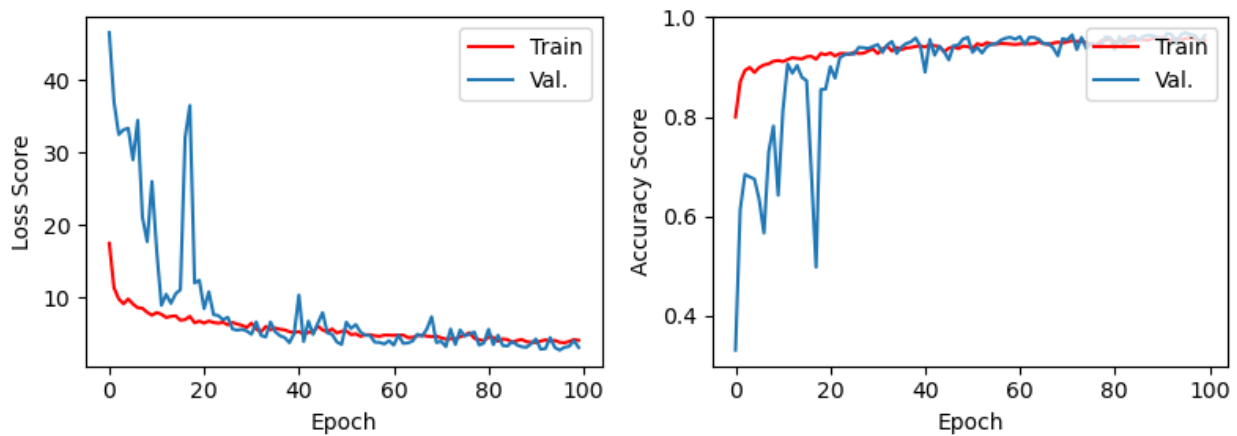


Figure 5.9: Tracking Progress: Evaluation of Jaccard Loss and Accuracy for the Model Architecture.

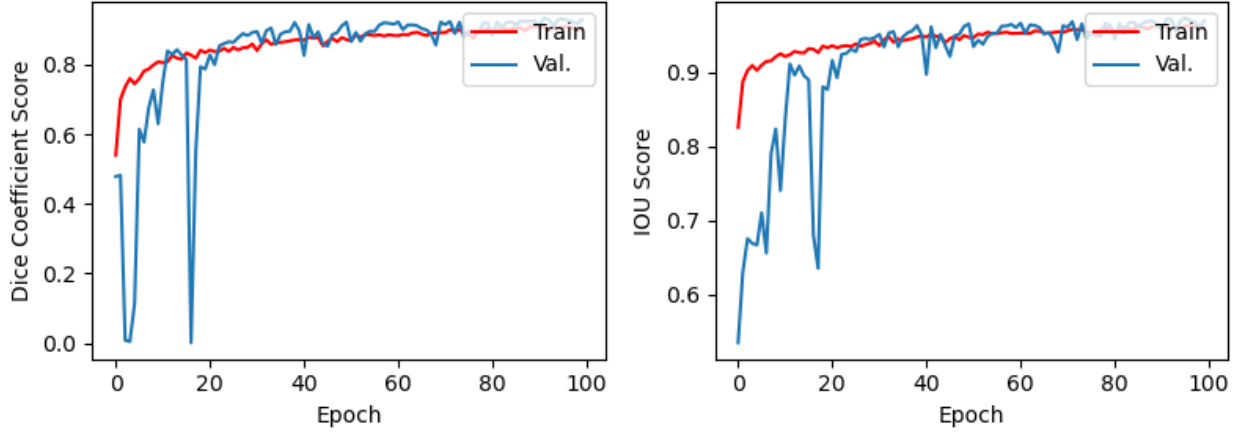


Figure 5.10: Tracking Progress: Evaluation of DC and IoU for Proposed Model Architecture.

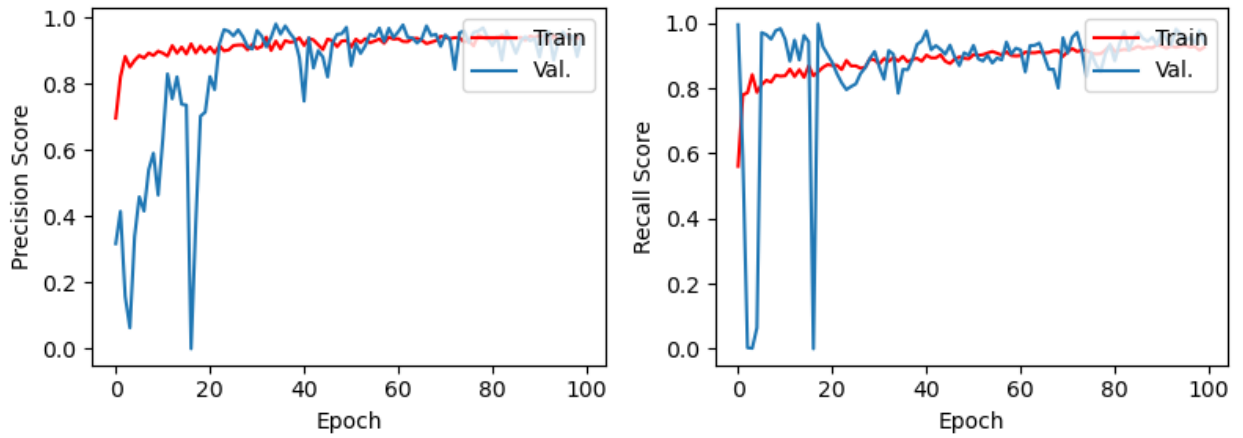


Figure 5.11: Tracking Progress: Evaluation of precision and recall for Proposed Model Architecture.

5.4.3. Proposed Skin Cancer Models Predictions

In Fig 5.12, several predictions from the suggested model are showcased. This visual representation offers a model's performance by displaying examples of its predictions for skin cancer lesions. These predictions provide insights into how the model categorizes and classifies different types of lesions. The suggested model performs well across all seven classes, despite the imbalance in data distribution as illustrated in Figure 5.1. When the model predicts accurately, the confidence level typically falls within the 97%–100% range. Figures 5.13 and 5.14 show several predictions from the U-net segmentation model.

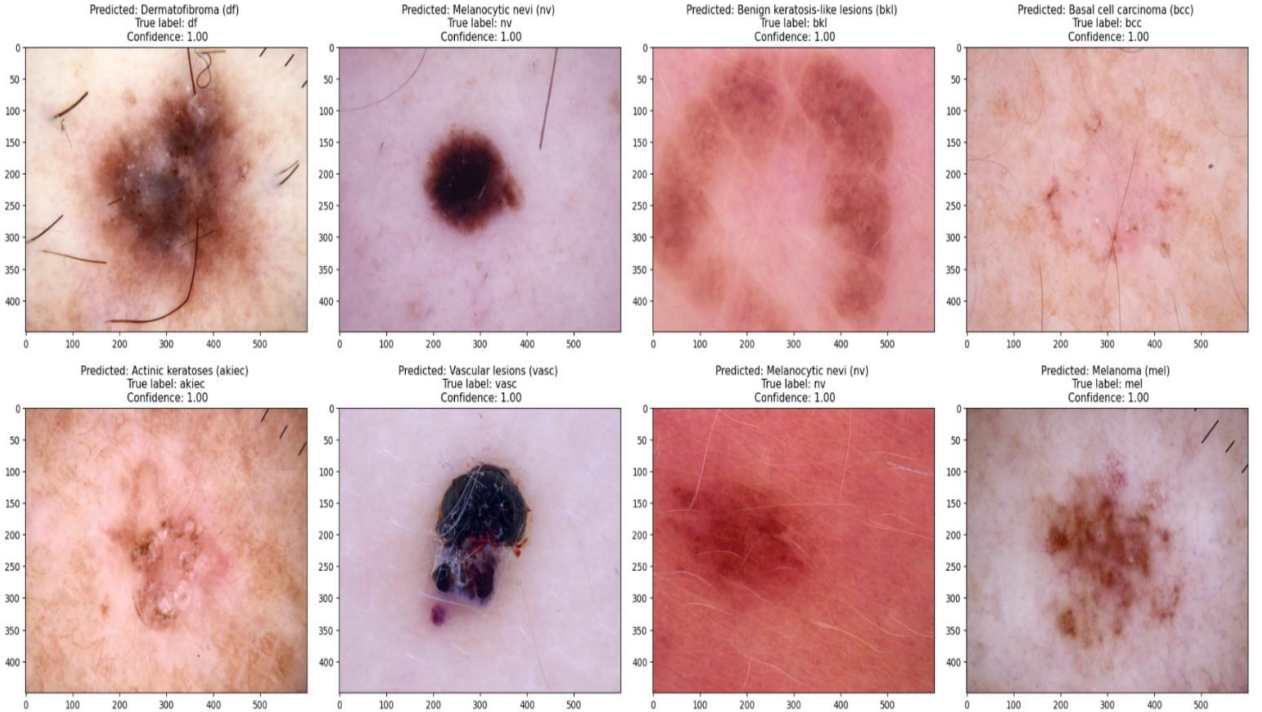


Figure 5.12: Sample classification predictions from the suggested model.

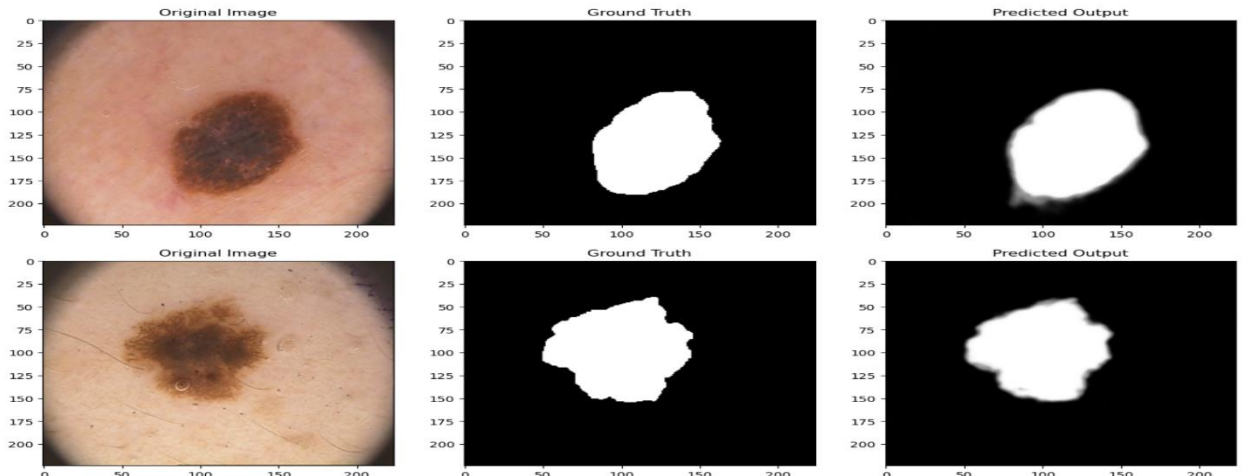


Figure 5.13: Sample predictions from the segmentation model.

Combining segmentation and classification models represents a promising approach to improving skin cancer diagnostic systems. In this integrated framework, the segmentation model precisely defines the lesion boundaries of skin cancer, effectively isolating the affected areas. These segmented regions are then localized or cropped and sent to the classification model for further analysis and diagnosis. Figure 5.14 illustrates this process by depicting the sequential workflow in which segmented lesions are accurately identified and then classified to determine the specific type of skin cancer. By combining these two methodologies, we can leverage the strengths of segmentation for precise delineation and classification for accurate diagnosis, ultimately improving the efficiency and reliability of skin cancer detection systems.

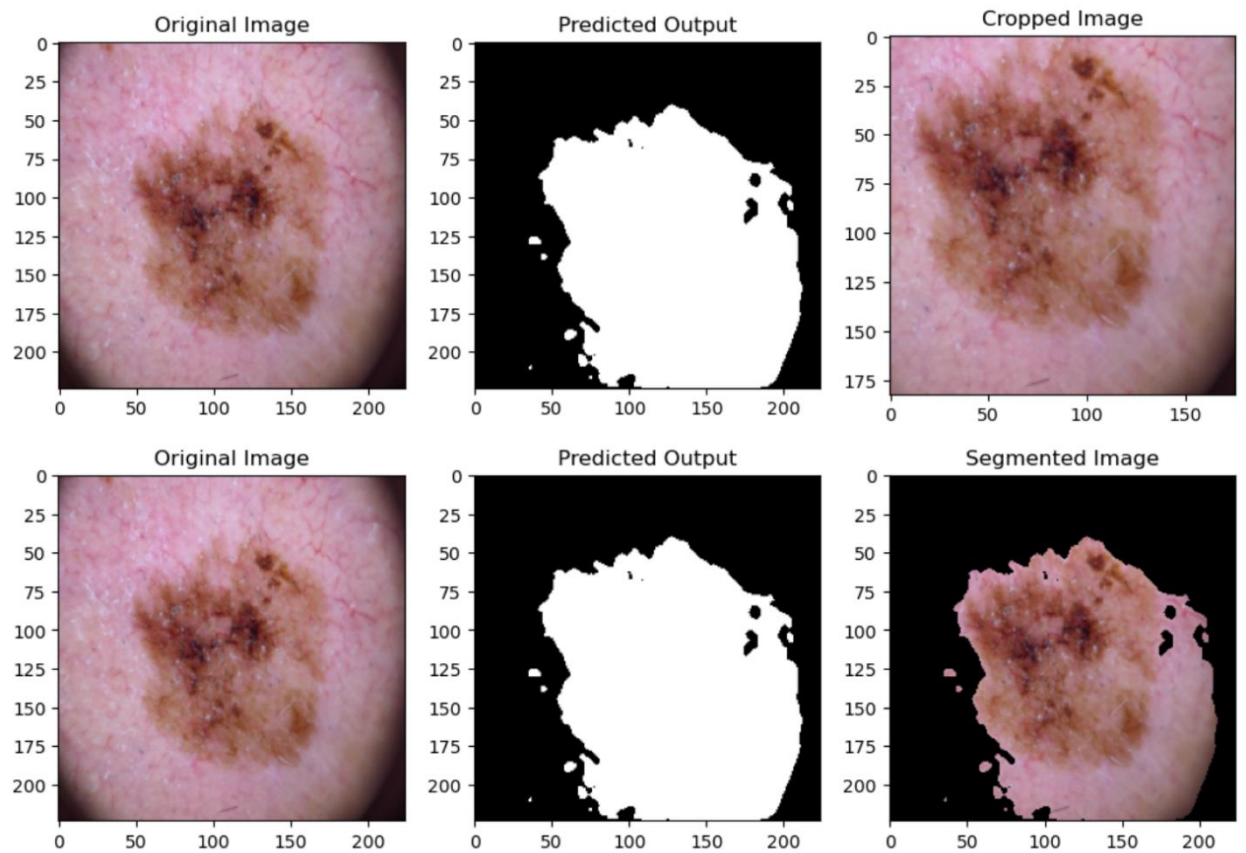


Figure 5.14: Segmentation-Driven Skin Cancer Diagnosis Model

5.4.4. Results for Brain Tumor Segmentation

Tables 5.7 and 5.8, along with Figures 5.15 and 5.16, present a comprehensive analysis of the performance metrics of the U-Net model across training and testing datasets. Demonstrating remarkable accuracy, Dice Coefficient, and IoU scores, the U-Net model underscores its effectiveness in precisely segmenting Brain Tumors.

Table 5.7: Performance Analysis: Metric Comparison across Brain Training Set.

Training Metrics			
Model Name	Accuracy	Dice Coefficient	iou
U-NET	0.9986	0.9276	0.8675
Attention ResUNet	0.9985	0.9182	0.8501
inceptionv3	0.9976	0.886	0.7999
resnet50	0.9981	0.9014	0.8248
resnext50	0.998	0.9014	0.8245

Training Metrics Scores

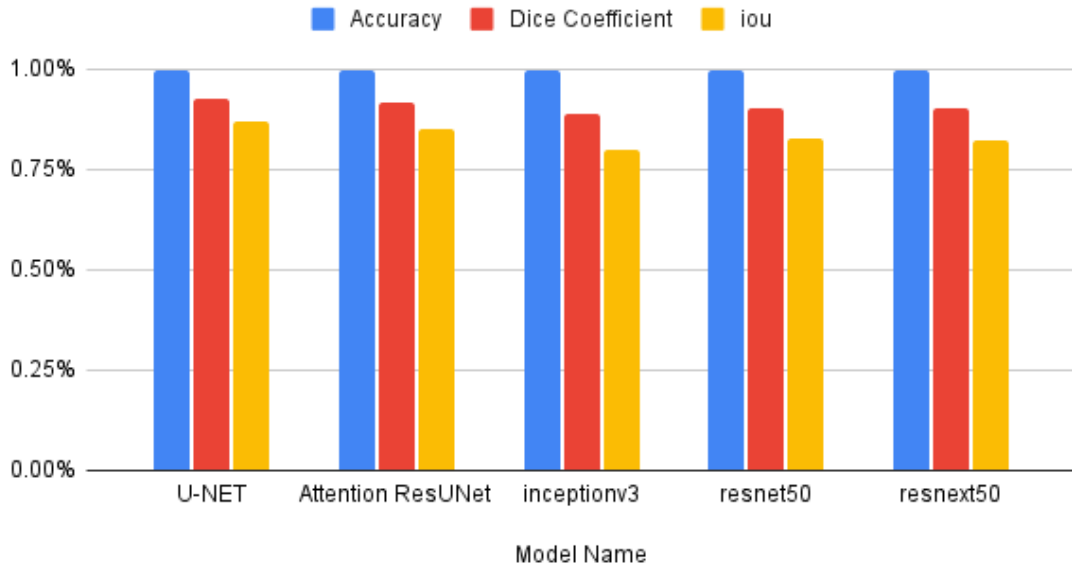


Figure 5.15: Performance Analysis: Metric Comparison across Brain Training Set.

Table 5.8: Performance Analysis: Metric Comparison across Brain Testing Set.

Testing Metrics			
Model Name	Accuracy	Dice Coefficient	iou
U-NET	0.9984	0.9127	0.8411
Attention-Res-UNet	0.9982	0.9022	0.8252
inceptionv3	0.9975	0.8673	0.7698
resnet50	0.9977	0.8801	0.7898
resnext50	0.9976	0.8721	0.7783

Testing Metrics Scores

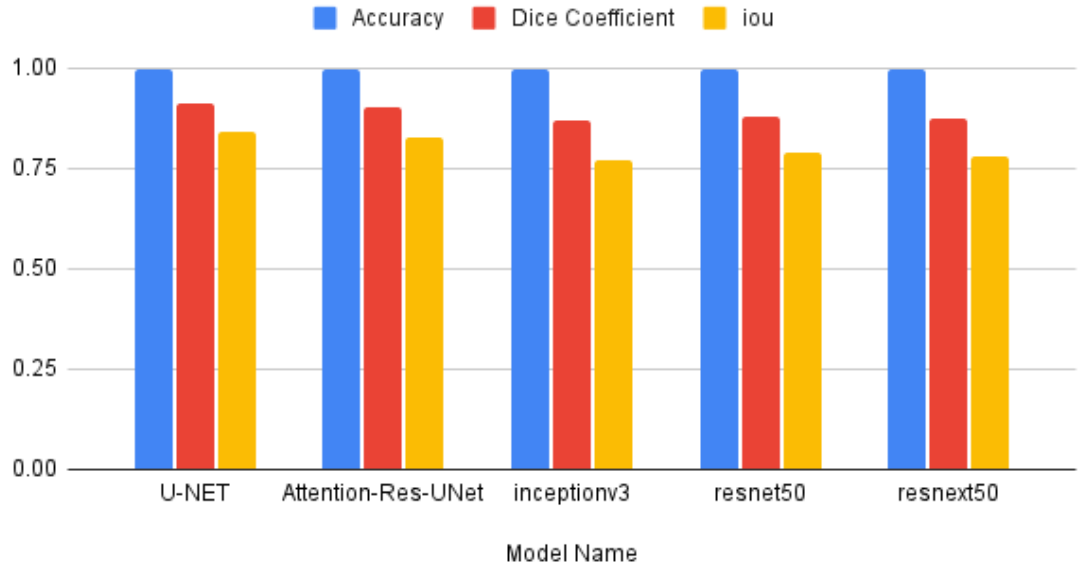


Figure 5.16: Performance Analysis: Metric Comparison across Brain Testing Set.

Table 5.9 and Figure 5.17 present a comprehensive comparison between our proposed method for brain tumor detection and segmentation and several other prominent approaches found in existing literature. Each method is evaluated based on three key metrics: accuracy, dice similarity coefficient (DSC), and intersection over union (IOU).

Table 5.9: Comparison between the proposed method and the other papers.

Model Name	accuracy	dsc	iou
B Wang et al. [26]	-	82	69.5
MN Trinh et al. [27]	-	91.51	84.58
S Jin et al. [30]	-	75.17	60.23
MA Naser & MJ Deen [33]	89	-	-
Q Yang et al. [34]	93.7	-	-
S Ghosh et al. [39]	-	91.81	-
B Zhan et al. [41]	-	85.7	75.81
F Özyurt et al. [45]	95.62	-	-
The Proposed Method	99.86	92.76	86.75

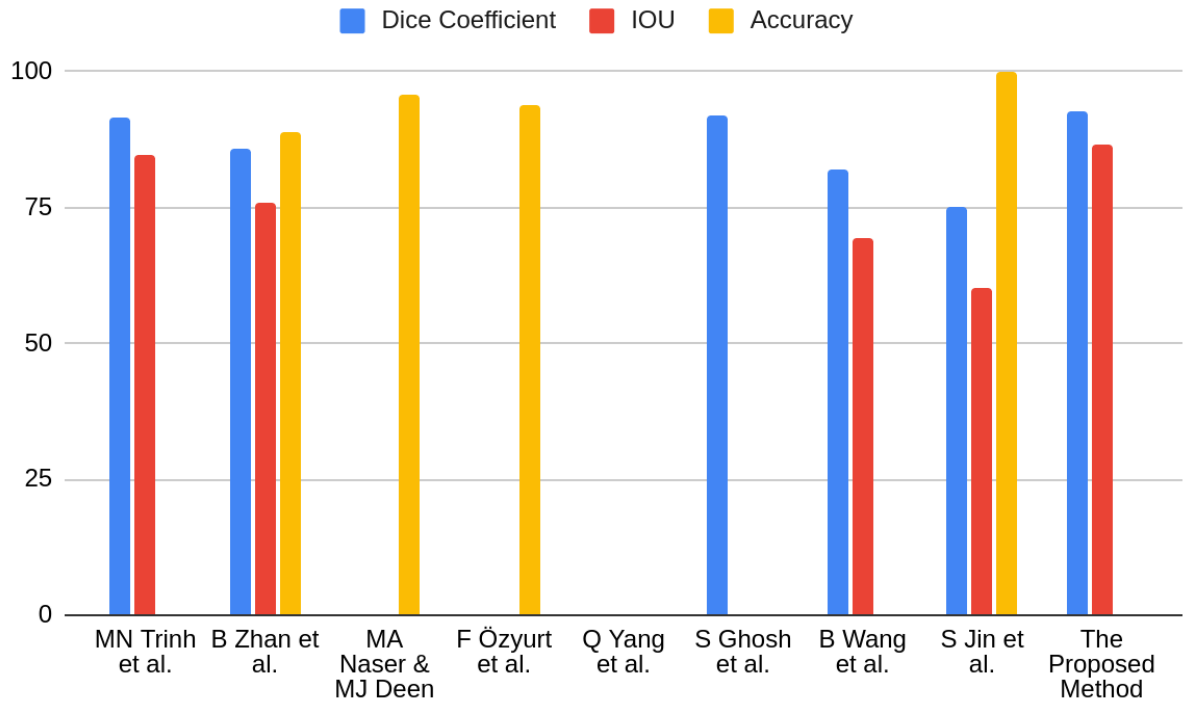


Figure 5.17: Benchmarking Proposed Method Against Existing Papers: A Comparative Study.

5.4.3. Proposed Brain Tumor Model Predictions

Figure 5.18 illustrates a sample prediction generated by the best-trained U-Net model. The image showcases the model's proficiency in accurately segmenting Brain tumors, highlighting its ability to delineate boundaries and identify areas of interest. This prediction exemplifies the model's robust performance in real-world scenarios, further emphasizing its potential for aiding in the automated diagnosis and treatment of Brain Tumor.

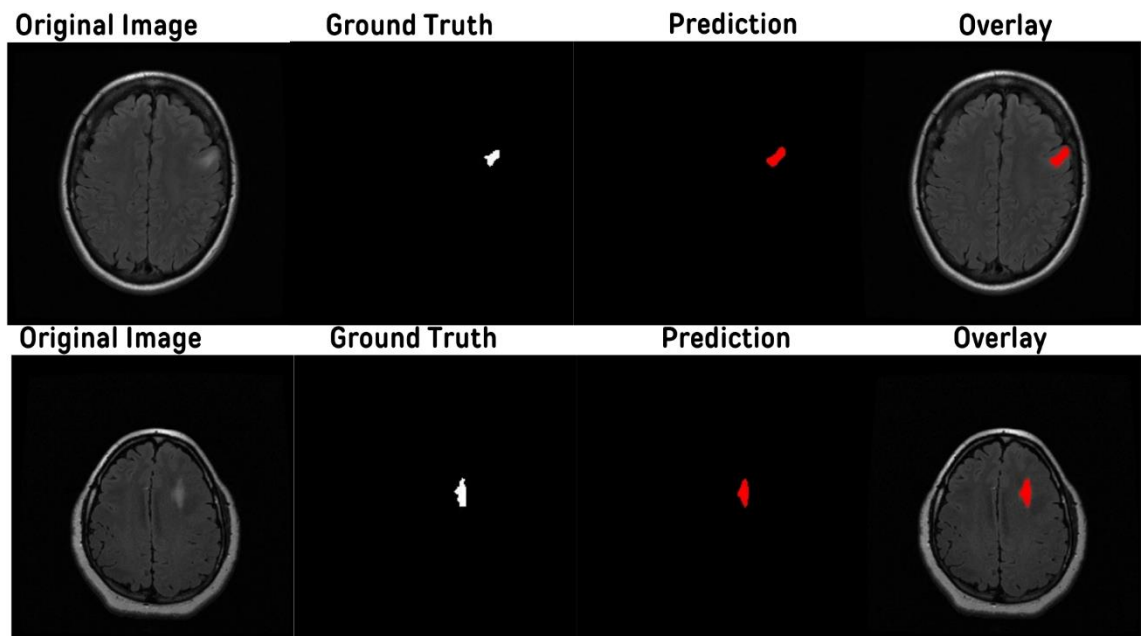


Figure 5.18 Sample prediction from the Brain segmentation model.

5.5. Business Value

- Precision Medical Diagnosis: Our AI project revolutionizes the accuracy and efficiency of skin and brain tumor diagnosis. Powered by advanced machine learning algorithms and extensive data sets, it offers reliable assessments, potentially reducing misdiagnoses and enabling early detection of cancerous growths.
- Efficiency and Cost Savings: Traditional diagnostic methods often entail time-consuming and costly procedures like biopsies or MRI scans. Our AI project provides a non-invasive and swift alternative, saving both time and resources for patients and healthcare providers alike.
- Accessible Healthcare Solutions: Leveraging the power of AI, our project extends diagnostic capabilities to regions with limited access to specialized medical expertise. Remote communities or underserved areas can benefit from timely and accurate assessments, leading to improved health outcomes.
- Empowering Healthcare Professionals: Rather than replacing healthcare professionals, our AI project serves as a valuable tool to augment their decision-making process. It offers additional insights and assists in prioritizing cases, enabling doctors to focus their expertise where it is most impactful.
- Continuous Advancements: Through ongoing refinement and updates, our AI project continuously enhances its diagnostic accuracy. By incorporating feedback from medical experts and accumulating more data over time, it remains at the forefront of cancer detection technology.

5.6. The Platforms GUI

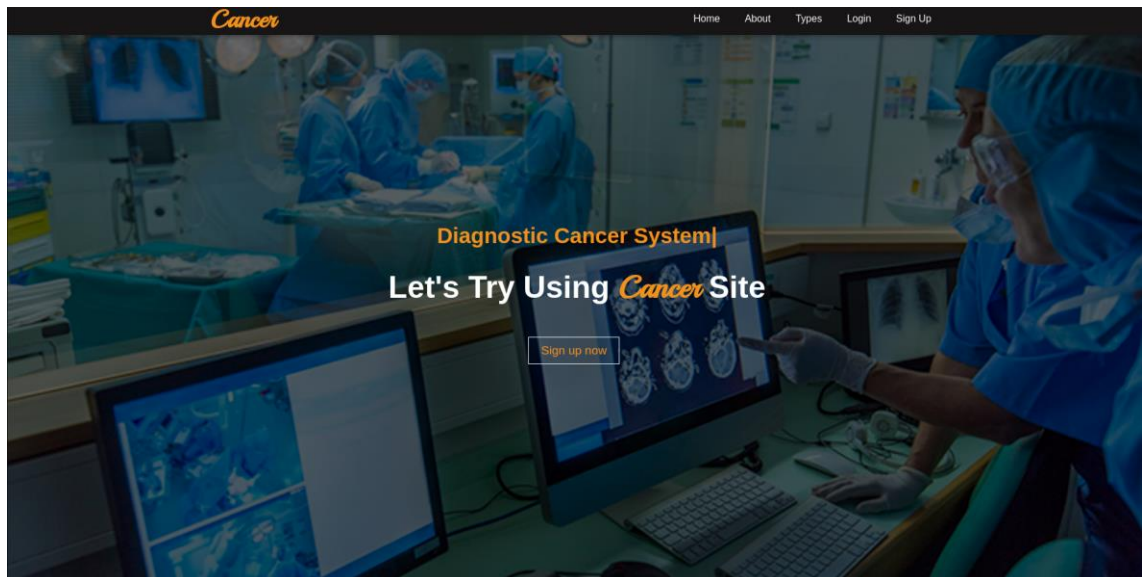


Figure 5.19 Home for the website.

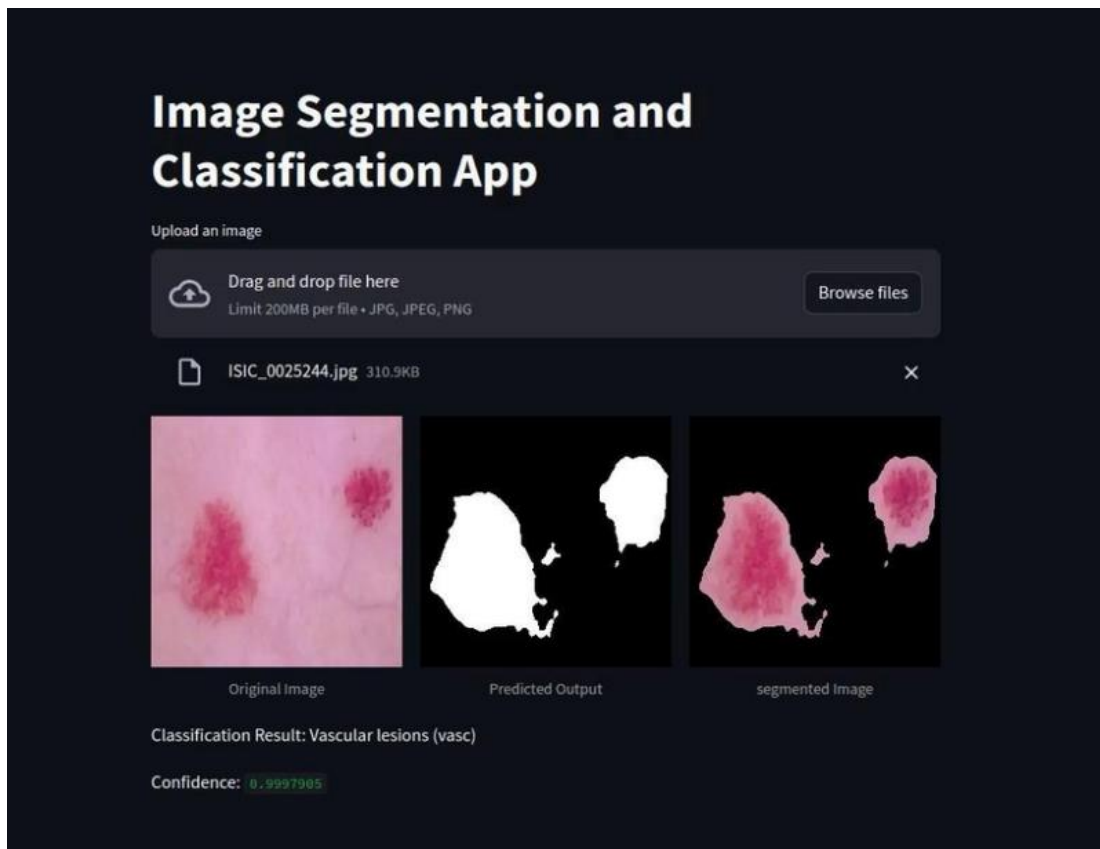


Figure 5.20 Streamlit APP for skin cancer.



Figure 5.21 Desktop APP.

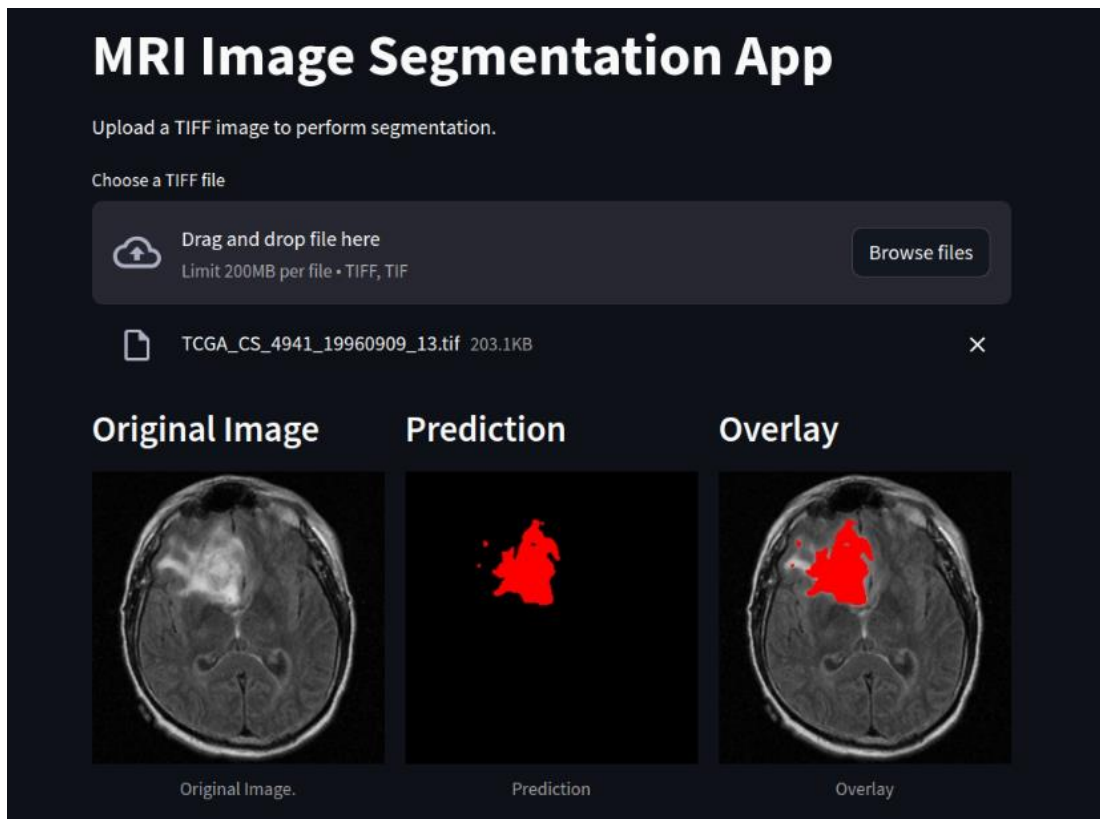


Figure 5.22 Streamlit APP for brain tumor.

Chapter Six

CONCLUSION

This thesis represents a significant stride forward in the realm of medical diagnostics, harnessing the power of technology to confront two of the most pressing health challenges: skin cancer and brain tumors. Through the development of a comprehensive project encompassing a website, desktop application, and Streamlit app, the potential for early detection and precise localization of these ailments has been greatly amplified.

By leveraging datasets like HAM1000 and PH2 for skin cancer classification and the LGG dataset for brain tumor segmentation, this project has laid the foundation for a transformative approach to healthcare. Through meticulous analysis and implementation of machine learning algorithms, coupled with intuitive user interfaces, this endeavor offers a beacon of hope for both patients and medical professionals alike.

Furthermore, at the heart of this project lie advanced deep learning architectures such as Convolutional Neural Networks (CNNs) and U-Net. These sophisticated models have been instrumental in extracting intricate patterns and features from medical imaging data, enabling the accurate classification of skin lesions and the precise segmentation of brain tumors. Through the fusion of these deep learning techniques with large-scale datasets, the efficacy of diagnostic processes has been significantly enhanced, paving the way for more timely interventions and personalized treatment strategies.

As the digital landscape continues to evolve, the fusion of technology and medicine becomes increasingly indispensable. This work not only showcases the capabilities of modern computational techniques but also underscores the imperative of interdisciplinary collaboration in addressing complex health issues. In the closing chapters of this book, we glimpse a future where the boundaries between traditional healthcare and cutting-edge innovation blur, ultimately leading to improved outcomes and enhanced quality of life for individuals worldwide.

Our future work aims to enhance our AI project's impact in healthcare through comprehensive data integration from diverse sources, including genomic data, patient medical histories, and environmental factors, to improve diagnostic accuracy and personalize treatments. We plan to extend our diagnostic capabilities to include multiple imaging modalities such as X-rays, CT scans, and histopathological images, allowing for comprehensive cancer diagnosis. Real-time monitoring features will be developed to track tumor growth and treatment response, aiding clinicians in adapting treatment strategies. Integrating our AI into clinical workflows with user-friendly interfaces will support healthcare professionals in making informed decisions. We will ensure regulatory compliance and ethical adherence by collaborating with authorities and legal experts. Additionally, we will create educational resources and interactive interfaces to empower patients with knowledge about their conditions and treatment options, fostering engagement and adherence to personalized health recommendations. This holistic approach aims to improve patient care and outcomes by seamlessly integrating advanced AI capabilities into the healthcare ecosystem.

Future Work

- Comprehensive Data Integration: Expand the scope of our AI project by integrating diverse datasets from various sources, including genomic data, patient medical histories, and environmental factors. This will enhance diagnostic accuracy and enable personalized treatment recommendations.
- Multi-Modal Diagnosis: Extend the capabilities of our AI project to encompass multiple imaging modalities beyond skin and brain scans. This could include X-rays, CT scans, or histopathological images, enabling comprehensive diagnosis across several types of cancer.
- Real-Time Monitoring: Develop features for real-time monitoring of tumor growth and treatment response. By analyzing sequential imaging studies, our AI project can track changes in tumor size and morphology, assisting clinicians in adapting treatment strategies accordingly.
- Clinical Decision Support: Integrate our AI project into clinical workflows to provide decision support for healthcare professionals. Develop user-friendly interfaces and algorithms that facilitate seamless interaction between the AI system and medical practitioners.
- Regulatory Compliance: Ensure compliance with regulatory standards and ethical guidelines governing the use of AI in healthcare. Collaborate with regulatory authorities and legal experts to navigate complex healthcare regulations and obtain necessary approvals for deployment.
- Patient Education and Engagement: Develop educational resources and interactive interfaces to empower patients with knowledge about their condition and treatment options. Foster patient engagement and adherence to treatment plans through personalized health recommendations generated by our AI project.

R e f e r e n c e s

- [1] S Panda, AS Tiwari, MR Prusty. Comparative study on different Deep Learning models for Skin Lesion Classification using transfer learning approach. International Journal of Scientific and Research Publications. 2021;11(1):219-32.
- [2] Y Wang, Y Wang, J Cai, TK Lee, C Miao, ZJ Wang. Ssd-kd: A self-supervised diverse knowledge distillation method for lightweight skin lesion classification using dermoscopic images. Medical Image Analysis. 2023 Feb 1;84:102693.
- [3] K Sirokin, M Escudero-Viñolo, P Carballeira, JC SanMiguel. Improved skin lesion recognition by a self-supervised curricular deep learning approach. arXiv preprint arXiv:2112.12086. 2021 Dec 22.
- [4] Aldhyani TH, Verma A, Al-Adhaileh MH, Koundal D. Multi-class skin lesion classification using a lightweight dynamic kernel deep-learning-based convolutional neural network. Diagnostics. 2022 Aug 24;12(9):2048.
- [5] S Maqsood, R Damaševičius. Multiclass skin lesion localization and classification using deep learning-based features fusion and selection framework for smart healthcare. Neural Networks. 2023 Mar 1;160:238-58.
- [6] AR Baig, Q Abbas, R Almakki, ME Ibrahim, L AlSuwaidan, AE Ahmed. Light-Dermo: A Lightweight Pretrained Convolution Neural Network for the Diagnosis of Multiclass Skin Lesions. Diagnostics. 2023 Jan 19;13(3):385.
- [7] B Shetty, R Fernandes, AP Rodrigues, R Chengoden, S Bhattacharya, K Lakshmanan. Skin lesion classification of dermoscopic images using machine learning and convolutional neural network. Scientific Reports. 2022 Oct 28;12(1):18134.
- [8] MS Ali, MS Miah, J Haque, MM Rahman, MK Islam. An enhanced technique of skin cancer classification using deep convolutional neural network with transfer learning models. Machine Learning with Applications. 2021 Sep 15;5:100036.
- [9] F Zhuang, Z Qi, K Duan, D Xi, Y Zhu, H Zhu, H Xiong, Q He. A comprehensive survey on transfer learning. Proceedings of the IEEE. 2020 Jul 7;109(1):43-76.
- [10] A Hosna, E Merry, J Gyambo, Z Alom, Z Aung, MA Azim. Transfer learning: a friendly introduction. Journal of Big Data. 2022 Oct 22;9(1):102.
- [11] A Mohammed, R Kora. A comprehensive review on ensemble deep learning: Opportunities and challenges. Journal of King Saud University-Computer and Information Sciences. 2023 Feb 1.
- [12] Y Nie, P Sommella, M Carratu, M Ferro, M O'nils, J Lundgren. Recent Advances in Diagnosis of Skin Lesions Using Dermoscopic Images Based on Deep Learning. IEEE Access. 2022 Aug 17.

- [13] D Popescu, M El-Khatib, L Ichim. Skin lesion classification using collective intelligence of multiple neural networks. *Sensors*. 2022 June 10;22(12):4399.
- [14] MA Khan, MY Javed, M Sharif, T Saba, A Rehman. Multi-model deep neural network based features extraction and optimal selection approach for skin lesion classification. In 2019 international conference on computer and Information Sciences (ICCIS) 2019 Apr 3 (pp. 1-7) Aljouf, Kingdom of Saudi Arabia. IEEE.
- [15] V Anand, S Gupta, A Altameem, SR Nayak, RC Poonia, AK Saudagar. An enhanced transfer learning-based classification for diagnosis of skin cancer. *Diagnostics*. 2022 Jul 5;12(7):1628.
- [16] TM Alam, K Shaukat, WAKhan, IAHameed, LA Almuqren, MA Raza, M Aslam, S Luo. An efficient deep learning-based skin cancer classifier for an imbalanced dataset. *Diagnostics*. 2022 Aug 31;12(9):2115.
- [17] S Aladhadh, M Alsanea, M Aloraini, T Khan, S Habib, M Islam. An effective skin cancer classification mechanism via medical vision transformer. *Sensors*. 2022 May 25;22(11):4008.
- [18] S Jain, U Singhania, B Tripathy, EA Nasr, MK Aboudaif, AK Kamrani. Deep learning-based transfer learning for classification of skin cancer. *Sensors*. 2021 Dec 6;21(23):8142.
- [19] MA Al-Masni, DH Kim, TS Kim. Multiple skin lesions diagnostics via integrated deep convolutional networks for segmentation and classification. *Computer methods and programs in biomedicine*. 2020 Jul 1;190:105351.
- [20] A Panthakkan, SM Anzar, S Jamal, W Mansoor. Concatenated Xception-ResNet50—A novel hybrid approach for accurate skin cancer prediction. *Computers in Biology and Medicine*. 2022 Nov 1;150:106170.
- [21] RD Seeja, A Suresh. Deep learning-based skin lesion segmentation and classification of melanoma using support vector machine (SVM). *Asian Pacific journal of cancer prevention: APJCP*. 2019;20(5):1555.
- [22] A Tajerian, M Kazemian, M Tajerian, A Akhavan Malayeri. Design and validation of a new machine-learning-based diagnostic tool for the differentiation of dermatoscopic skin cancer images. *PLoS One*. 2023 Apr 14;18(4):e0284437.
- [23] P Tschandl, C Rosendah, H Kittler. The HAM10000 dataset, a large collection of multi-source dermatoscopic images of common pigmented skin lesions. *Scientific Data*. 2018; 5: 180161. Search in. 2018;2.
- [24] SA Hicks, I Strümke, V Thambawita, M Hammou, MA Riegler, P Halvorsen, S Parasa. On evaluation metrics for medical applications of artificial intelligence. *Scientific reports*. 2022 Apr 8;12(1):5979.

- [25] SQ Nisa, AR Ismail. Comparative Performance Analysis of Deep Convolutional Neural Network for Gastrointestinal Polyp Image Segmentation.
- [26] B Wang, P Geng, T Li, Y Yang, X Tian, G Zhang, X Zhang. A deep model towards accurate boundary location and strong generalization for medical image segmentation. *Biomedical Signal Processing and Control*. 2024 Feb 1;88:105623.
- [27] MN Trinh, VD Nguyen, VT Pham, TT Tran. An EfficientNet-encoder U-Net Joint Residual Refinement Module with Tversky–Kahneman Baroni–Urbani–Buser loss for biomedical image Segmentation. *Biomedical Signal Processing and Control*. 2023 May 1;83:104631.
- [28] FP Poll, SK Shil, MA Hossain, A Ayman, YM Jan. Detection and classification of HGG and LGG brain tumor using machine learning. In *2018 International Conference on Information Networking (ICOIN)* 2018 Jan 10 (pp. 813-817). IEEE.
- [29] S Chatterjee, FA Nizamani, A Nürnberg, O Speck. Classification of brain tumours in MR images using deep spatiotemporal models. *Scientific Reports*. 2022 Jan 27;12(1):1505.
- [30] S Jin, S Yu, J Peng, H Wang, Y Zhao. A novel medical image segmentation approach by using multi-branch segmentation network based on local and global information synchronous learning. *Scientific Reports*. 2023 Apr 25;13(1):6762.
- [31] A Shomirov, J Zhang, MM Billah. Brain tumor segmentation of HGG and LGG MRI images using WFL-based 3D U-net. *Journal of Biomedical Science and Engineering*. 2022 Oct 28;15(10):241-60.
- [32] SG Choi, CB Sohn. Detection of HGG and LGG Brain Tumors using U-Net. *Medico-legal Update*. 2019 Jan 1;19(1).
- [33] MA Naser, MJ Deen. Brain tumor segmentation and grading of lower-grade glioma using deep learning in MRI images. *Computers in biology and medicine*. 2020 Jun 1;121:103758.
- [34] Q Yang, H Zhang, J Xia, X Zhang. Evaluation of magnetic resonance image segmentation in brain low-grade gliomas using support vector machine and convolutional neural network. *Quantitative Imaging in Medicine and Surgery*. 2021 Jan;11(1):300.
- [35] J Walsh, A Othmani, M Jain, S Dev. Using U-Net network for efficient brain tumor segmentation in MRI images. *Healthcare Analytics*. 2022 Nov 1;2:100098.
- [36] P Zheng, X Zhu, W Guo. Brain tumour segmentation based on an improved U-Net. *BMC Medical Imaging*. 2022 Nov 18;22(1):199.
- [37] R Ranjbarzadeh, A Bagherian Kasgari, S Jafarzadeh Ghoushchi, S Anari, M Naseri, M Bendechache. Brain tumor segmentation based on deep learning and an attention

mechanism using MRI multi-modalities brain images. *Scientific Reports*. 2021 May 25;11(1):1-7.

[38] A İşin, C Direkoglu, M Şah. Review of MRI-based brain tumor image segmentation using deep learning methods. *Procedia Computer Science*. 2016 Jan 1;102:317-24.

[39] S Ghosh, A Chaki, KC Santosh. Improved U-Net architecture with VGG-16 for brain tumor segmentation. *Physical and Engineering Sciences in Medicine*. 2021 Sep;44(3):703-12.

[40] F Ullah, M Nadeem, M Abrar, M Al-Razgan, T Alfakih, F Amin, A Salam. Brain Tumor Segmentation from MRI Images Using Handcrafted Convolutional Neural Network. *Diagnostics*. 2023 Aug 11;13(16):2650.

[41] Z Liu, L Tong, L Chen, Z Jiang, F Zhou, Q Zhang, X Zhang, Y Jin, H Zhou. Deep learning based brain tumor segmentation: a survey. *Complex & intelligent systems*. 2023 Feb;9(1):1001-26.

[42] B Zhan, E Song, H Liu, Z Gong, G Ma, CC Hung. CFNet: A medical image segmentation method using the multi-view attention mechanism and adaptive fusion strategy. *Biomedical Signal Processing and Control*. 2023 Jan 1;79:104112.

[43] SK Mathivanan, S Sonaimuthu, S Murugesan, H Rajadurai, BD ShivaHare, MA Shah. Employing deep learning and transfer learning for accurate brain tumor detection. *Scientific Reports*. 2024 Mar 27;14(1):7232.

[44] AM Zubair Rahman, M Gupta, S Aarathi, TR Mahesh, V Vinoth Kumar, S Yogesh Kumaran, S Guluwadi. Advanced AI-driven approach for enhanced brain tumor detection from MRI images utilizing EfficientNetB2 with equalization and homomorphic filtering. *BMC Medical Informatics and Decision Making*. 2024 Apr 30;24(1):113.

[45] F Özyurt, E Sert, E Avci, E Dogantekin. Brain tumor detection based on Convolutional Neural Network with neutrosophic expert maximum fuzzy sure entropy. *Measurement*. 2019 Dec 1;147:106830.



Skin Cancer Classification and Segmentation using Deep Learning

Citation: Elgohary, Rania; Tarek, Mostafa.; EzzAlRegal, Mohamed; Ahmed, Abdulrahman; Samir, Amr; Ehab, Nour; M.B. Badawi

*Inter. Jour. of Telecommunications, IJT'2024,
Vol. 04, Issue 01, pp. 01-23, 2024.*

Editor-in-Chief: Youssef Fayed.

Received: 01/04/2024.

Accepted: 10/05/2024.

Published: 10/05/2024.

Publisher's Note: The International Journal of Telecommunications, IJT, stays neutral regarding jurisdictional claims in published maps and institutional affiliations.



Copyright: © 2023 by the authors. Submitted for possible open access publication under the terms and conditions of the International Journal of Telecommunications, Air Defense College, ADC, (<https://ijt.journals.ekb.eg/>).

Rania Elgohary¹, Mostafa Tarek¹, Mohamed EzzAlRegal¹, Abdulrahman Ahmed¹, Amr Samir¹, Nour Ehab¹, and M.B. Badawy^{1,2,*}

¹ Department of Artificial Intelligence, College of Information Technology, Misr University for Science and Technology (MUST), 6th of October City 12566, Egypt.

² Mechanical Engineering Department, Faculty of Engineering, Alexandria University, El-Chatby, Alexandria 21544, Egypt.

* Correspondence author(s). E-mail(s): mohammed.badawi@must.edu.eg,

Contributing authors: Rania.elgohary@must.edu.eg, mostafat4438@gmail.com, mezz7409@gmail.com, abdulrahmn47@gmail.com, amrsalatif@gmail.com, nuorehaab21@gmail.com

Abstract: This paper integrates medical science and artificial intelligence, focusing on using convolutional neural networks (CNNs) to improve skin cancer diagnosis accuracy. Given the rising global incidence of skin cancers such as melanoma and basal cell carcinoma, this research is becoming increasingly important. This study uses the HAM10000 and PH2 datasets, which are known for their diverse skin cancer images, and employs a CNN-based approach informed by previous research findings.

The proposed methodology includes extensive preprocessing and augmentation to increase the dataset's variability, allowing for thorough training and evaluation. The CNN model, which was developed using advanced training methods and includes convolutional and pooling layers, is the result of previous research demonstrating the efficacy of CNNs in skin lesion detection. Furthermore, the U-NET-based segmentation model contributes to the comprehensive analysis by precisely delineating lesion boundaries, which improves the understanding of skin cancer. The CNN model's performance is evaluated using a variety of metrics, including accuracy, classification reports, confusion matrices, and segmentation-specific metrics like the Dice coefficient and IOU. These metrics provide valuable insights into the changing landscape of skin cancer diagnosis, allowing for the development of effective, precise, and accessible healthcare solutions in the dynamic field of dermatology. The experimental results for skin cancer classification are promising, indicating that the proposed approach outperforms other models. The best-trained classification model had an impressive 99.5% accuracy, 99.5% precision, and 99.5% recall. The test data was 97.204% accurate, 97.5% precise, and 97.2% recall. In addition, the U-NET model performed admirably in skin cancer lesion segmentation, with segmentation metrics such as an accuracy of 96.68%, precision of 95.39%, recall of 94.24%, Dice coefficient of 93.58%, and IOU of 97.09% for training data and an accuracy of 96.14%, precision of 93.44%, recall of 94.09%, Dice coefficient of 92.55%, and IOU of 96.43% for testing data.

Keywords: Deep learning; computer vision; skin cancer; multi-class classification; segmentation; PH2 dataset

Abbreviation	Definition
CNN	Convolutional Neural Network
VGG	Visual Geometry Group
Resnet	Residual Network
IOU	Intersection over Union
Lr	Learning Rate
SSD-KD	Single Shot MultiBox Detector with Knowledge Distillation
Xception	Extreme Inception
SVM	Support Vector Machine

1. Introduction

To improve diagnostic approaches for skin cancer, it is critical to understand the significant global concern caused by the disease's rising prevalence. Skin cancer, including types such as melanoma and basal cell carcinoma, represents a significant public health challenge, with its prevalence on the rise worldwide. Skin cancer, including types such as melanoma and basal cell carcinoma, represents a significant public health challenge, with its prevalence on the rise worldwide. Early detection and classification of skin lesions are critical for effective intervention and treatment. With sunlight exposure, genetic factors, and lifestyle choices all contributing to rising rates of skin cancer, there is an urgent need for novel solutions that can keep up with the growing demand for precise diagnostics.

This research is especially important considering this context, as it harnesses the capabilities of Convolutional Neural Networks (CNNs) and utilizes the HAM10000 and PH2 datasets to address the challenges of skin cancer diagnosis. By integrating medical expertise with innovative technology, the proposed study has the potential to revolutionize the field. Additionally, with the incorporation of the segmentation model, which precisely delineates lesion boundaries, this research offers a comprehensive approach to improving skin cancer diagnosis accuracy. In the broader context of dermatological healthcare, this study aims to make a significant contribution to the ongoing fight against skin cancer. By incorporating advanced deep learning techniques into the diagnostic process, we hope to provide a solution that not only addresses the current challenges posed by skin cancer but also anticipates and adapts to the changing landscape of this complex health issue.

Panda et al. [1] compared various deep learning models using a transfer learning approach, emphasizing the method's effectiveness in skin lesion classification. Similarly, Wang et al. [2] investigated deep learning-based melanoma segmentation and classification, with the latter developing the SSD-KD method, a self-supervised approach for lightweight classification. Sirotnik et al. [3] proposed an improved recognition system using a self-supervised curricular deep learning approach, while Aldhyani et al. [4] created a multi-class skin lesion classification system using a dynamic kernel deep-learning-based CNN. Maqsood and Damaševičius [5] proposed a framework for localizing and classifying multiple skin lesions, focusing on feature fusion and selection for smart healthcare applications. Similarly, Baig et al. [6] presented novel CNN-based diagnostic tools for multi-class skin lesions, emphasizing lightweight and machine-learning-based approaches.

Shetty et al. [7] and Ali et al. [8] emphasized the use of convolutional neural networks (CNNs) in skin lesion classification, leveraging machine learning techniques to improve accuracy. Zhuang et al. [9] and Hosna et al. [10] provided thorough overviews and introductions to transfer learning, a critical technique in this field. Additional studies by Mohammed and Kora [11], Nie et al. [12], and Popescu et al. [13] investigated the opportunities and challenges of ensemble deep learning, advances in dermoscopic image diagnosis, and neural network collective intelligence, respectively. Khan et al. [14] and Anand et al. [15] investigated the extraction and optimal selection of features for skin lesion classification via multi-model deep neural networks and enhanced transfer learning-based classification systems. Alam et al. [16], Aladhadh et al. [17], and Jain et al. [18] made additional contributions to the field by addressing issues with imbalanced datasets, the use of medical vision transformers, and transfer learning in skin cancer classification. Finally, Al-masni et al. [19] and Panthakkan et al. [20] proposed integrated deep convolutional networks and a novel hybrid approach that combines Xception and ResNet50 for accurate skin cancer prediction, respectively, building on the foundation laid by RD Seeja and A Suresh [21], who used deep learning for skin lesion segmentation and melanoma classification using SVM, and the diagnostic tool developed by A Tajerian et al. [22], who used machine learning for dermatoscopic skin cancer image differentiation, recent advances have significantly improved the field. Researchers have made significant progress by addressing challenges such as imbalanced datasets, integrating medical vision transformers, and leveraging transfer learning techniques.

This paper addresses the need to improve skin cancer diagnostic methods by combining medical science and artificial intelligence, with a focus on Convolutional Neural Networks (CNNs) for improved accuracy. Using the large HAM10000 dataset, which is known for its diverse skin cancer images, a CNN-based approach informed by previous research is employed. The dataset's variability is increased for training and evaluation through extensive preprocessing and augmentation.

2. Methodology

2.1. Data Collection

The datasets employed in this research are the "HAM10000" dataset and the "PH2" dataset. The "HAM10000" dataset comprises skin cancer images depicting various skin lesions. This dataset comprises a total of 10,015 images, each with dimensions (450, 600, 3). Each image is linked to a specific diagnosis, categorized into seven classes: Melanocytic nevi (nv), Melanoma (mel), Benign keratosis-like lesions (bkl), Basal cell carcinoma (bcc), Actinic keratoses (akiec), Vascular lesions (vasc), and Dermatofibroma (df). The dataset also provides additional information for each image, including diagnosis and age. The "PH2" dataset is another dataset used in this research, which consists of skin lesion images as well. It includes a total of 200 images, with dimensions of 768 × 560 pixels. These images were acquired in RGB color as BMP files.

2.2. Data Preprocessing

HAM10000: Following the retrieval of image files, all images were resized from 450x600 pixels to 28x28 pixels. Subsequently, the dataset was partitioned into training and testing sets, with 80% of the data allocated to the training set and the remaining 20% to the test set. Both the training and test sets were normalized to ensure consistency in the data distribution. Additionally, a label mapping was created, consisting of a dictionary that associates the names of the seven classes with key values ranging from 0 to 6, facilitating classification tasks.

PH2: All images were resized from 768x560 pixels to 224x224 pixels. Subsequently, the dataset was partitioned into training and testing sets, with 80% of the data allocated to the training set and the remaining 20% to the test set, ensuring a balanced distribution for training and evaluation. This resizing process enables compatibility with models that expect input images of uniform dimensions.

2.3. Data Augmentation

HAM10000: To address the class imbalance and augment the training dataset, various methods were employed. Skin images were augmented using transformations such as rotation, width shift, height shift, shear, horizontal flip, and vertical flip. This augmentation strategy increased the number of images from 10,015 to 45,756, while preserving identical dimensions of twenty-eight pixels in width, twenty-eight pixels in height, and three-color channels. By introducing variability into the training set, this augmentation approach enhances the model's generalization and robustness to different skin lesion variations.

PH2: Random rotation and horizontal flipping were applied to augment the PH2 dataset. These transformations introduce variations in the dataset, which helps in improving the model's ability to generalize to unseen data and enhances its robustness. This augmentation strategy diversifies the dataset while maintaining consistency in dimensions, facilitating more effective training of the model.

2.4. Model Architecture:

Classification using the HAM10000 dataset: The model consists of twelve layers. The model initiates with convolutional layers, proficient at capturing intricate patterns within images. The initial layer deploys sixteen filters, followed by a max-pooling layer strategically down-sampling spatial dimensions. This pattern iterates, progressively escalating complexity with 32, 64, and 128 filters in subsequent convolutional layers. The corresponding max-pooling layers strike a balance between preserving crucial features and reducing spatial dimensions, culminating in a final convolutional layer followed by a flattening operation. This transition readies the data for the fully connected layers, establishing a connection between spatial hierarchies and the dense layers. The subsequent dense layers, featuring 64 and 32 neurons, act as a potent feature extractor, refining the learned representations. The output is realized through a dense layer with seven neurons, each representing a distinct class in the present classification task. The SoftMax activation function ensures the model provides well-calibrated probabilities for each class, facilitating confident predictions. This comprehensive architecture carefully considers both spatial intricacies and hierarchical feature extraction, contributing to the model's robust performance in computer vision tasks. Figure 1 shows the used classification model architecture. Table 1 shows the hyperparameters for Classification Methodology.

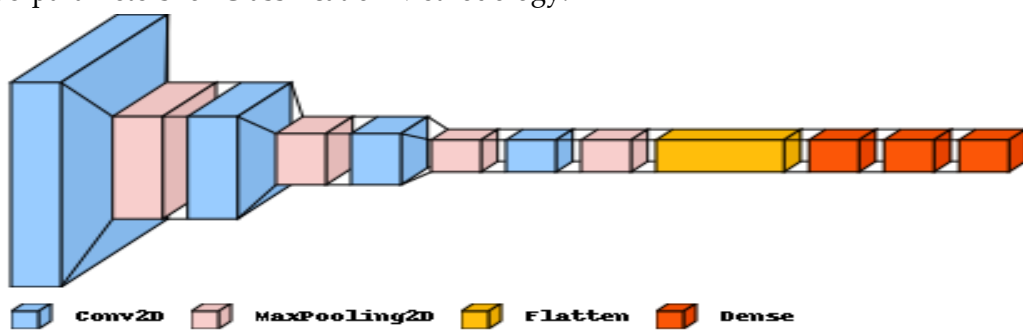


Figure 1: Proposed Classification Model Architectural Framework.

Table 1: Hyperparameters for classification process.

Hyperparameter	Value	Description
Learning Rate	0.001	The rate at which the model adjusts its weights during training.
Rotation Range	10	Range (in degrees) for random rotations applied to the images.
Width Shift Range	0.2	Range for random horizontal shifts applied to the images.
Height Shift Range	0.2	Range for random vertical shifts applied to the images.
Shear Range	0.2	Shear intensity (in radians) for geometric transformations.
Horizontal Flip	TRUE	Randomly flip images horizontally during training.
Vertical Flip	TRUE	Randomly flip images vertically during training.
Batch Size	64	Number of samples processed per gradient update during training.
Epochs	20	Number of complete passes through the entire training dataset.

Segmentation using the PH2 dataset: The model architecture includes one encoder and one decoder pathway. The encoder pathway initiates with four convolutional layers, followed by max-pooling layers for down-sampling, progressively increasing the complexity with deeper layers. Each convolutional block is composed of two convolutional layers with batch normalization and ReLU activation, ensuring effective feature extraction while mitigating the risk of overfitting. Additionally, spatial dropout is incorporated to enhance the model's robustness by introducing randomness during training.

The decoder pathway mirrors the encoder in terms of the number of layers, with four transposed convolutional layers for up-sampling. These layers are used to sample the feature maps to the original image resolution. This symmetric architecture facilitates the precise localization of skin lesion boundaries. Furthermore, the final layer employs a 1x1 convolution followed by a sigmoid activation function. Figure 2 shows the used Segmentation model architecture.

The Jaccard distance loss function is used to train the model by calculating the difference between predicted and ground truth segmentation masks. The segmentation model is trained for 100 epochs with the Adam optimizer and a learning rate of 0.003. Throughout the training process, different evaluation measures such as Intersection over Union (IoU), Dice coefficient, precision, recall, and accuracy are tracked to assess the model's performance on both the training and validation sets. Table 2 shows the hyperparameters for Segmentation Methodology.

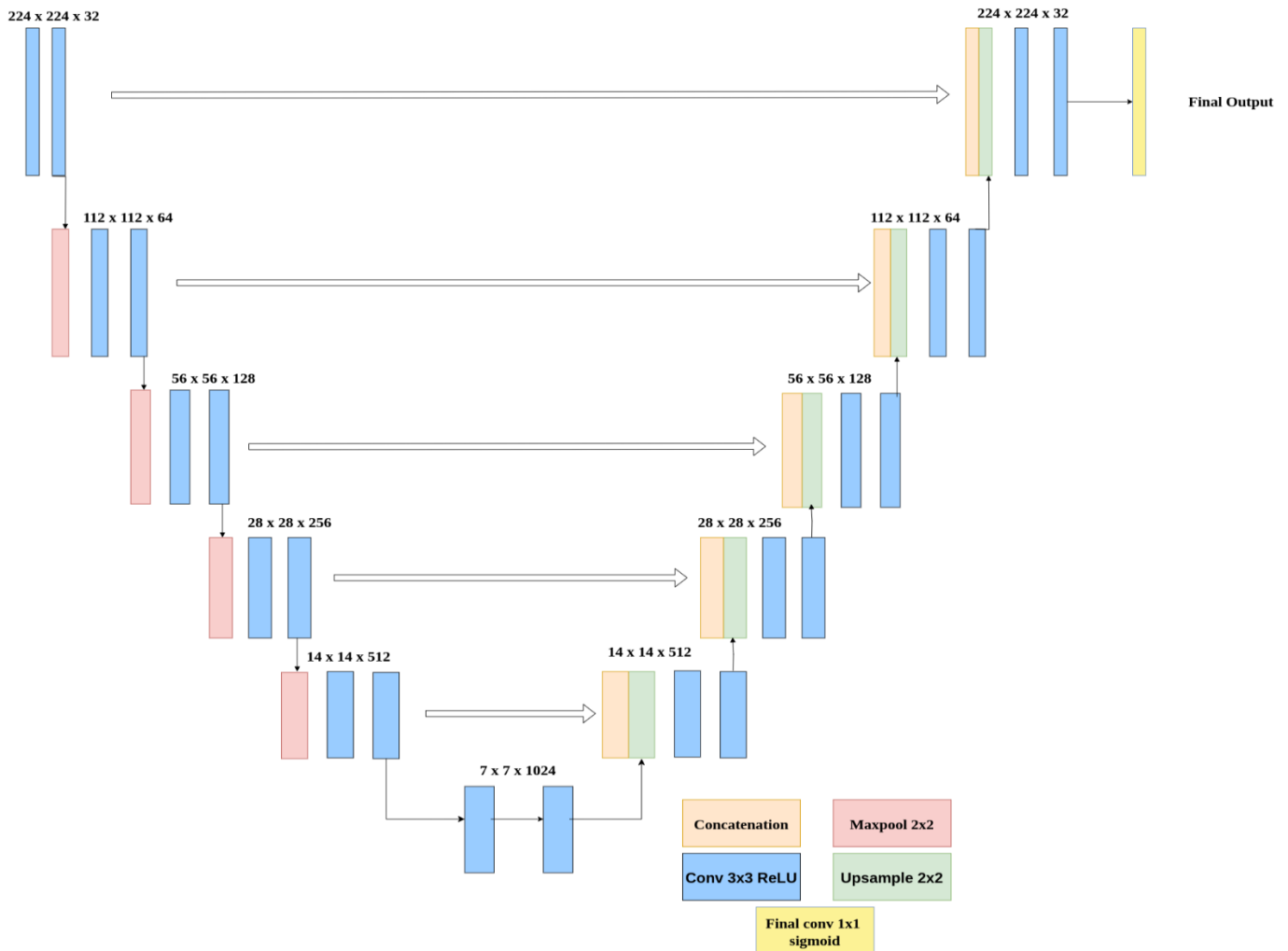


Figure 2: Segmentation Model Architectural Framework.

Table 2: Hyperparameters for Segmentation process.

Hyperparameter	Value	Description
Rotation Range	-40 to 40	Range (in degrees) for random rotations applied to the images.
Horizontal Flip	TRUE	Randomly flip images horizontally during training.
Dropout	0.4	Dropout rate for spatial dropout applied to convolutional layers.
Learning Rate	0.003	The rate at which the model adjusts its weights during training.
Optimizer	Adam	Optimizer algorithm used for training the model.
Batch Size	16	Number of samples processed per gradient update during training.
Epochs	Variable	Number of complete passes through the entire training dataset.

3. Dataset Insights

The HAM10000 dataset [23], also known as the Human Against Machine with ten thousand training images dataset, features high-quality images of skin lesions. It encompasses several types of skin lesions, ranging from benign to malignant. The lesions are categorized into seven distinct classes. However, there is an imbalance among the classes in the dataset, as illustrated in Table 3 and Figure 3.

Table 3: Class Distribution Analysis of the dataset.

Class	Counts
Melanocytic nevi (nv)	6705
Melanoma (mel)	1113
Benign keratosis-like lesions (bkl)	1099
Basal cell carcinoma (bcc)	514
Actinic keratoses and intraepithelial carcinoma (akiec)	327
Vascular lesions (vasc)	142
Dermatofibroma (df)	115

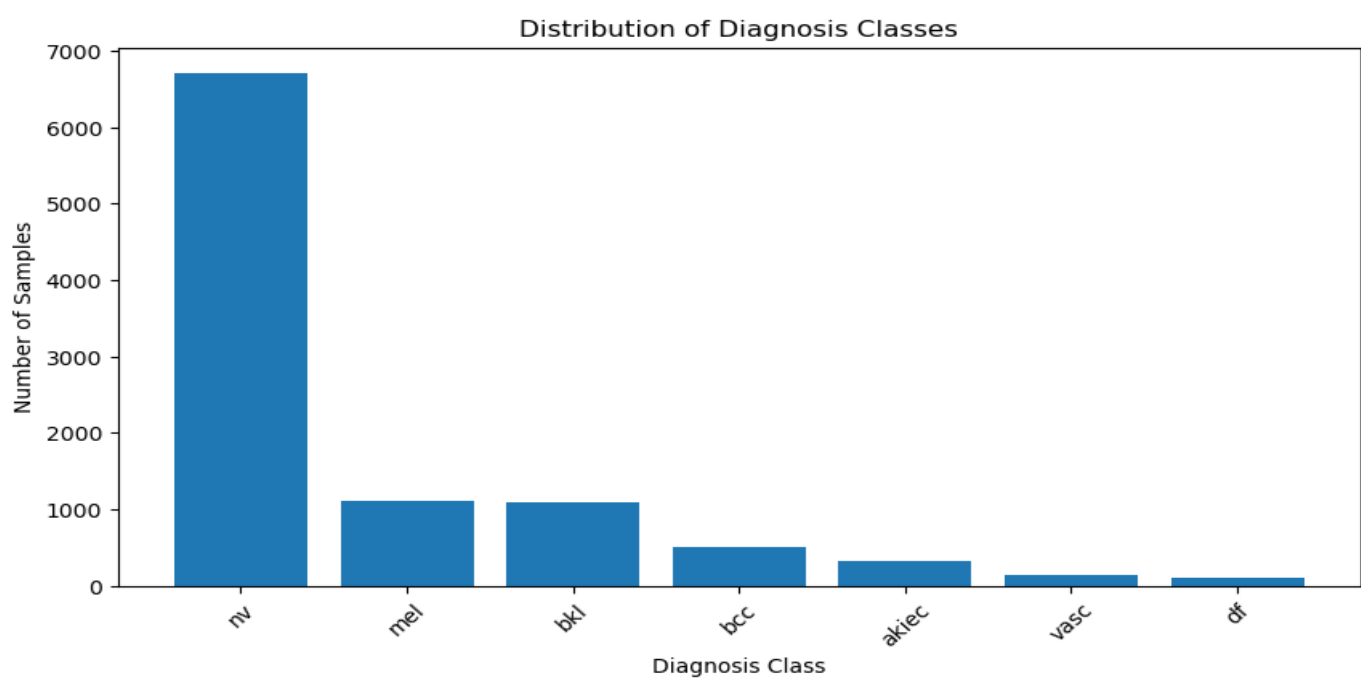


Figure 3: Class Distribution Analysis of the dataset.

To address the challenge of an unbalanced dataset within the HAM1000 dataset, a strategy of duplicating images was employed for augmentation purposes. This duplication process did not result in any new augmentation transformations, and to preserve the NV class's integrity in the HAM1000 dataset, no augmentation tech-

niques were used. During data preparation for training and testing, augmentation transformations such as rotation, shifting, and flipping were applied to the training set only, leaving the original dataset unchanged.

Table 4 and Figure 4 summarize the data augmentation strategies used to address the unbalanced dataset in HAM1000. The approach involved duplicating images for augmentation without introducing new transformations, while maintaining the integrity of the NV class. Augmentation techniques such as rotation, shifting, and flipping were exclusively applied to the training set.

Table 4: Class Distribution after using the factor.

Class	Counts	Factor used	Counts + (Counts*factor) + Counts
Melanoma (mel)	1113	4	6678
Benign keratosis-like lesions (bkl)	1099	4	6594
Basal cell carcinoma (bcc)	514	11	6682
Actinic keratoses and intraepithelial carcinoma (akiec)	327	17	6213
Vascular lesions (vasc)	142	45	6674
Dermatofibroma (df)	115	52	6210

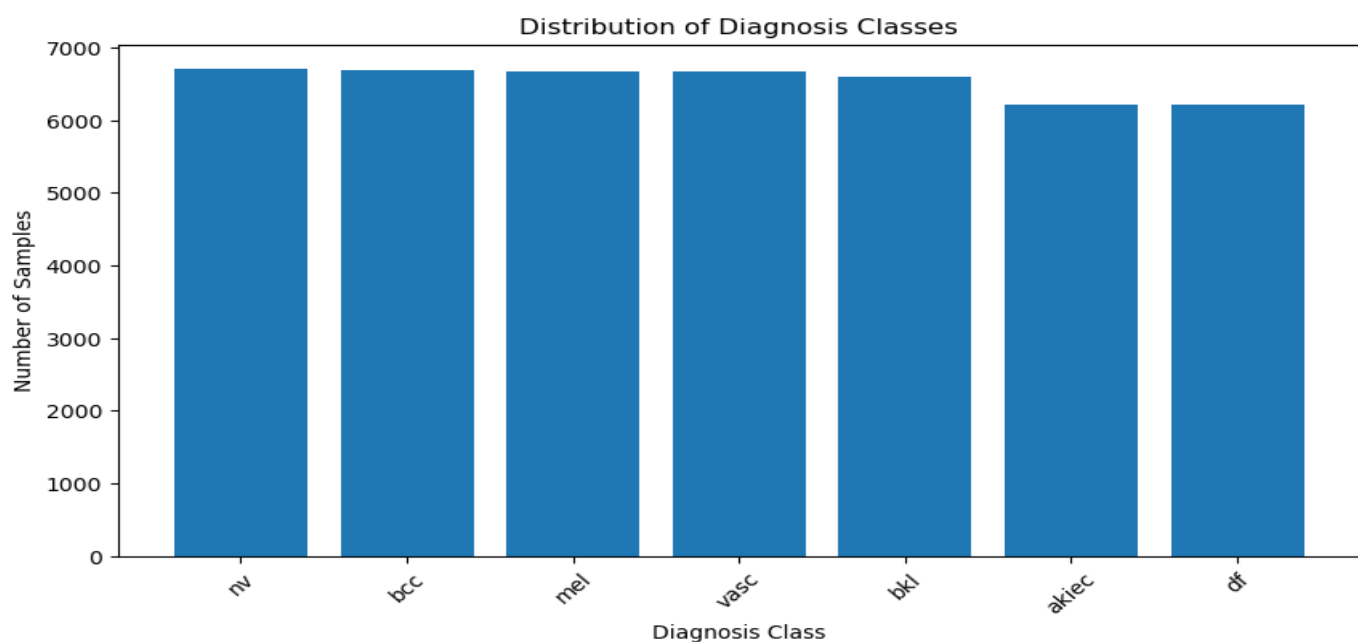


Figure 4: All Class Distribution after using the factor.

The PH2 dataset [20] is a well-known dataset in the field of dermatology and medical image analysis. It consists of 200 high-resolution images acquired in RGB color format as BMP files, with dimensions of 768×560 pixels.

4. Evaluation Metrics for both classification and segmentation

Before we delve into the results obtained from training various deep learning algorithms on the HAM10000 and PH2 datasets for predicting skin cancer, it is essential to understand the significance of each metric used in the evaluation process. Accuracy, precision, and recall for classification and Jaccard Distance, Intersection over Union (IoU), Dice Coefficient, precision, recall, and Accuracy for segmentation.

4.1 Accuracy [24]

Definition: Accuracy is a measure of the overall correctness of the model. It calculates the ratio of correctly predicted instances to the total instances.

$$\text{Accuracy} = \frac{\text{True Positives} + \text{True Negatives}}{\text{Total Predictions}} \quad (1)$$

Usefulness: While accuracy provides a general sense of how well the model is performing, it might not be the best metric for imbalanced datasets. In the case of skin cancer classification, where the occurrence of malignant cases might be significantly lower than benign cases, accuracy alone may not provide a complete picture.

4.2 Precision [24]

Definition: Precision measures the accuracy of positive predictions. It calculates the ratio of true positives to the total predicted positives.

$$\text{Precision} = \frac{\text{True Positives}}{\text{True Positives} + \text{False Positives}} \quad (2)$$

Usefulness: Precision is crucial in scenarios where false positives are costly. In skin cancer classification, high precision means that when the model predicts a sample as malignant, it is likely to be correct. It is particularly important in medical contexts where misdiagnosing benign cases as malignant could lead to unnecessary treatments.

4.3 Recall [24]

Definition: Recall measures the ability of the model to capture all the relevant instances. It calculates the ratio of true positives to the total actual positives.

Equation:

$$\text{Recall} = \frac{\text{TruePositives}}{\text{TruePositives} + \text{FalseNegatives}} \quad (3)$$

Usefulness: Recall is vital when the cost of false negatives is high. In the context of skin cancer classification, high recall indicates that the model is effective in identifying malignant cases, minimizing the chances of missing potentially dangerous lesions.

4.4 Jaccard Distance [25]

Definition: The Jaccard distance, also known as the Intersection over Union (IoU), quantifies the dissimilarity between the predicted and ground truth segmentation masks. It measures the ratio of the intersection to the union of the two masks. A lower Jaccard distance indicates better segmentation accuracy.

$$JaccardIndex = \frac{|A \cap B|}{|A \cup B|} \quad (4)$$

$$JaccardDistance = 1 - JaccardIndex \quad (5)$$

Where:

- A and B are the ground truth and predicted segmentation masks, respectively.
- $|A \cap B|$ denotes the number of pixels common to both masks.
- $|A \cup B|$ represents the total number of pixels in both masks.

Usefulness: Jaccard distance is useful for evaluating the similarity between two segmentation masks. It provides a measure of how well the predicted segmentation aligns with the ground truth. A lower Jaccard distance indicates better segmentation accuracy.

4.5 Intersection over Union (IoU) [25]

Definition: IoU is a measure of the overlap between the predicted and ground truth segmentation masks. It calculates the ratio of the intersection to the union of the two masks, providing insights into the model's ability to accurately delineate skin lesion boundaries. Higher IoU values signify better segmentation performance.

$$IoU(A, B) = \frac{|A \cap B|}{|A \cup B|} \quad (6)$$

Where:

- A and B are the ground truth and predicted segmentation masks, respectively.
- $|A \cap B|$ denotes the number of pixels common to both masks.
- $|A \cup B|$ represents the total number of pixels in both masks.

Usefulness: IoU is commonly used in image segmentation tasks to assess the quality of segmentation results. Higher IoU values indicate better agreement between the predicted and ground truth segmentation masks, reflecting improved segmentation accuracy.

4.6 Dice Coefficient [25]

Definition: The Dice coefficient assesses the similarity between the predicted and ground truth segmentation masks. It computes the ratio of twice the intersection to the sum of the volumes of the two masks. A higher Dice coefficient indicates greater overlap and similarity between the predicted and ground truth masks.

Equation:

$$Dice(A, B) = \frac{2|A \cap B|}{|A| + |B|} \quad (7)$$

Where:

- A and B are the ground truth and predicted segmentation masks, respectively.
- $|A \cap B|$ denotes the number of pixels common to both masks.
- $|A|$ and $|B|$ denotes the total number of pixels in each mask.

Usefulness: The Dice coefficient is particularly useful in evaluating the performance of segmentation models. It provides a robust measure of segmentation accuracy, especially in scenarios with class imbalance, where accurately capturing small structures is essential.

5. Results and Discussion

5.1. Results for classification

As shown in Table 5 and Figure 5, DeepConvNet achieved the highest accuracy, precision, and recall scores, indicating its effectiveness in accurately classifying skin cancer lesions. Auto Encoder, while having a relatively high precision score, exhibited lower accuracy and recall scores compared to DeepConvNet, suggesting that it may have struggled with correctly identifying some instances of skin cancer. CNN decay lr, VGG16, ResNet50, InceptionV3, and Xception all demonstrated varying degrees of performance, with accuracy, precision, and recall scores falling below those of DeepConvNet but still showcasing some level of effectiveness in skin cancer classification.

Table 5: Performance Analysis: Metric Comparison across Training Algorithms.

Training Metrics			
Model Name	Accuracy	Precision	Recall
DeepConvNet	99.5	99.5	99.5
Auto Encoder	70.17	82.26	58.09
CNN with decay lr	81.23	89.72	73.28
VGG16	67.13	84.03	54.65
ResNet50	66.99	66.99	66.99
InceptionV3	66.97	85.86	54.2
Xception	66.8	85.92	54.31

Training Metrics Scores

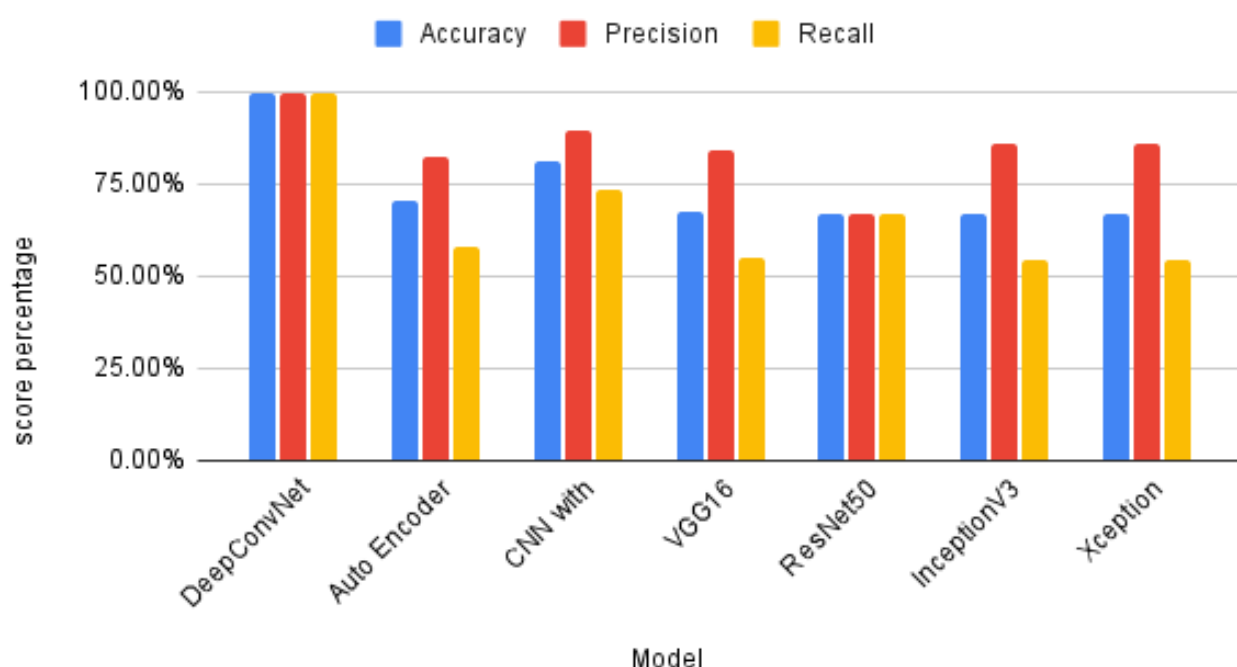


Figure 5: Performance Analysis: Metric Comparison across Training Algorithms.

Table 6 and Figure 6 show that the DeepConvNet outperformed all other testing algorithms in terms of accuracy, precision, and recall, demonstrating its ability to accurately categorize skin cancer lesions.

Table 6: Performance Analysis: Metric Comparison across Testing Algorithms.

Testing Metrics			
Model Name	Accuracy	Precision	Recall
DeepConvNet	97.204	97.5	97.2
Auto Encoder	70.17	82.49	58.17
CNN with decay lr	73.64	81.1	67.9
VGG16	66.99	83.52	60.03
ResNet50	66.83	66.83	66.83
InceptionV3	66.89	85.19	60.58
Xception	66.73	83.29	61.04

Testing Metrics Scores

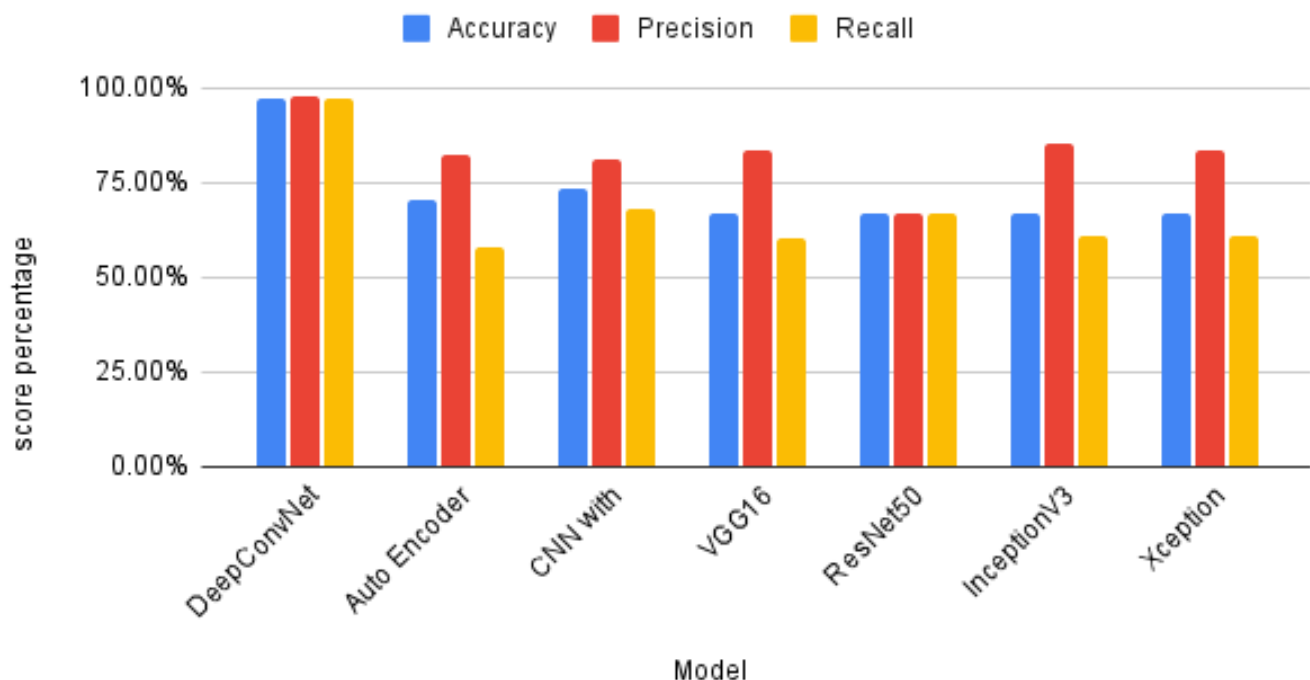


Figure 6: Performance Analysis: Metric Comparison across Testing Algorithms.

Figure 7 illustrates the progressive enhancement in accuracy over time, showcasing the positive trend in performance as training progresses.

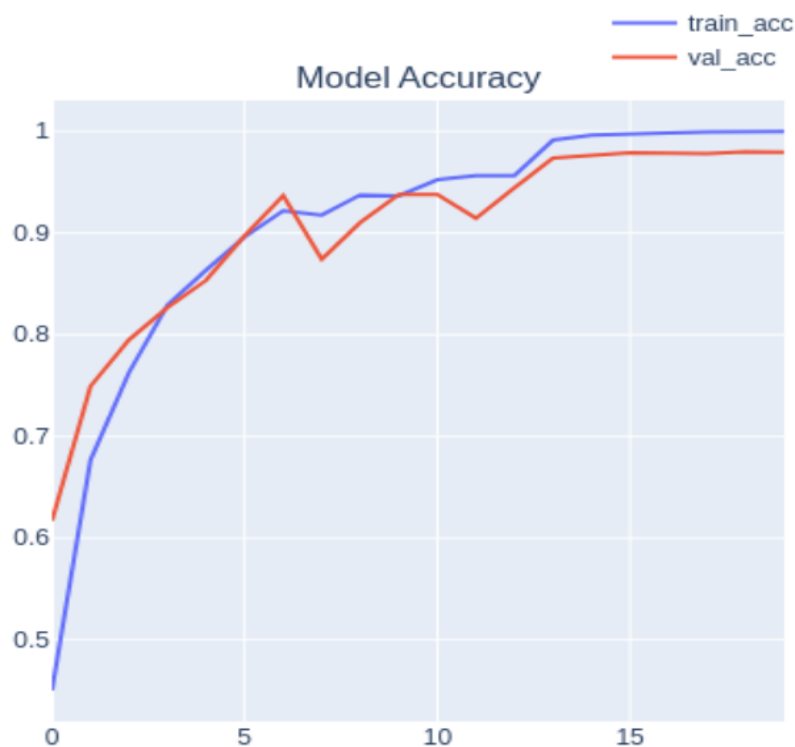


Figure 7: Tracking Progress: Evaluation of Accuracy for Proposed Model Architecture.

Figure 8 demonstrates the concurrent decline in loss over time, highlighting the iterative refinement and optimization of the model.



Figure 8: Tracking Progress: Evaluation of Loss for Proposed Model Architecture.

Figure 9 provides a visual representation of the model's performance through a confusion matrix graph for each class of data on the test set, including its performance on the unbalanced classes, as presented in Table and Figure 3. Each row in the confusion matrix corresponds to the actual class labels, while each column represents the predicted class labels. The values in the cells of the matrix indicate the number of instances that were classified into each class.

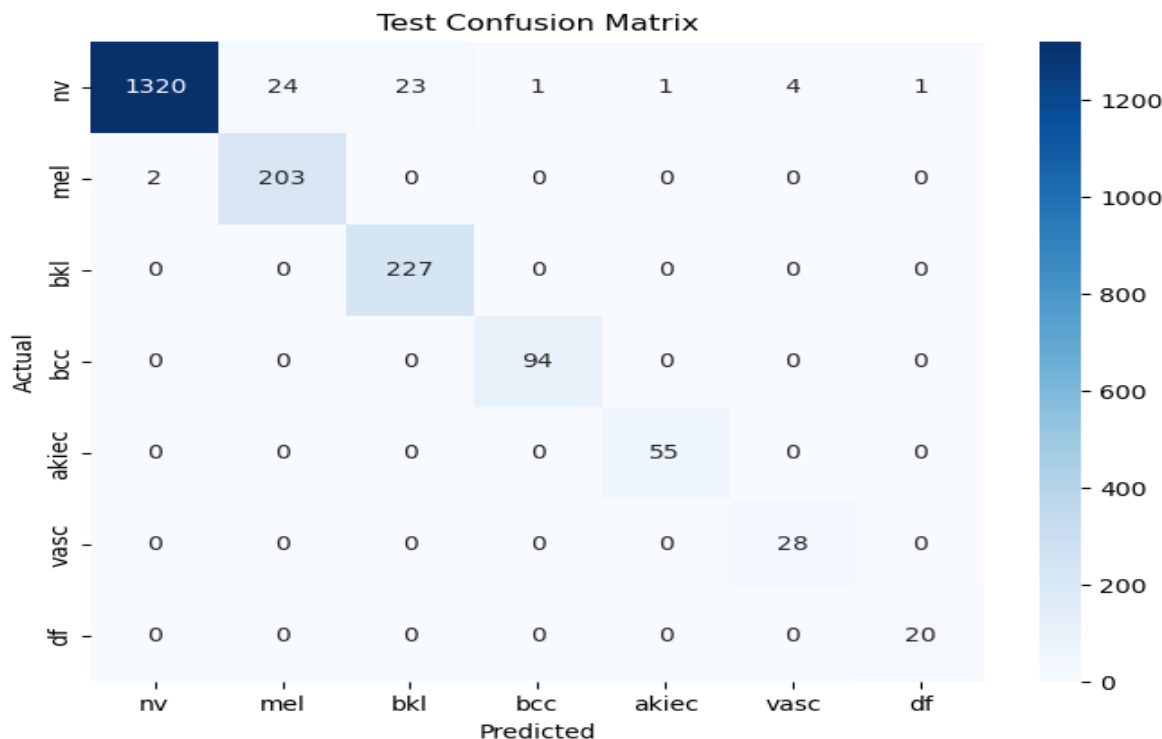


Figure 9: Visualizing Model Performance: Confusion Matrix Graph for Test Data.

This research paper provides a comprehensive overview of recent advances in skin lesion classification using deep learning models. The complexities of improving diagnostic accuracy and efficiency in skin disease detection are examined in detail using a variety of methodologies demonstrated by leading researchers, including transfer learning, knowledge distillation, and innovative network architectures.

1. S Panda et al. [1]: The research paper on skin lesion classification utilizing Deep Learning models employed various methods to achieve its objectives. The study utilized transfer learning with pre-trained models such as VGG16, ResNet50, InceptionV3, and Xception to classify skin lesions into different categories. The models were trained on a dataset consisting of images of various skin diseases, including melanoma, nevus, and seborrheic keratosis. The training process involved 30 epochs with a batch size of 16 for training and 10 for validation.

2. Y Wang et al. [2]: In a comparative study of skin lesion classification methods, deep learning models, traditional machine learning algorithms, and knowledge distillation techniques have been evaluated for their effectiveness in improving diagnostic accuracy. Deep learning models have shown promise in achieving higher accuracy rates due to their ability to learn complex patterns. Knowledge distillation techniques aim to enhance the performance of lightweight models by transferring knowledge from larger models. These methods have demonstrated improvements in accuracy, sensitivity, and specificity in skin lesion classification tasks. Lever-

aging advanced techniques like knowledge distillation can enhance the diagnostic accuracy of skin disease classification, contributing to more efficient diagnostic tools for skin diseases.

3. TH Aldhyani et al. [4]: The study focuses on the development and implementation of a lightweight dynamic kernel deep-learning-based convolutional neural network for multi-class skin lesion classification. The methodology employed in the research includes the use of variable size kernels and activation functions in the network, with a strategic allocation of fewer kernels in the initial layers for efficient utilization. Additionally, class-wise data balancing was performed to ensure unbiased training.

4. S Maqsood & R Damaševičius [5]: In this study on multiclass skin lesion localization and classification using deep learning, a novel approach was developed to enhance the accuracy and efficiency of skin cancer detection. The methodology involved the utilization of a customized Convolutional Neural Network (CNN) for automatic feature extraction, incorporating well-known networks such as Xception, ResNet-50, ResNet-101, and VGG16 to reduce computation time. The feature selection process was optimized using a unique Univariate Measurement of Pairwise Dependence (UMPD) approach, which effectively selected the best features for recognition.

5. B Shetty et al. [7]: In this research study on skin lesion classification, a variety of methods were employed to enhance the accuracy of the classification models. Machine learning models including Decision Tree, Random Forest, Support Vector Machine, K-Nearest Neighbor, Logistic Regression, Gaussian Naïve Bayes, and Linear Discriminant Analysis were evaluated, with Random Forest exhibiting the highest accuracy among them.

6. MS Ali et al. [8]: The research focuses on utilizing a deep convolutional neural network (DCNN) model combined with transfer learning techniques to enhance the classification of skin cancer based on dermoscopy images. The proposed DCNN model was developed to accurately classify skin lesions, particularly in the early stages of cancer. By training the model on a large dataset and fine-tuning it over multiple epochs, the researchers achieved significant improvements in classification accuracy compared to existing deep learning models. The results demonstrated that the DCNN model outperformed traditional transfer learning models such as AlexNet, ResNet, VGG-16, DenseNet, and MobileNet in terms of accuracy and execution time. Through a comprehensive evaluation on the HAM10000 dataset, the DCNN model showed superior performance in distinguishing between benign and malignant skin lesions, with promising implications for early detection and treatment of skin cancer.

7. V Anand et al. [15]: The research focuses on enhancing the classification of skin cancer through a transfer learning approach using the VGG16 architecture. The proposed model incorporates additional layers, including a flatten layer and dense layers with LeakyReLU and sigmoid activation functions, to improve accuracy. Data augmentation techniques are employed during pre-processing to increase dataset randomness and stability.

8. TM Alam et al. [16]: In their study of an Efficient Deep Learning-Based Skin Cancer Classifier for an Imbalanced Dataset, Alam et al. used a comprehensive methodology to address the challenges posed by imbalanced data.

9. S Aladhadh et al. [17]: In their research employed a two-tier framework to address the challenges associated with accurate skin cancer classification. The first stage involved data augmentation techniques to enhance the training dataset, mitigating issues related to insufficient labeled data. Subsequently, they developed a Medical Vision Transformer (MVT)-based classification model for skin cancer. This innovative approach involved splitting input images into patches and feeding them to the transformer in a sequence structure, akin to word embedding. The final classification was performed using a Multi-Layer Perceptron (MLP). The experimental results, conducted on the Human Against Machine (HAM10000) dataset, demonstrated the superiority of the proposed MVT-based model over existing state-of-the-art techniques.

10. RD Seeja & A Suresh [21]: The study focuses on utilizing deep learning technology for skin lesion segmentation and classification of melanoma. The methodology employed in this research involves the initial segmentation of dermoscopy images using a Convolutional Neural Network (CNN) based U-net algorithm. Subsequently, color, texture, and shape features are extracted from the segmented images using techniques such as Local Binary Pattern (LBP), Edge Histogram (EH), Histogram of Oriented Gradients (HOG), and Gabor method. These extracted features are then fed into various classifiers including Support Vector Machine (SVM), Random Forest (RF), K-Nearest Neighbor (KNN), and Naïve Bayes (NB) for the diagnosis of melanoma or benign lesions.

11. A Tajerian et al. [22]: In this study, we employed a methodological approach that leveraged dermoscopy images from the HAM10000 dataset to develop a machine-learning-based diagnostic tool for the classification of dermatoscopic skin cancer images. The process involved image pre-processing techniques such as labeling, resizing, and data augmentation to enhance the dataset. Transfer learning was utilized to create a model architecture based on EfficientNET-B1, incorporating a global average pooling 2D layer and a softmax layer with 7 nodes for classification.

Table 7 and Figure 10 present a comparison between the proposed method, implemented through the Deep-ConvNet architecture, and several previous research papers. Various training metrics, including accuracy, precision, and recall, are used for each model.

Table 7: Comparison between the proposed method and the other papers.

Training Metrics			
Paper	Accuracy	Precision	Recall
S Panda et al. [1]	-	97	95.2
Y Wang et al. [2]	84.6	-	-
TH Aldhyani et al. [4]	97.8	98.1	98
S Maqsood & R Damaševičius [5]	98.57	-	-
B Shetty et al. [7]	91.77	-	-
MS Ali et al. [8]	93.16	96.57	93.66
V Anand et al. [15]	89.09	-	-

TM Alam et al. [16]	91	-	-
S Aladhadh et al. [17]	96.14	96	96.50
RD Seeja & A Suresh [21]	85.19	42.59	50
A Tajerian et al. [22]	94	88	85
Current Proposed Method DeepConvNet	99.5	99.5	99.5

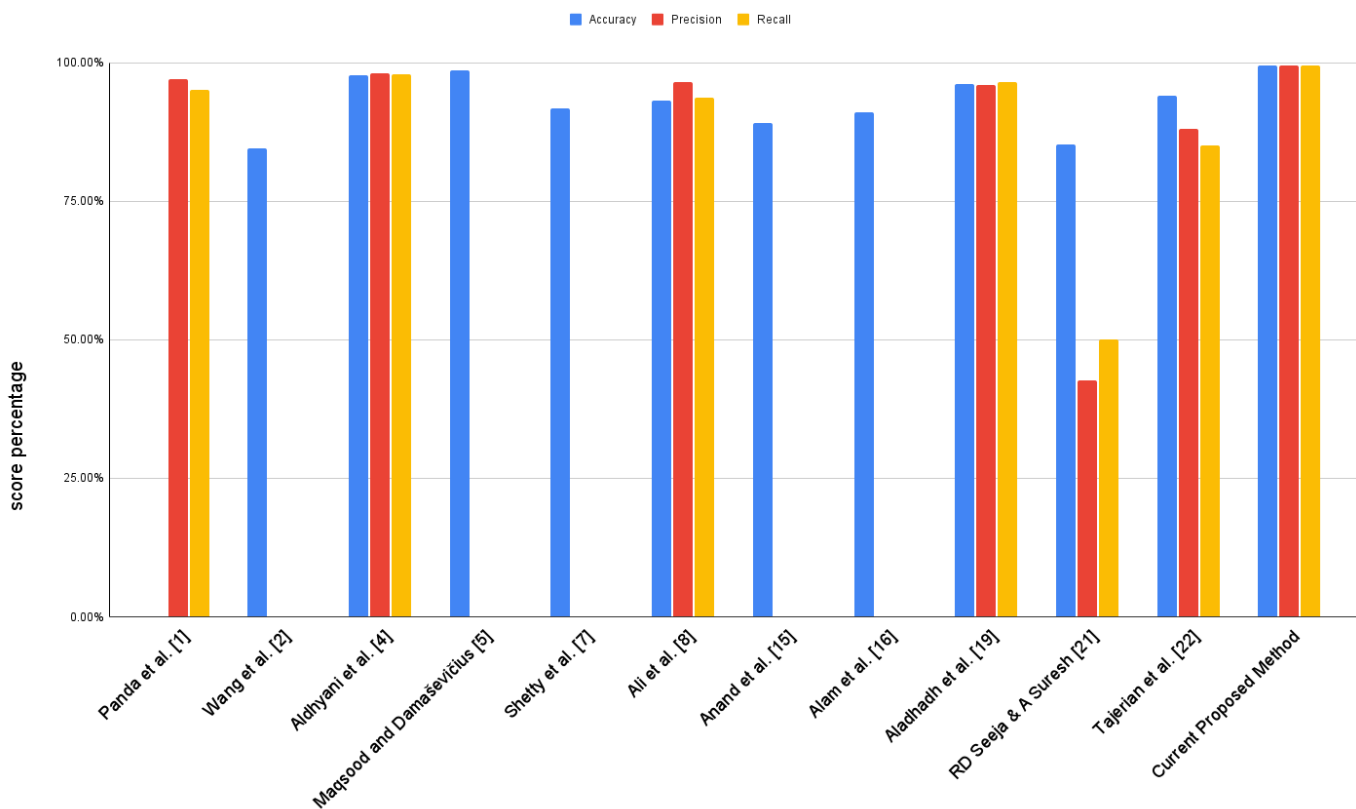


Figure 10: Benchmarking Proposed Method Against Existing Papers: A Comparative Study.

5.2. Results for Segmentation

In Table 8 and Fig 11, the U-Net model's performance metrics are examined across both training and testing datasets. The U-Net model achieves high accuracy, precision, recall, Dice Coefficient, and IoU scores, underscoring its efficacy in accurately segmenting skin cancer lesions.

Table 8: Performance Analysis: Metric Comparison across Training and Testing Sets.

Training Metrics					
Model Name	Accuracy	Precision	Recall	Dice Coefficient	IoU
U-NET	96.68	95.39	94.24	93.58	97.09
Testing Metrics					
Model Name	Accuracy	Precision	Recall	Dice Coefficient	IoU
U-NET	96.14	93.44	94.09	92.55	96.43



Figure 11: Performance Analysis: Metric Comparison across Training and Testing Sets.

Figures 12, 13, and 14 illustrate the progressive enhancement in accuracy, accompanied by a concurrent decline in Jaccard loss and improvement in Dice Coefficient, IoU, precision, and recall over time. These visuals represent the iterative refinement and optimization of the model, showcasing a positive trend in performance as training progresses.

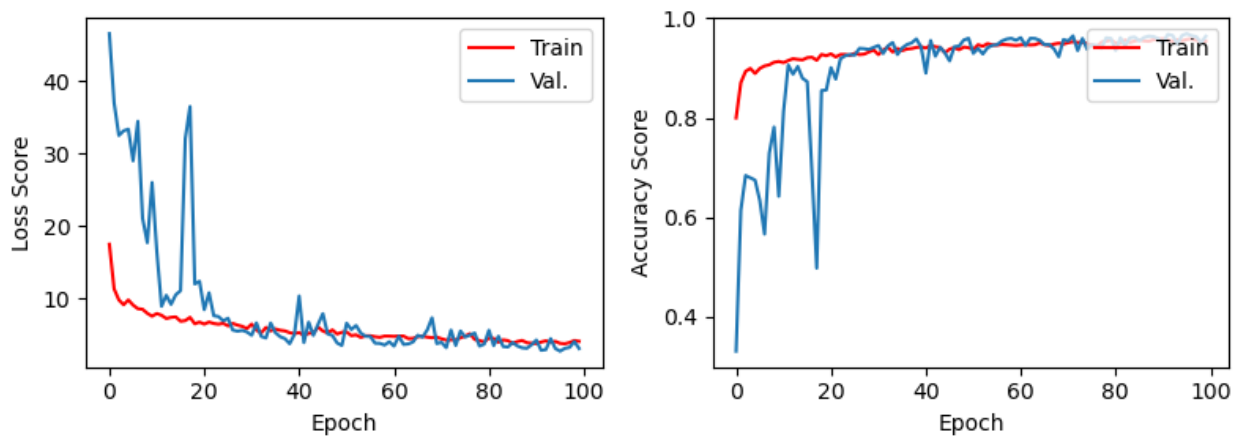


Figure12: Tracking Progress: Evaluation of Jaccard Loss and Accuracy for the Model Architecture.

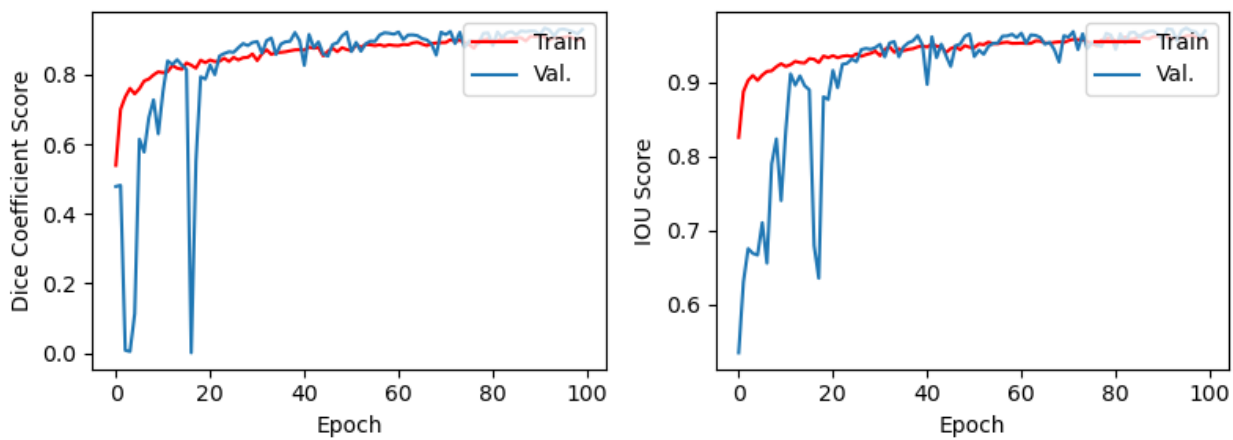


Figure 13: Tracking Progress: Evaluation of Dice Coefficient and IoU for Proposed Model Architecture.

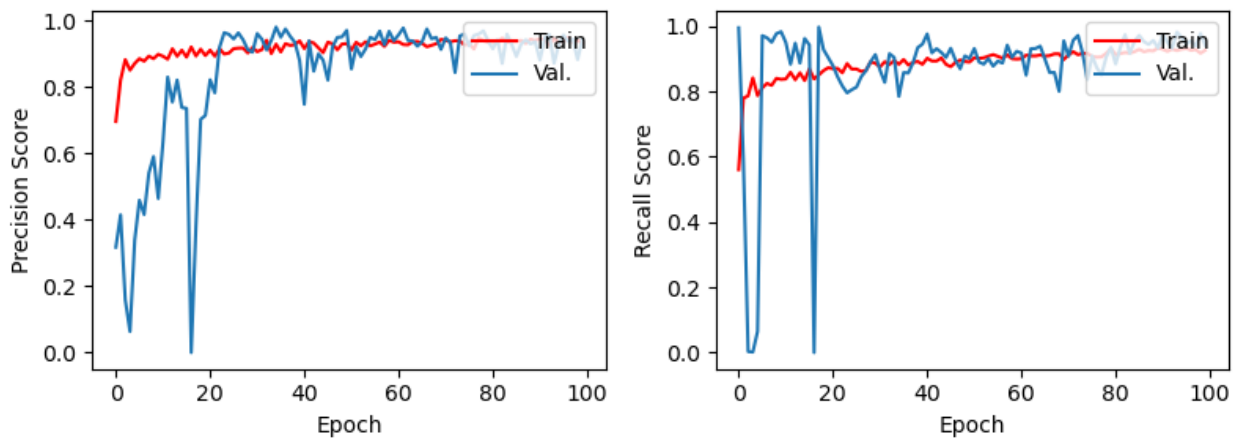


Figure 14: Tracking Progress: Evaluation of precision and recall for Proposed Model Architecture.

5.3 Proposed Model Prediction

In Fig 15, several predictions from the suggested model are showcased. This visual representation offers a model's performance by displaying examples of its predictions for skin cancer lesions. These predictions provide insights into how the model categorizes and classifies different types of lesions. The suggested model performs well across all seven classes, despite the imbalance in data distribution as illustrated in Figure 3. When the model predicts accurately, the confidence level typically falls within the 97%–100% range. Figures 16 and 17 show several predictions from the U-net segmentation model.

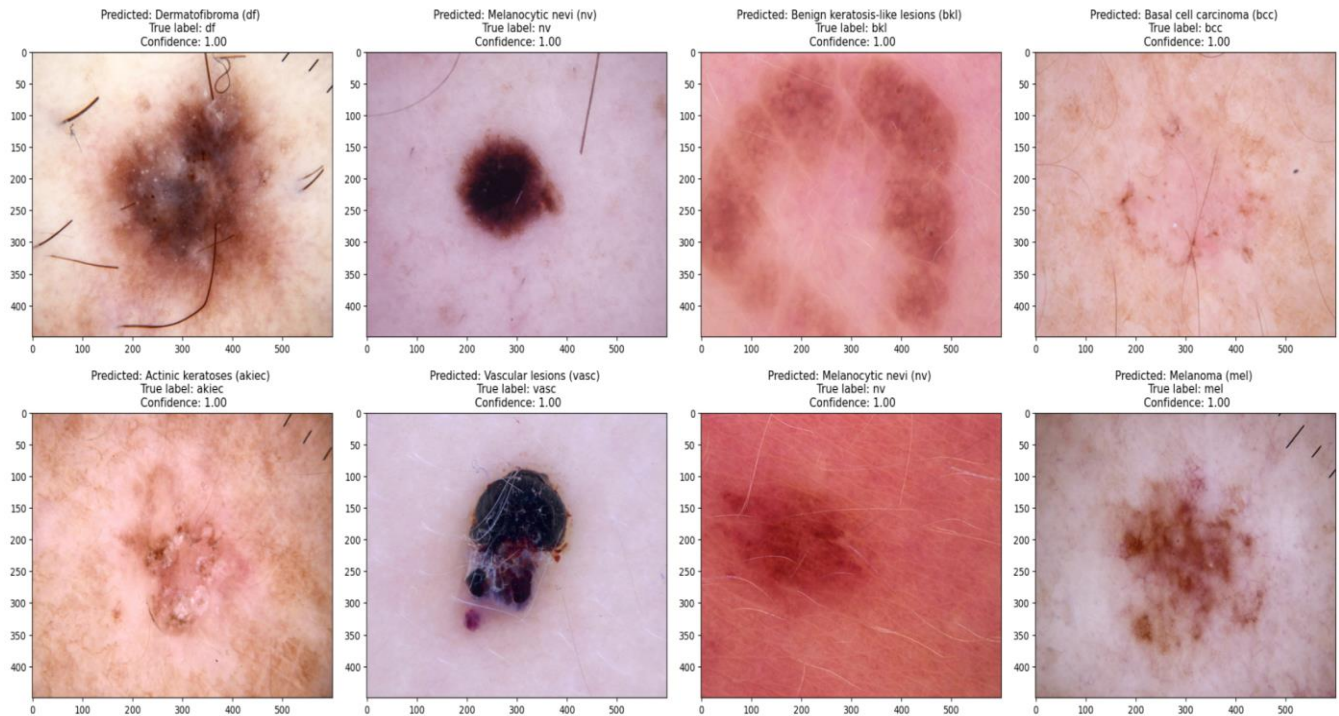


Figure 15: Sample classification predictions from the suggested model.

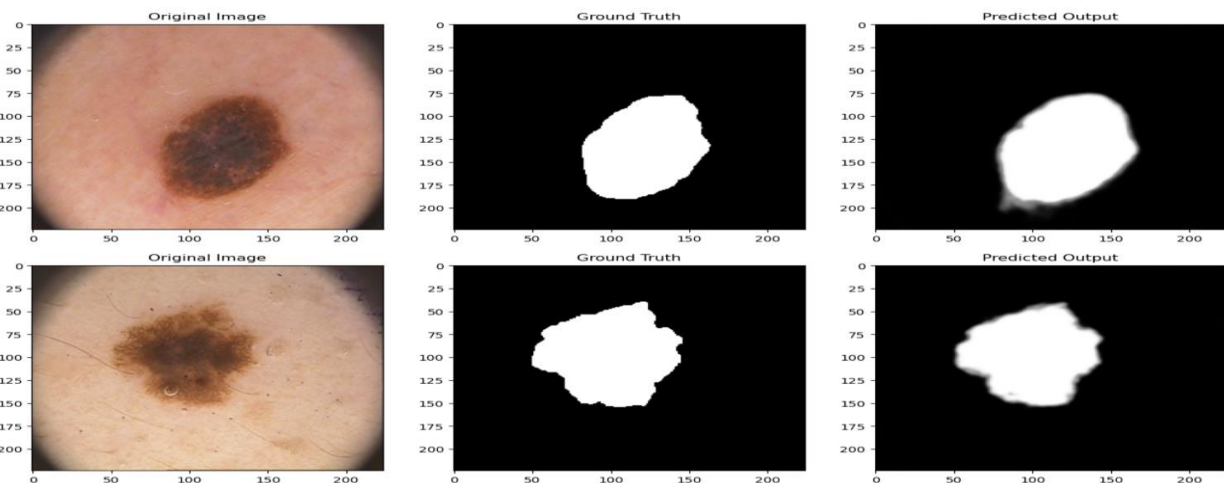


Figure 16: Sample predictions from the segmentation model.

Combining segmentation and classification models represents a promising approach to improving skin cancer diagnostic systems. In this integrated framework, the segmentation model precisely defines the lesion boundaries of skin cancer, effectively isolating the affected areas. These segmented regions are then localized or cropped and sent to the classification model for further analysis and diagnosis. Figure 17 illustrates this process by depicting the sequential workflow in which segmented lesions are accurately identified and then classified to determine the specific type of skin cancer. By combining these two methodologies, we can leverage the strengths of segmentation for precise delineation and classification for accurate diagnosis, ultimately improving the efficiency and reliability of skin cancer detection systems.

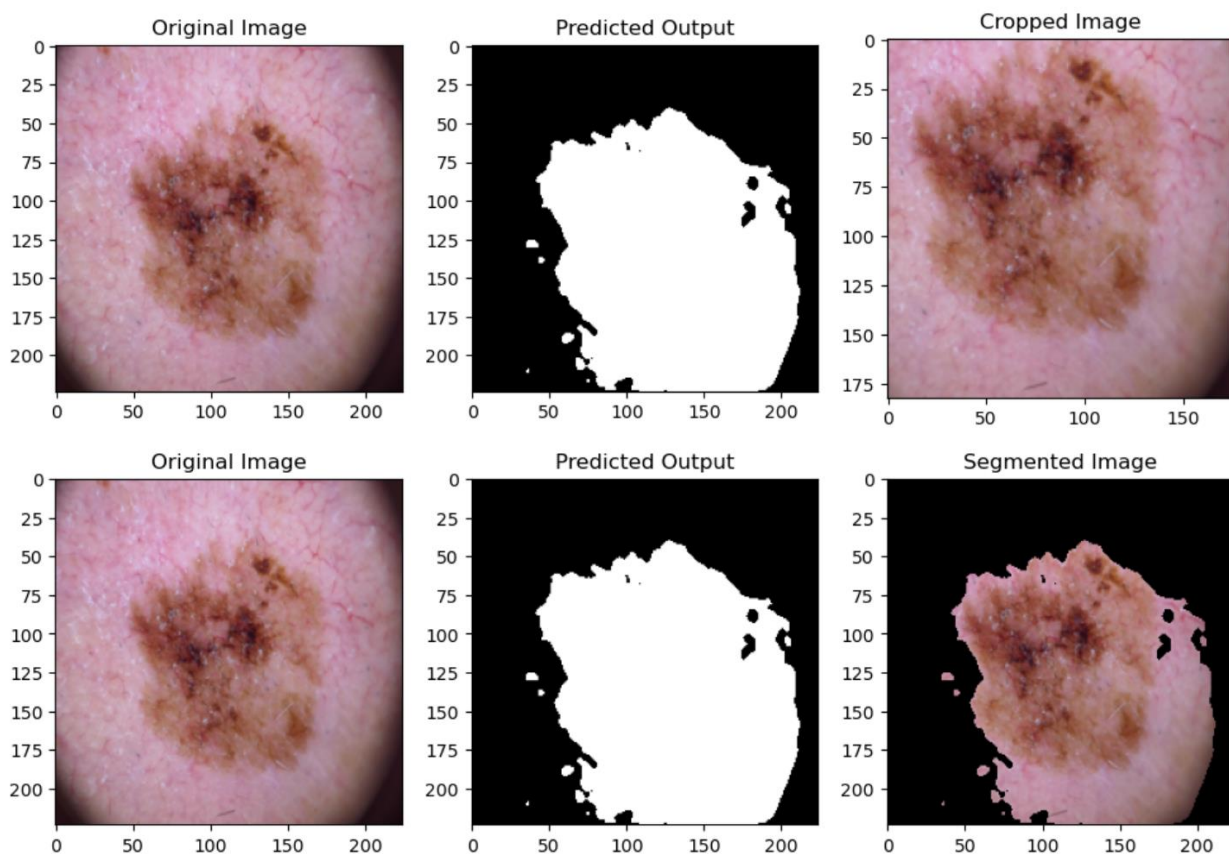


Figure 17: Segmentation-Driven Skin Cancer Diagnosis Model

7. Conclusion

The research highlights the significant advances made at the intersection of medical science and artificial intelligence, particularly in skin cancer diagnosis. The study found that integrating convolutional neural networks (CNNs) and leveraging the HAM10000 and PH2 datasets improved the accuracy and reliability of skin cancer classification and segmentation. The research proposed DeepConvNet architecture emerged as a front-runner, outperforming existing algorithms in accurately identifying several types of skin cancer lesions. With accuracy, precision, and recall scores of 99.5%, our model demonstrated its ability to accurately diagnose skin cancer lesions with unprecedented precision. The results obtained from the segmentation phase of our study underscore its pivotal role in advancing skin cancer diagnostics. Through segmentation, we achieved precise delineation of lesion boundaries, enabling accurate localization and isolation of affected areas. This level of precision not only enhances the efficiency of subsequent diagnostic processes but also facilitates targeted analysis by focusing exclusively on relevant regions of interest.

Finally, our research adds significantly to the ongoing efforts in dermatology healthcare by providing an innovative and accessible solution for skin cancer diagnosis. By leveraging the power of CNNs and advanced deep learning techniques, our proposed method paves the way for efficient, precise, and scalable solutions to reduce the global burden of skin cancer.

References

1. S Panda, AS Tiwari, MR Prusty. Comparative study on different Deep Learning models for Skin Lesion Classification using transfer learning approach. International Journal of Scientific and Research Publications. 2021;11(1):219-32.

2. Y Wang, Y Wang, J Cai, TK Lee, C Miao, ZJ Wang. Ssd-kd: A self-supervised diverse knowledge distillation method for light-weight skin lesion classification using dermoscopic images. *Medical Image Analysis*. 2023 Feb 1;84:102693.
3. K Sirotkin, M Escudero-Viñolo, P Carballeira, JC SanMiguel. Improved skin lesion recognition by a self-supervised curricular deep learning approach. *arXiv preprint arXiv:2112.12086*. 2021 Dec 22.
4. Aldhyani TH, Verma A, Al-Adhaileh MH, Koundal D. Multi-class skin lesion classification using a lightweight dynamic kernel deep-learning-based convolutional neural network. *Diagnostics*. 2022 Aug 24;12(9):2048.
5. S Maqsood, R Damaševičius. Multiclass skin lesion localization and classification using deep learning-based features fusion and selection framework for smart healthcare. *Neural Networks*. 2023 Mar 1;160:238–58.
6. AR Baig, Q Abbas, R Almakki, ME Ibrahim, L AlSuwaidan, AE Ahmed. Light-Dermo: A Lightweight Pretrained Convolution Neural Network for the Diagnosis of Multiclass Skin Lesions. *Diagnostics*. 2023 Jan 19;13(3):385.
7. B Shetty, R Fernandes, AP Rodrigues, R Chengoden, S Bhattacharya, K Lakshmann. Skin lesion classification of dermoscopic images using machine learning and convolutional neural network. *Scientific Reports*. 2022 Oct 28;12(1):18134.
8. MS Ali, MS Miah, J Haque, MM Rahman, MK Islam. An enhanced technique of skin cancer classification using deep convolutional neural network with transfer learning models. *Machine Learning with Applications*. 2021 Sep 15;5:100036.
9. F Zhuang, Z Qi, K Duan, D Xi, Y Zhu, H Zhu, H Xiong, Q He. A comprehensive survey on transfer learning. *Proceedings of the IEEE*. 2020 Jul 7;109(1):43–76.
10. A Hosna, E Merry, J Gyalmo, Z Alom, Z Aung, MA Azim. Transfer learning: a friendly introduction. *Journal of Big Data*. 2022 Oct 22;9(1):102.
11. A Mohammed, R Kora. A comprehensive review on ensemble deep learning: Opportunities and challenges. *Journal of King Saud University-Computer and Information Sciences*. 2023 Feb 1.
12. Y Nie, P Sommella, M Carratu, M Ferro, M O’nils, J Lundgren. Recent Advances in Diagnosis of Skin Lesions Using Dermoscopic Images Based on Deep Learning. *IEEE Access*. 2022 Aug 17.
13. D Popescu, M El-Khatib, L Ichim. Skin lesion classification using collective intelligence of multiple neural networks. *Sensors*. 2022 June 10;22(12):4399.
14. MA Khan, MY Javed, M Sharif, T Saba, A Rehman. Multi-model deep neural network based features extraction and optimal selection approach for skin lesion classification. In: 2019 international conference on computer and Information Sciences (IC-CIS) 2019 Apr 3 (pp. 1-7) Aljouf, Kingdom of Saudi Arabia. IEEE.
15. V Anand, S Gupta, A Altameem, SR Nayak, RC Poonia, AK Saudagar. An enhanced transfer learning-based classification for diagnosis of skin cancer. *Diagnostics*. 2022 Jul 5;12(7):1628.
16. TM Alam, K Shaukat, WAKhan, IAHameed, LA Almuqren, MA Raza, M Aslam, S Luo. An efficient deep learning-based skin cancer classifier for an imbalanced dataset. *Diagnostics*. 2022 Aug 31;12(9):2115.
17. S Aladhadh, M Alsanea, M Aloraini, T Khan, S Habib, M Islam. An effective skin cancer classification mechanism via medical vision transformer. *Sensors*. 2022 May 25;22(11):4008.
18. S Jain, U Singhania, B Tripathy, EA Nasr, MK Aboudaif, AK Kamrani. Deep learning-based transfer learning for classification of skin cancer. *Sensors*. 2021 Dec 6;21(23):8142.
19. MA Al-Masni, DH Kim, TS Kim. Multiple skin lesions diagnostics via integrated deep convolutional networks for segmentation and classification. *Computer methods and programs in biomedicine*. 2020 Jul 1;190:105351.
20. A Panthakkan, SM Anzar, S Jamal, W Mansoor. Concatenated Xception-ResNet50—A novel hybrid approach for accurate skin cancer prediction. *Computers in Biology and Medicine*. 2022 Nov 1;150:106170.
21. RD Seeja, A Suresh. Deep learning-based skin lesion segmentation and classification of melanoma using support vector machine (SVM). *Asian Pacific journal of cancer prevention: APJCP*. 2019;20(5):1555.

22. A Tajerian, M Kazemian, M Tajerian, A Akhavan Malayeri. Design and validation of a new machine-learning-based diagnostic tool for the differentiation of dermatoscopic skin cancer images. *PLoS One.* 2023 Apr 14;18(4):e0284437.
23. P Tschandl, C Rosendah, H Kittler. The HAM10000 dataset, a large collection of multi-source dermatoscopic images of common pigmented skin lesions. *Scientific Data.* 2018; 5: 180161. Search in. 2018;2.
24. SA Hicks, I Strümke, V Thambawita, M Hammou, MA Riegler, P Halvorsen, S Parasa. On evaluation metrics for medical applications of artificial intelligence. *Scientific reports.* 2022 Apr 8;12(1):5979.
25. SQ Nisa, AR Ismail. Comparative Performance Analysis of Deep Convolutional Neural Network for Gastrointestinal Polyp Image Segmentation.

الملخص

هذه الرسالة تقدم استكشافاً شاملاً للتقنيات الحوسبة المتقدمة في مجال التشخيص الطبي، مركزة على تحديد وتصنيف الأفات السرطانية في الجلد وتقسيم الأورام الدماغية. من خلال تطوير وتنفيذ مشروع شامل يضم موقعًا إلكترونيًا وتطبيق سطح المكتب وتطبيق Streamlit ، تسعى الدراسة إلى استغلال التكنولوجيا للكشف المبكر والتحديد الدقيق لهذه الحالات الصحية الحرجة.

من خلال استخدام مجموعات البيانات البارزة مثل HAM1000 و PH2 لتحليل سرطان الجلد ومجموعة بيانات LGG لتقسيم الأورام الدماغية، تأسست الدراسة أساس قوي للابتكار التشخيصي. من خلال استخدام خوارزميات التعلم الآلي المتقدمة، بما في ذلك الشبكات العصبية التكاملية المركزية (CNNs) وU-Net ، يهدف المشروع إلى استخراج وتفسير الأنماط المعقدة الكامنة في بيانات التصوير الطبي، مما يسهل التشخيص الدقيق وتحفيظ العلاج.

بالإضافة إلى عرض قدرات التقنيات الحديثة في المنهجيات الحوسبة، تؤكد الرسالة على أهمية التعاون بين التخصصات في مواجهة التحديات الصحية. من خلال دمج التكنولوجيا الحديثة بسلامة مع الخبرة السريرية، تسعى الدراسة إلى تقليل الفجوة بين الممارسات الصحية التقليدية والنمذج الحوسبة الناشئة.

مع استمرار تطور المناظر الرقمية، تحمل دمج التكنولوجيا والطب وعداً هائلاً بتحديث العمليات التشخيصية وتحسين نتائج المرضى. من خلال هذا الجهد، تتطلع إلى مستقبل حيث تتلاشى الحدود بين التخصصات، مما يدخلنا في عصر الطب الدقيق والتدخلات الصحية الشخصية.



جامعة مصر للعلوم والتكنولوجيا

كلية تكنولوجيا المعلومات

تقرير مقدم كمطلوب مشروع التخرج للحصول على درجة البكالوريوس في تكنولوجيا
المعلومات

الكشف عن السرطان باستخدام التعلم العميق

مقدم من

اسم الطاب	الرقم الجامعي	القسم
مصطفى طارق	٩٤٠٧١	ذكاء اصطناعي
محمد عز الرجال	٩٤٣٠٣	ذكاء اصطناعي
عمرو سمير	٩٤٢١٨	ذكاء اصطناعي
عبد الرحمن احمد	٩٠٣٦٩	ذكاء اصطناعي
نور ايها	٩٠٣٣٠	ذكاء اصطناعي

تحت إشراف

أ.د./ رانيه الجوهرى

د./ محمد بدوى

الهيئة المعاونة

أ.م./ شيماء يوسف

أ.م./ شيرين محمد

يونيو / 2024



جامعة مصر للعلوم والتكنولوجيا

كلية تكنولوجيا المعلومات

تقرير مقدم كمطلوب مشروع التخرج للحصول على درجة البكالوريوس في تكنولوجيا
المعلومات

الكشف عن السرطان باستخدام التعلم العميق

تحت إشراف

ا.د. رانيه الجوهرى

د. محمد بدوى

الهيئة المعاونة

ا.م. شيماء بهاء

ا.م. شيرين يوسف

يونيو / 2024